DEVELOPMENT OF PROCESS EVALUATION OF IMPROVED FISCHER-TROPSCH SLURRY CATALYSTS. QUARTERLY TECHNICAL PROGRESS REPORT, 1 APRIL--30 JUNE 1988

AIR PRODUCTS AND CHEMICALS, INC.
ALLENTOWN, PA

1988

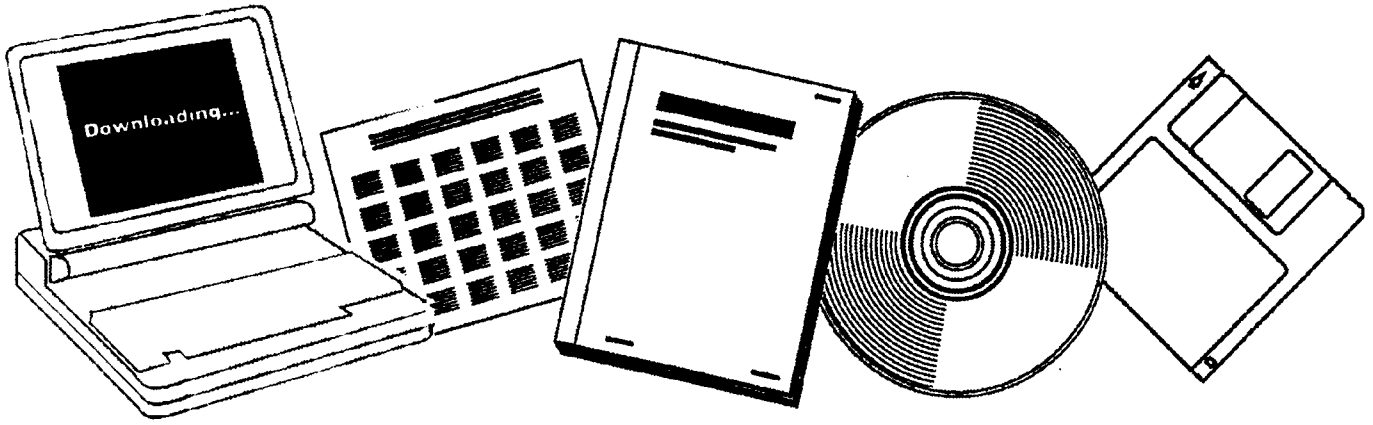

One Source. One Search. One Solution.

NTIS

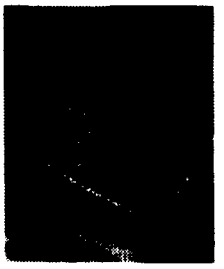

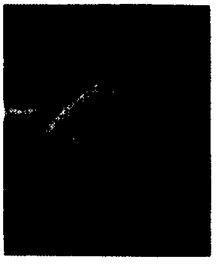

Providing Permanent, Easy Access to U.S. Government Information

National Technical Information Service is the nation's largest repository and disseminator of government-initiated scientific, technical, engineering, and related business information. The NTIS collection includes almost 3,000,000 information products in a variety of formats: electronic download, online access, CD-ROM, magnetic tape, diskette, multimedia, microfiche and paper.

Search the NTIS Database from 1990 forward

NTIS has upgraded its bibliographic database system and has made all entries since 1990 searchable on **www.ntis.gov.** You now have access to information on more than 600,000 government research information products from this web site.

Link to Full Text Documents at Government Web Sites

Because many Government agencies have their most recent reports available on their own web site, we have added links directly to these reports. When available, you will see a link on the right side of the bibliographic screen.

Download Publications (1997 - Present)

NTIS can now provides the full text of reports as downloadable PDF files. This means that when an agency stops maintaining a report on the web, NTIS will offer a downloadable version. There is a nominal fee for each download for most publications.

For more information visit our website:

www.ntis.gov

U.S. DEPARTMENT OF COMMERCE
Technology Administration
National Technical Information Service
Springfield, VA 22161

DOE/PC/80011-T7

DOE/PC/80011—T7

DE92 016986

DEVELOPMENT AND PROCESS EVALUATION OF IMPROVED FISCHER-TROPSCH SLURRY CATALYSTS

7th QUARTERLY TECHNICAL PROGRESS REPORT

FOR THE PERIOD 1 APRIL TO 30 JUNE 1988

by

Howard P. Withers

Air Products and Chemicals, Inc.

Allentown, PA 18195

and

Dragomir B. Bukur and Michael P. Rosynek

Departments of Chemical Engineering and Chemistry

Texas A&M University

College Station, TX 77843

WORK PERFORMED UNDER DOE CONTRACT NO. DE-AC22-85PC80011

FOR THE UNITED STATES DEPARTMENT OF ENERGY

THE PITTSBURGH ENERGY TECHNOLOGY CENTER

PITTSBURGH, PENNSYLVANIA

DISCLAIMER

Project Manager - George Cinquegrane
Liquid Fuels Division
Pittsburgh Energy Technology Center
Pittsburgh, Pennsylvania

Program Manager - John Shen
Office of Coal Preparation & Liquefaction
Department of Energy
Washington, DC

TABLE OF CONTENTS

I. ABSTRACT

Six fixed bed runs and a single slurry reactor run have been completed during the last reporting period. In fixed bed reactors, process variable studies using 100 Fe/5 Cu/4.2 K/20 Al_2O_3, 100 Fe/5 Cu/4.2 K, and Ruhrchemie LP 33/81 catalysts were made. The alumina–containing catalyst completes the series of supported catalysts planned to be tested. The activity of the supported catalysts decreases as the binder/support concentration increases for both alumina– and silica–containing catalysts, and the decline in activity exceeds that expected from the dilution of active metal with support alone. The unsupported catalyst containing 100 Fe/5 Cu/4.2 K was tested to distinguish clearly between support and promoter effects. The unsupported catalyst had similar activity as the catalysts containing 8 parts support, but produced greater amounts of lower molecular weight products. The Ruhrchemie catalyst was tested after calcination, while in the previous fixed bed tests, the catalyst was uncalcined. Calcination did not have a significant effect on activity, but the calcined catalyst produced more high molecular weight products than the uncalcined catalyst.

Three of the fixed bed tests were long term stability runs. The 100 Fe/5 Cu/4.2 K/8 SiO_2 catalyst was tested at 235 °C, 1.48 MPa, 2.0 Nl/g–cat·h, using both (H_2/CO) = 1.0 (up to 270 h) and 0.67 feed gas (270–552 h). The catalyst deactivated during the test, with a faster rate of deactivation using (H_2/CO) = 1.0 feed than with (H_2/CO) = 0.67. A 100 Fe/1.0 Cu/0.2 K catalyst has also been subjected to a stability test, and the catalyst deactivated rapidly during the initial period of the run. The run was terminated after the first balance due to excessive deactivation, and a retest of this catalyst is currently in progress. In the retest, the deactivation of the catalyst is also significant. The Ruhrchemie LP 33/81 catalyst was also evaluated in a long term stability test. A power failure at 382 h interrupted the run, but prior to the interruption the catalyst was stable. From the beginning of the first mass balance at 58.5 h to immediately before the power failure 342.5 h, the (H_2+CO) conversion dropped from 60.6 to 53.6 %. Following the power outage, the catalyst was stable at a lower activity, and gave an (H_2+CO) conversion of about 50 %. After

the fifth balance, the feed ratio was increased to 1.0 and the (H_2+CO) conversion increased to 57.2 %. The catalyst remained stable with the (H_2/CO) = 1.0 feed.

The Ruhrchemie LP 33/81 catalyst was also tested in a slurry reactor run which incorporated both a stability test and a process variable study. Five balances were completed at a fixed set of conditions (250 °C, 1.48 MPa, 2.0 Nl/g–cat·h, H_2/CO = 0.67) up to about 340 h. The (H_2+CO) conversion was steady, dropping from an initial level of 46.0 % to 44.2 %. Following the stability portion of the run, process variables were varied in 8 balances over 235–265 °C, 1.48–2.96 MPa, 1.0–4.0 Nl/g–cat·h, (H_2/CO) = 0.67 and 1.0 to determine their effect on catalyst activity and selectivity. Varying the process conditions accelerated catalyst deactivation, and by 619 h the conversion at the original process conditions dropped to 35.9 %. As the catalyst deactivated, selectivity shifted towards production of lower molecular weight compounds.

Metal exposures (dispersions) of selected precipitated iron catalysts, both unsupported and silica–supported, were determined by temperature–programmed desorption of adsorbed H_2, following reduction treatment in either H_2 or CO at 300 °C. Calculated metal exposures showed little dependence on either the presence of potassium and/or copper promoter or the support identity, and varied within the range 2 to 5 %. Both the isothermal and temperature–programmed reduction behaviors of a commercial Ruhrchemie iron catalyst in H_2 and in CO closely resembled those of the 100 Fe/5 Cu/4.2 K/25 SiO_2 catalyst prepared during the present investigation. Reduction of the calcined catalyst occurred in two steps: $Fe_2O_3 \rightarrow Fe_3O_4 \rightarrow Fe$, and the SiO_2 support inhibited the second step of the process, compared to the behavior of 100 Fe/5 Cu/4.2 K. X–ray photoelectron spectroscopic data revealed that, unlike the behavior observed for 100 Fe/5 Cu/4.2 K/25 SiO_2, treatment of the Ruhrchemie catalyst in H_2 at 300 °C leads to substantially more zero–valent surface iron than does reduction in CO at the same temperature. Infrared spectroscopic studies of 25 wt % Fe/SiO_2, using NO as a probe adsorbate, have demonstrated the marked susceptibility of surface Fe^{2+} and Fe^0 toward reoxidation by O_2 at 25 °C.

II. OBJECTIVE AND SCOPE OF WORK

The objective of this contract is to develop a consistent technical data base on the use of iron-based catalysts in Fischer-Tropsch (F-T) synthesis reactions. This data base will be developed to allow the unambiguous comparison of the performance of these catalysts with each other and with state-of-the-art iron catalyst compositions. Particular attention will be devoted to generating reproducible kinetic and selectivity data and to developing reproducible improved catalyst compositions. To accomplish these objectives, the following specific tasks will be undertaken.

TASK 1 - Project Work Plan

The objective of this task is to establish a detailed project work plan covering the entire period of performance of the contract. This includes estimated costs and manhours expended by month for each task.

TASK 2 - Slurry Catalyst Improvement

The primary purpose of this task is to develop improved iron-based catalysts, both precipitated and supported, that show enhanced activity and selectivity in slurry phase testing. This will be accomplished by gaining systematic understanding of the role of promoters, binders, supports and activation procedures in determining the activity and selectivity of iron-based catalysts. The catalyst development program will incorporate extensive physical and chemical characterization of these materials with the objective to establish correlations between the physical/chemical properties of these catalysts and the corresponding catalytic behavior for synthesis gas conversion.

TASK 3 - Process Evaluation Research

The purpose of this task is to subject the most improved catalysts (based on activity and selectivity) to a thorough process evaluation. This involves long term stability studies, investigation of a wide range of process variables, and determination of kinetic parameters.

Task 4 - Economic Evaluation

The aim of this task is to develop the relative economic impact for each improved ctatlyst composition and compare these economics with the economics of using the base case catalyst.

I. SUMMARY OF PROGRESS

The initial series of tests of supported catalysts has been completed. The remaining alumina-containing catalyst, 100 Fe/5 Cu/4.2 K/20 Al_2O_3, was tested in run FA-76-0968. An unsupported catalyst containing the same promoter concentrations as the supported catalysts (5 Cu/4.2 K) was also tested to determine the undisguised effect of supports and promoters (run FA-31-1118). A total of six different catalysts have now been tested in the binder/support effect series: unsupported, silica-containing with 8, 25, and 100 parts SiO_2/100 parts Fe, and alumina-containing with 8 and 20 parts Al_2O_3/100 parts Fe. Each catalyst was tested using the same set of nominal process conditions: 220, 235, and 250 °C, 1.48 and 2.96 (1 balance) MPa, 2 and 4 Nl/g-cat-h, with (H_2/CO) = 1.0 synthesis gas. Catalyst activity decreased as the support concentration increased for both alumina- and silica-containing catalysts, even when differences in the metal content of catalysts was accounted for. The unsupported catalyst and 8 parts SiO_2 catalyst were the most active tested, followed by the 8 parts Al_2O_3 catalyst. These support levels also increased selectivity towards high molecular weight products (C_{12}+). The 100 Fe/5 Cu/4.2 K/8 SiO_2 catalyst is among the most active catalyst tested to date, and has desirable selectivity behavior (low methane, high C_{12}+) as well.

A fixed bed test of calcined Ruhrchemie LP 33/81 catalyst was made. In previous tests of this catalyst, the catalyst was not calcined. The activity of the calcined and uncalcined catalyst were very similar at the same nominal process conditions. The (H_2+CO) conversion with calcined catalyst was slightly greater than uncalcined at 235 °C, 1.48 MPa, 2 Nl/g-cat-h, 49.1 % compared to 43.7 %, but at higher temperature (250 °C) or space velocity (4.0 Nl/g-cat-h) the conversions were virtually the same. The selectivities of the calcined and uncalcined catalysts were different. Calcination seemed to shift the product distribution towards higher molecular weight compounds, with less methane and more C_{12}+ products formed using the calcined catalyst. The selectivity of the calcined catalyst was similar to the high potassium promoted (supported promoter level)

catalysts tested in the current study, while our supported catalysts containing 25 or less parts support were significantly more active than Ruhrchemie LP 33/81, whose composition, 100 Fe45 Cu/4 K/25 SiO_2 is similar to our 25 parts SiO_2 catalyst.

Three stability runs in fixed bed reactors have been completed, and a single fixed bed run is currently in progress. The 100 Fe/5 Cu/4.2 K/8 SiO_2 catalyst was tested in run FA–63–1308 at 235 °C, 1.48 MPa, 2.0 Nl/g–cat-h using (H_2/CO) = 0.67 and 1.0 feed gas, and 8 mass balances were made in over 550 h on stream. The catalyst deactivated steadily during the run, with a faster rate of deactivation using (H_2/CO) = 1.0 synthesis gas as opposed to (H_2/CO) = 0.67. More CH_4 and C_2–C_4 products were formed as the catalyst deactivated. A precipitated, unsupported catalyst (100 Fe/1.0 Cu/0.2 K) was tested in run FA–15–1698, which had been tested previously at varied process conditions, and was found to be the most active of the unsupported, promoted catalysts. The catalyst deactivated rapidly during the first stability test, with the conversion dropping from an initial 78.0 % (H_2+CO) conversion to 51.1 % over a 45 h interval. This run was terminated after the first mass balance, and a new test of the same catalyst was initiated in run FA–15–1768. This run is still in progress, however, the catalyst has again undergone significant deactivation. At 235 °C, 1.48 MPa, 2.0 Nl/g–cat-h, with (H_2/CO) = 0.67 feed gas, the initial (H_2+CO) conversion at 25.5 h was 55.1 %, but at 174 h, the (H_2+CO) conversion has dropped to 31.2 %. A stability test of Ruhrchemie LP 33/81 catalyst, run FB–99–1588, was also made. The catalyst was stable, and at 250 °C, 1.48 MPa, 2.0 Nl/g–cat-h, using (H_2/CO) = 0.67 feed gas the (H_2+CO) conversions was 58.3 % at 100 h, dropping to 53.6 % by 340 h. A power failure at 382 h caused an immediate decrease in conversion, dropping to about 50 %, but the catalyst continued to be stable at lower activity. After the fifth balance, the feed gas was switched to a (H_2/CO) = 1.0 ratio, and the conversion increased to 57.2 % (479 h). The catalyst activity remained nearly constant with the higher feed ratio gas, dropping to 55.7 % by 630 h.

A slurry reactor test of the Ruhrchemie LP 33/81 catalyst has been completed. The run was

made as both a stability test and a process variable study. In the first part of the run, conditions were held constant at 250 °C, 1.48 MPa, 2.0 Nl/g-cat-h, (H_2/CO) = 0.67 for 5 mass balances (about 340 h on stream). Catalyst activity was stable during this period, with the (H_2+CO) conversions measured in the range 42.6–46.4 %. Following the stability test, process conditions were varied to determine their effect on catalyst activity and selectivity. The conditions ranged from 235–265 °C, 1.48–2.96 MPa, 1.0–4.0 Nl/g-cat-h, (H_2/CO) = 0.67–1.0, and 8 mass balances, including a repeat of the initial conditions, were completed. Changing of process conditions increased the rate of catalyst deactivation, and during the repeat of conditions at 619 h the (H_2+CO) conversion was 35.9 %.

Three precipitated iron catalyst compositions were selected for resynthesis, on the basis of overall catalytic performance for the Fischer–Tropsch reaction. Approximately 100 g batches of each of the following compositions were prepared, using the controlled–pH, continuous precipitation technique that has been detailed previously and employed for all prior catalyst syntheses:

100 Fe/1 Cu/0.2 K

100 Fe/3 Cu/0.2 K

100 Fe/5 Cu/4.2K/8 SiO_2

Elemental analyses were performed by atomic absorption spectroscopy for each material, and were found to be within acceptable limits.

Metal exposures (dispersions) are an indication of the fraction of total reduced metal that is available for adsorption or reaction at the surface of precipitate crystallites. Exposures were determined for 12 representative catalyst compositions by temperature–programmed desorption of adsorbed H_2, following calcination at 300 °C and subsequent reduction in either H_2 or CO at the same temperature. Assuming dissociative adsorption of H_2, fractional metal exposures were calculated from the total amount of desorbed H_2 in each case. The observed values showed relatively little variation. Most were within the range H/Fe = 0.02 to 0.05 and appeared to be

largely independent of the presence of either copper or potassium promoter or, surprisingly, SiO_2 and Al_2O_3 supports. Resulting exposures were, in general, somewhat higher for samples reduced in CO than for those treated in H_2.

Reduction and surface properties of a commercial Ruhrchemie iron catalyst were characterized using isothermal and temperature–programmed reduction and X–ray photoelectron spectroscopic techniques. Both temperature–programmed and isothermal (300 °C) reduction behaviors of this material closely resembled those of the 100 Fe/5 Cu/4.2 K/25 SiO_2 catalyst that has been synthesized and characterized previously during this investigation. Reduction of the precalcined catalyst in either H_2 or CO occurs in two consecutive steps:

$$Fe_2O_3 \rightarrow Fe_3O_4 \rightarrow Fe$$

Compared to the behavior of the unsupported 100 Fe/5 Cu/4.2 K composition prepared during this study, the presence of SiO_2 significantly decreased the rate of reduction of the Ruhrchemie catalyst at 300 °C in both H_2 and CO. In marked contrast to the behavior observed previously for 100 Fe/5 Cu/4.2 K/25 SiO_2, however, XPS measurements indicated that reduction in H_2 at 300 °C was more effective at producing zero–valent surface iron species than was treatment in CO at the same temperature.

Infrared spectroscopic studies have been made to investigate the effect of potassium promoter in influencing the susceptibility of reduced, silica–supported iron to reoxidation by O_2 at 25 °C. Using NO as a probe adsorbate, these measurements have demonstrated that reoxidation occurs rapidly at ambient temperature in a two–step process that eliminates surface adsorption sites. The presence of potassium promoter or the use of high (730 °C) reduction temperatures greatly increase the tendency toward reoxidation.

We have continued our analysis of fixed bed reactor hot trap products collected in previous runs. Our results for the activation/reduction study runs show the presence of at least two chain

growth probabilities (α's) in the hydrocarbon distribution. The values for low molecular products ranged from 0.66–0.74 while for higher products the range was 0.84–0.94. The analysis of the wax had little effect on the lumped hydrocarbon distribution for these runs, with only minor shifts between the C_5–C_{11} and C_{12}+ products.

IV. DETAILED DESCRIPTION OF TECHNICAL PROGRESS

TASK 1 — Project Work Plan

The project work plan was completed during the first quarter of this project and the detailed work plan was submitted to APCI.

TASK 2 — Slurry Catalyst Improvement

2.1. Wax Analysis Results.

We have continued our work on analyzing the products collected in the hot trap of the fixed bed reactor systems during previous runs. These results are incorporated into the existing data to extend the range of carbon numbers included in the mass balances and selectivity calculations. The results for selected reduction/activation study fixed bed catalyst tests are summarized in Table 1.

Our analysis of the higher molecular weight products clearly shows that at least two chain growth probabilities (α's) are needed to characterize the product distribution. Anderson–Schulz–Flory (ASF) plots are shown in Figs. 1 and 2 for runs FA–25–2737 and FA–25–3077 (reported in the Technical Progress Report for 1 October – 31 December 1987). High methane and C_2–C_4 yields were obtained in run FA–25–2737, while run FA–25–3077 produced large amount of C_{12}+ products. Both runs showed product distributions which did not fit the simple, single α, ASF model. Huff and Satterfield (1984) and Stenger (1985) have discussed multiple–α product distributions, and we have used the two–α model described by Huff and Satterfield to represent our data:

$$m_n = \beta(1-\alpha_I)\alpha_I^{n-1} + (1-\beta)(1-\alpha_I I)\alpha_{II}^{n-1} \qquad (1)$$

where m_n is the mole fraction of products containing n carbon atoms (hydrocarbon and oxygenate), β is the fraction of type I sites on the catalyst, and α_I and α_{II} are the chain growth probabilities associated with the type I and type II sites, respectively.

The constants appearing in Eq. (1) are obtained in the following manner: at low carbon number, the product distribution is dominated by the type I site, and α_I is calculated from the

slope of the log-linear plot in the usual manner as α_I = exp (slope). Similarly, at higher carbon numbers the product distribution is dominated by the type II site, and α_{II} can be calculated from the slope at large n. β is calculated using these known values of α, and the best estimate of β, in the least squares sense, is given by:

$$\beta = \frac{\sum_{j=1}^{N}(m_j + m_{II}^j)(m_I^j - m_{II}^j)w_j}{\sum_{j=1}^{N}(m_I^j - m_{II}^j)^2 w_j} \tag{2}$$

where $m^j = (1-\alpha)\alpha^{j-1}$ for the type I or II site, N is the maximum carbon number in the distribution, and w_j is the weighting factor associated with carbon number j. The weighting factor is needed to account for the large range of mole fractions, which typically span several orders of magnitude in any one sample; without weighting, the estimate of β is based almost entirely on the first few carbon numbers. The values of β appearing in Table 1 were obtained using a weight given by $w_j = e^j$.

The reduction conditions effect both the nature of the sites (*i.e.*, α_I and α_{II}) and the number of sites (or the relative activity of the sites), β. The use of H_2 reductant, runs FA–25–3237 (250 °C) and FB–25–3227 (280 °C), has little effect on α_I, but compared to CO reductant (FB–25–0098 and FA–25–2967), H_2 decreases α_{II} and increases β, causing more lower molecular weight products to be formed. High reduction pressure (run FA–25–3517) decreased β significantly to 0.68, although this reduction procedure had a detrimental effect on catalyst stability. The remaining CO reductions resulted in β ranging from 0.81 to 0.92. In the presence of H_2 reductant, β was always high (0.91–0.92) including the H_2+CO reduction (run FB–25–3377).

Deviations between the model (Eq. 1) and the experimental data occur for several reasons. In Fig. 1, the negative deviations in the C_7–C_{19} range are caused by errors in fitting the parameters (α_I, α_{II}, and β) separately. Overprediction of the mole fractions arise in the region where the type I and II contributions overlap, while our estimation technique assumes that the parameters can be evaluated individually. These errors are typically small. Negative deviations in the C_7–C_{10} mole

fractions apparent in Fig. 2 are caused by product loss to evaporation during sample handling. The disparity in the C_{12}–C_{20} carbon number products may be due to product losses as well, and we have also found that errors in this range of carbon numbers result from overestimation of the amount of analyzed wax. By erroneously including more wax than was analyzed into the product distribution, the mole fractions of higher carbon numbers are higher than expected. The result is a negative deviation in the distribution where the organic liquid and wax analyses overlap. An underestimation of the organic liquid analyzed caused by less than 100 % recovery in the organic analysis or sample weight error, should give the same type of deviations.

The addition of the wax analysis results into the product distribution had little effect on the lumped hydrocarbon distributions, which are also shown in Table 1. Only minor shifts in the C_5–C_{11} and $C_{12}+$ fractions occurred, due to the redistribution of C_9–C_{11} products from the wax to the C_5–C_{11} fraction. The fixed bed reactor wax is primarily $C_{12}+$. Small amounts of oxygenates are usually present in the wax, and after analysis, they are reclassified and no longer counted as hydrocarbons. This reclassification decreases the fraction of total hydrocarbons formed, which changes the methane and C_2–C_4 fractions slightly.

2.2. Fixed Bed Catalyst Studies.

Three additional fixed bed catalyst process variable studies using our standard testing procedure have been completed. A calcined sample of the Ruhrchemie LP 33/81 catalyst has been tested (run FB–99–1348) for comparison with previous tests of uncalcined LP 33/81 catalyst. A supported catalyst containing a nominal 20 parts Al_2O_3/100 parts Fe has also been tested (run FA–76–0968) to complete the series of Al_2O_3 catalysts. An unsupported catalyst containing the same promoter concentrations as the Al_2O_3– and SiO_2–containing catalysts (5 Cu/4.2 K nominal) was run to determine the undisguised effect of support on catalyst performance (run FA–31–1118).

2.2.1. Run FB–99–1348 (Calcined Ruhrchemie LP 33/81).

Six mass balances were performed in run FB–99–1348, and the results are summarized in Table

2. This run was made to test Ruhrchemie LP 33/81 catalyst after calcination, and the 30/60 mesh catalyst was reduced with pure CO for 12 h at 280 °C prior to exposure to synthesis gas. The Ruhrchemie catalyst has a nominal composition of 100 Fe/4 Cu/4 K/25 SiO_2 (weight basis), which is similar to our 100 Fe/5 Cu/4.2 K/25 SiO_2 catalyst. A test of uncalcined Ruhrchemie LP 33/81 catalyst was made in run FB–99–3477, reported in the Technical Progress Report for 1 October–31 December 1988, and selected activity and selectivity aspects of these two runs are compared in Table 3.

During the first balance at 235 °C, 1.48 MPa, and 2 Nl/g–cat·h, the mass closure was low and the conditions were repeated again during balance 3. The activity of the catalyst between the two balances was essentially constant, and during balance 3 the (H_2+CO) conversion was 49.1 %. At higher space velocity, 4 Nl/g–cat·h, the conversion dropped to 33.8 %. The effect of temperature at 220, 235, and 250 °C at 2 Nl/g–cat·h and 1.48 MPa, showed the expected increase in (H_2+CO) conversion: 25.9 (balance 5), 49.1 (balance 3), and 60.3 % (balance 4). The conversion at 220 °C was lower than expected, and partial deactivation apparently occurred during the test at 250 °C. Catalyst deactivation was evident during balance 6 at 235 °C and 2.96 MPa, at constant (P/SV) as balances 1 and 3. At the higher pressure, the (H_2+CO) conversion dropped to 36.7 %, while at the lower pressure the conversion was 49.1 %.

The activity of both calcined and uncalcined catalysts was very similar. At 235 °C and 2 Nl/g–cat·h, the calcined catalyst was slightly more active, giving an (H_2+CO) conversion of 49.1 % compared to the 43.7 % conversion for the uncalcined catalyst. At higher space velocity (4 Nl/g–cat·h) or higher temperature (250 °C) the calcined and uncalcined catalyst gave the same conversions (Table 3). Catalyst deactivation in run FB–99–1348 (calcined) during balances 5 and 6 (220 °C, 1.48 MPa and 235 °C, 2.96 MPa) caused the (H_2+CO) conversions to be lower than expected at these conditions. At the same conditions, the uncalcined catalyst was not deactivated, thus the lower activity of the calcined catalyst was due to deactivation as opposed to calcination.

Before deactivation occurred, the calcined catalyst produced smaller amounts of methane, C_2–C_4, and C_5–C_{11} products than the uncalcined catalyst. At 235 °C, 2 Nl/g–cat·h, the calcined catalyst formed roughly half the CH_4 and C_2–C_4 products as the uncalcined catalyst, 4.3 versus 7.9 % (CH_4) and 17.6 and 36.4 % (C_2–C_4), while the amount of C_{12}+ products increased from 29.4 to 61.1 %. Similar differences in the selectivity occurred at 235 °C, 4 Nl/g–cat·h and at 250 °C, 2 Nl/g–cat·h, and are compared in Table 3. We had difficulties during the test of the uncalcined catalyst with atomic closures (the H balance was consistently low) which may have some impact on selectivity, however, large errors in the hydrocarbon distribution are not expected.

The ASF plots for the calcined Ruhrchemie LP 33/81 catalyst showed a strong break in the distribution at about C_{10}, which reflects the tendency of the calcined catalyst to produce large amounts of high molecular weight products. ASF plots for the balances at 235 and 250 °C (2 Nl/g–cat·h, 1.48 MPa) are shown in Figs. 3 and 4. Temperature had only a slight effect on the parameters, decreasing α_I from 0.64 to 0.63 and β from 0.82 to 0.80, and α_{II} remained unchanged at 0.92; the weight % hydrocarbon distributions at the two temperatures are also similar.

2.2.2. Run FA–76–0968 (100 Fe/5 Cu/4.2 K/20 Al_2O_3).

Run FA–76–0958 was the test of 100 Fe/5 Cu/4.2 K/20 Al_2O_3 catalyst, and the results of the six mass balances performed are summarized in Table 4. The catalyst was ground to 30/60 mesh before charging the reactor, and reduced using CO at 280 °C for 12 h. During the first two balances, at 235 °C, 1.48 MPa, 2 (balance 1) and 4 Nl/g–cat·h (balance 2), the (H_2+CO) conversions were 68.3 and 35.3 %, increasing to 73.4 % in balance 3 at 250 °C and 2 Nl/g–cat·h. The conversions are lower than the conversions obtained using the 8 parts Al_2O_3 catalyst (run FA–73–0828, reported in the Technical Progress Report for 1 January – 31 March 1988). The conversions obtained are higher than or comparable to the conversions using 25 parts SiO_2: 55.0 (balance 1), 38.5 (balance 2), and 67.6 % (balance 3) which were run at the same nominal conditions as the alumina–containing catalyst.

Catalyst deactivation occurred before the fourth balance at 220 °C, 2 Nl/g–cat-h. The (H_2+CO) conversion obtained during this balance was lower than expected, 22.1 % as compared to 31.1 % for the silica–containing catalyst (25 parts SiO_2) and 31.7 % for the 8 parts Al_2O_3 catalyst. A repeat of the conditions of balance 1 in balance 5 showed that the (H_2+CO) conversion had dropped from the original 68.3 % conversion to only 31.5 % over a 96 h time interval. Balance 6 was made at high pressure, 2.96 MPa, at constant (P/SV) as balances 1 and 5. The (H_2+CO) was 30.5 %, which is comparable to the balance 5 conversion, thus the high pressure did not further deactivate the catalyst.

This catalyst was selective towards high molecular weight products, with a maximum of 61.9 % C_{12}+ products at 235 °C, 4 Nl/g–cat-h in balance 2. The space velocity had little effect on selectivity as the weight % hydrocarbon distribution and the olefin/paraffin ratios were comparable between balances 1 and 2 (2 and 4 Nl/g–cat-h, respectively). Higher temperature (250 °C, balance 3) increased the percentages of CH_4, C_2–C_4, and C_5–C_{11} products as is normally expected, from 3.72, 16.6, and 19.2 % (235 °C, balance 1) to 4.84, 21.0, and 21.5 % (250 °C). The C_{12}+ fraction decreased from 60.5 to 52.7 %. The deactivated catalyst produced more of the gaseous hydrocarbons than the fresh catalyst. In balance 5, the catalyst produced 5.02 % CH_4 and 21.5 % C_2–C_4, an increase from balance 1 at the same conditions, and the C_{12}+ products decreased to 53.2 %. Higher pressure (comparing balances 5 and 6) had little effect on the weight % hydrocarbon distribution.

2.2.3. Run FA–31–1118 (100 Fe/5 Cu/4.2 K).

Six mass balances were performed during run FA–31–1118, and the results are summarized in Table 5. The catalyst was ground to 30/60 mesh and reduced, after loading, at 280 °C for 12 h with CO reductant. The 100 Fe/5 Cu/4.2 K catalyst was tested to determine precipitated catalyst behavior in the absence of support, at the high potassium and copper promoter levels used in the supported catalysts. The initial activity of the catalyst was high and comparable to the 100 Fe/5 Cu/4.2 K/8 SiO_2 catalyst (run FA–63–0418, reported in the Technical Progress

Report for 1 January – 31 March 1988), giving (H_2+CO) conversions of 78.3 (235 °C, 1.48 MPa, 2 Nl/g-cat·h), 54.8 (235 °C, 4 Nl/g-cat·h), and 65.4 % (250 °C, 4 Nl/g-cat·h) during balances 1–3. At the same nominal conditions, the silica–containing catalyst achieved 76.7, 52.8, and 65.1 % conversions. Balance 3 at 250 °C deactivated the catalyst, and the (H_2+CO) conversion dropped to 33.0 % during balance 4 at 220 °C, while compared to the silica–containing catalyst, a conversion of approximately 60 % was expected. Balance 5 was run at the same conditions as balance 1, and the conversion was found to have dropped from 78.3 to 47.2 %.

The unsupported catalyst showed a greater tendency to produce low molecular weight products (CH_4, C_2–C_4, and C_5–C_{11}) than either the alumina– or silica–containing catalysts with 8 parts support per 100 parts iron. At 235 and 250 °C (4 Nl/g-cat·h) the weight % of methane was 4.84 and 5.74 %, while the 8 parts SiO_2 catalyst produced 3.27 and 3.69 % and the Al_2O_3 catalyst produced 4.19 and 4.91 % at the same nominal conditions. As the catalyst deactivated, the C_2–C_4 and C_5–C_{11} percentages remained constant: 21.8 and 22.2 % (balance 2) to 23.6 and 24.4 % (balance 5). The increase in pressure during balance 6 to 2.96 MPa decreased methane and shifted some C_5–C_{11} products to C_{12}+. Between balances 5 and 6 (1.48 and 2.96 MPa, 235 °C), CH_4 decreased from 5.96 to 4.62 % and C_5–C_{11} decreased from 24.4 to 19.5 %. The C_{12}+ products increased from 46.0 to 52.8 % with the increase in pressure.

2.2.4. Discussion and Comparison of Supported Catalysts.

A summary of the selectivity and activity results is given in Table 6 for the three silica–containing catalysts (runs FA–63–0418, FA–66–0548, and FA–69–0668, reported in the Technical Progress Report for 1 January – 31 March 1988), the two alumina–containing catalysts, (runs FA–73–0828, reported in the Technical Progress Report for 1 January – 31 March 1988, and FA–76–0968), the unsupported catalyst using supported catalyst promoter levels (run FA–31–1118), and the calcined Ruhrchemie LP 33/81 catalyst (run FB–99–1348). The effect of support concentration can be studied over the range 0–100 parts SiO_2 and 0-20 parts Al_2O_3/100 parts Fe. The

impregnation technique used to prepare the alumina–containing catalysts was limited to a maximum support concentration of about 30 parts Al_2O_3/100 parts Fe, so a catalyst with high alumina concentration (*i.e.*, 100 parts) was not available for testing.

Catalyst activity, as measured by (H_2+CO) conversion, decreases as the support concentration increases. The (H_2+CO) conversions obtained at 235 °C at the two space velocities used in the tests are compared in Figure 5. The 8 parts SiO_2 and the unsupported catalysts had the highest activities, and on a per Fe basis, gave essentially the same (H_2+CO) conversions. The 8 parts Al_2O_3 catalyst also had high activity. The similarity in conversions for the unsupported and 8 parts supported catalysts show that the high activity is not due to surface areas alone. The very high potassium concentrations are responsible for the increase in catalyst activity over previous unsupported catalyst tests. While the BET surface areas of the SiO_2–containing catalysts increase from 94, 148, and 250 m^2/g at 8, 25, and 100 parts SiO_2/100 parts Fe, the (H_2+CO) conversions decrease at all conditions tested. The unsupported catalyst has a BET surface area of 38 m^2/g. The increased BET surface areas are caused by the addition of high surface area support and do not necessarily reflect a large increased active metal surface area in the presence of a support. Our measurements (Sect. 2.3.2 of this report) show that the fractional metal exposures for CO reduced, silica–containing catalysts are the same as for unsupported with the same promoter concentrations, thus crystallite size is constant. When alumina is added to the catalyst, the exposure roughly doubles. Egiebor and Cooper (1985) measured the BET surface areas of both fresh and used silica supported catalysts, with compositions of 100 Fe/4.2 Cu/6.7 K with 21, 50, and 73 parts SiO_2. Prior to use, these catalysts had surface areas of 151, 252, and 275 m^2/g, which agree with our values, but after use the surface areas decreased to 71, 17, and 28 m^2/g, respectively. The authors attributed the decrease in surface areas to carbon deposition on the catalyst during synthesis. Wax accumulation in catalyst pores may also contribute to low used catalyst surface areas. The high surface areas of fresh catalyst may not be representative of the actual area of the

activated catalyst. The high surface area catalysts have smaller pore diameters (Technical Progress Report for 1 October – 31 December 1988), increasing intraparticle diffusional limitations. Also, the catalysts with high support concentrations show stronger resistance to reduction and may not be fully activated.

The weight % hydrocarbon distributions of the supported catalysts and Ruhrchemie LP 33/81 (run FB-99-134S) are compared in Figs. 6 (235 °C, 1.48 MPa, 2 Nl/g–cat·h) and 7 (250 °C, 1.48 MPa, 2 or 4 Nl/g–cat·h). The addition of a small amount of support (8 parts/100 parts Fe) had a minor effect on conversion, but improves the selectivity by decreasing methane and C_2–C_4 formation, increasing the amount of C_{12}+ products. The calcined Ruhrchemie catalyst showed good C_{12}+ selectivity as well. An increase in the alumina concentration from 8 to 20 parts/100 parts Fe had no significant effect on the hydrocarbon distribution at any of the conditions tested. The selectivity of the catalyst with 8 parts SiO_2/100 parts Fe was better than (low methane, high C_{12}+) or comparable to the selectivities of all the supported catalysts, calcined Ruhrchemie LP 33/81, and unsupported catalyst. This catalyst is also one of the most active of the catalysts tested to date.

Our 100 Fe/5 Cu/4.2 K/25 SiO_2 catalyst and the Ruhrchemie LP 33/81 catalyst (100 Fe/4 Cu/4 K/25 SiO_2) have nearly the same compositions, yet behaved differently at similar operating conditions. Our catalyst was more active than the Ruhrchemie catalyst, but produced more gaseous hydrocarbons. At 235 °C, 2.0 Nl/g–cat·h, the (H_2+CO) conversions were 55.0 % for our catalyst and 49.1 % for the Ruhrchemie catalyst, while the methane was 5.7 and 4.3 % and the C_2–C_4 was 22.7 and 17.6 %, respectively. Similar differences were present at other conditions, which can be seen in Table 6. The 25 parts SiO_2 catalyst was also more selective towards lighter products than either of our 8 or 100 parts SiO_2 catalysts, regardless of differences in catalyst activity. We have noticed that higher support concentrations increase catalyst stability, in that more balances can be completed before catalyst deactivation becomes apparent. The 25 and 100 parts SiO_2 catalysts

were stable during the process variable studies, while the 8 parts SiO_2 and unsupported catalysts deactivated. All of these catalysts appeared robust at the single high pressure (2.96 MPa) mass balance. The Ruhrchemie catalyst has also been found to be a stable catalyst.

Dry (1981) discusses the results obtained at Sasol with supported catalysts. It is not possible to make quantitative comparisons between our work and that at Sasol, as Dry reports only relative values for potassium content, activity and hard wax selectivity, but some qualitative comparisons can be made. Using an Fe/Cu catalyst containing a relative K_2O concentration of 10 with 24 parts SiO_2/100 parts Fe (by weight), he reported a relative activity of 45 and a relative hard wax selectivity (*i.e.*, high molecular weight products) of 34. This was the most active catalysts of the series reported and had the highest hard wax selectivity. With an alumina supported catalyst (100 parts Al_2O_3) with a similar potassium loading (12), the activity decreased to 18 while the hard wax selectivity remained constant. With a second alumina catalyst, containing 23 parts Al_2O_3 and a potassium level of 3, activity increased to 35 and hard wax selectivity decreased to 10. Since higher potassium loading should increase activity at the levels reported, the decrease in activity with 23 and 100 parts Al_2O_3 can be attributed to the increase in support concentration, which is what we have observed for both alumina and silica supported catalysts. (Dry shows that high potassium concentrations, above 12, cause decreases in activity for SiO_2 supported iron). The decrease in hard wax selectivity is due to the change in potassium loading, where we have found that high potassium loadings give high selectivity to $C_{12}+$ products regardless of support.

The work of Egiebor and Cooper (1985) with 100 Fe/4.2 Cu/6.7 K and 21, 50, and 73 parts SiO_2 catalysts can also be compared to our results. They did not report their hydrocarbon distribution *per se*, but they noticed that the C_5–C_{11} fraction remained constant regardless of support concentration at a fixed set of conditions (300 °C, 0.71 MPa, H_2/CO = 1.0, 240 h^{-1}) and was 40–50 weight % of the total condensed products. They found that the reactant conversions changed only slightly as the support concentration increased, with no significant difference between the three

catalysts, which is not what we have experienced in our studies of supported catalysts.

2.3. Catalyst Preparation and Characterization.

We have completed the catalyst preparation and physical/chemical characterization portions of this investigation. Based on overall performances exhibited for the Fischer–Tropsch reaction, we resynthesized three of the precipitated iron catalysts, and have completed elemental analyses of their compositions. We have also determined metal exposures (dispersions) for several representative catalysts, in order to evaluate the effect of copper and potassium promoters and of silica and alumina supports on reduced iron crystallite size. Assessment of the reduction behavior of a commercial Ruhrchemie precipitated iron catalyst has been completed and compared to those of catalysts synthesized during this project. Infrared spectroscopic studies have been used to determine the effect of potassium promoter on the susceptibility of reduced silica–supported iron surfaces to reoxidation. Details of research results in each of these areas are provided in the following sections.

2.3.1. Catalyst Resyntheses.

Based on overall performances exhibited for the Fischer–Tropsch reaction during the catalyst testing phase of the project, three catalyst compositions were selected for resynthesis, in order to provide additional quantities of catalyst for further testing and to assess the reproducibility of the catalyst preparation method. Using the controlled–pH, continuous precipitation technique that has been described in previous reports, approximately 100 *g* (dry weight) of each catalyst was prepared. Elemental analyses of each material were performed using atomic absorption spectroscopy. Nominal and actual compositions (normalized to 100 parts Fe by weight) of the three resynthesized catalysts are summarized below:

Nominal Composition	Actual Composition
100 Fe/1 Cu/0.2 K	100 Fe/1.1 Cu/0.19 K
100 Fe/3 Cu/0.2 K	100 Fe/3.2 Cu/0.22 K
100 Fe/5 Cu/4.2 K/8 SiO_2	100 Fe/6.3 Cu/5.2 K/8 SiO_2

Although the analyzed copper and potassium contents of the silica–supported catalyst were somewhat higher than those of the previously synthesized catalyst having the same nominal composition (100 Fe/5.1 Cu/4.0 K/7.8 SiO_2), all elemental analyses were within acceptable limits.

2.3.2. Metal Exposure and Phase Identity Determinations.

In order to assess the influence of copper and potassium promoters and of silica and alumina supports on crystallite size in the reduced catalysts, metal exposure determinations were made for 12 selected catalyst compositions. Using the apparatus employed previously for temperature–programmed and isothermal reduction studies, samples of each calcined (16 *h* in air at 300 °C) catalyst were reduced for 16 *h* in either H_2 or CO ($GHSV =\sim 120{,}000$) at 300 °C. Following an He purge for 1 *h*, the samples were cooled in flowing H_2 to 25 °C, in order to saturate all available reduced surface sites with the adsorbate. The sample temperature was then ramped at 20 °C/min in flowing N_2 to 800 °C, and the quantity of desorbed H_2 was measured by monitoring the thermal conductivity of the effluent carrier gas. Assuming that H_2 adsorbs dissociatively and only on reduced Fe^0 sites, the concentration of the latter can be calculated. The results are summarized in Table 7.

In an attempt to determine the identity of bulk phases that are present in both precipitated and silica–supported iron catalyst, we performed X–ray powder diffraction (XRPD) measurements on selected catalysts. Prior to calcination, an unpromoted precipitated iron sample gave no discernible diffraction peaks, indicating that the material was either amorphous or contained very small (< 40 Å) crystallites. Unpromoted silica–supported catalysts containing 25 wt % Fe, as well as those containing 0.1 % K, 5 % K, 1 % Cu, and 5 % Cu promoters produced no measurable diffraction peaks following calcination in air for 16 *h* at 300 °C. Because of the difficulty experienced in obtaining

satisfactory diffraction peaks for these catalysts, no further XRPD experiments were performed.

2.3.3. Reduction Behavior of Ruhrchemie Catalyst.

The reduction behavior and resulting surface properties of a commercial Ruhrchemie catalyst were determined by application of the same temperature–programmed (TPR) and isothermal reduction methods and X–ray photoelectron spectroscopic (XPS) techniques used previously to characterize the catalysts synthesized during this investigation. The H_2 TPR profile of the precalcined Ruhrchemie catalyst, determined at a temperature program rate of 20 °C/min, is shown in Fig. 8. The peak at 340 °C is due to the first step of iron reduction ($Fe_2O_3 \rightarrow Fe_3O_4$), while the smaller peak at ~ 300 °C arises from reduction of copper oxide ($CuO \rightarrow Cu$). The broad peak centered at ~ 650 °C is due to reduction of Fe_3O_4 to metallic iron. The shapes and positions of the TPR peaks closely resemble those reported previously for the 100 Fe/5 Cu/4.2 K/25 SiO_2 catalyst that was prepared for study during this project (Fig. 9). The isothermal reduction profiles at 300 °C of the Ruhrchemie catalyst in H_2 and in CO are shown in Figs. 10 and 11, respectively. The results for both reductants are also very similar to those obtained previously for the 100 Fe/5 Cu/4.2 K/25 SiO_2 composition, demonstrating the similarity in reduction behavior of these two materials. It is apparent that the SiO_2 support inhibits the rate of the second reduction step in both H_2 and CO.

The chemical state of the Ruhrchemie catalyst surface following calcination and reduction treatments was determined by XPS measurements. Figs. 12–16 contain XPS spectra of this catalyst in the Fe 2p, Si 2p, K 2p/C 1s, O 1s, and Cu 2p regions, respectively. The Si 2p peak locations in Fig. 13 were used as references for each of the three series of spectra shown in the five Figures. The Fe $2p_{3/2}$ binding energy of 710.5 eV and the 3d → 4s shake–up satellite peak at ~ 719 eV in Fig. 12(a) confirm that the surface iron in the calcined catalyst was present as Fe_2O_3. Reduction in CO for 16 *h* at 300 °C (Fig. 12(b)) effected partial reduction to zero–valent iron, as shown by development of the small peak at ~ 707 eV, but most of the *surface* iron remained in the form of

unreduced Fe^{2+}/Fe^{3+} species. By contrast, reduction in H_2 under the same conditions resulted in a much greater percentage of reduced iron, as shown by the sharp peak at 706–707 eV in Fig. 12(c) that is characteristic of Fe^0. This behavior differs markedly from that observed previously for the precipitated iron catalysts synthesized during this investigation. For each of the latter, reduction in CO at 300 °C always leads to a much larger percentage of zero-valent surface iron than does treatment in H_2 under the same conditions. Since the preparation method employed for the two catalysts is presumably similar, the reason for these contrasting reduction behaviors is not clear.

Reduction of the Ruhrchemie catalyst in CO at 300 °C results in substantial deposition of surface carbon, as shown by the large peak at ~ 284 eV in Fig. 14(b). Unlike the case of unsupported catalysts, little surface enrichment in potassium occurs following reduction in H_2, as demonstrated by the failure of peaks in the K 2p region (293–296 eV) in Fig. 14(c) to increase as a result of H_2 treatment. Similar behavior has been observed previously for the $100Fe/5Cu/4.2K/25SiO_2$ precipitated catalyst; evidently, the SiO_2 support inhibits the surface migration and spreading of potassium promoter. Reduction in either H_2 or CO at 300 °C results in complete conversion of surface CuO (Fig. 16(a)) to the metallic state (Figs. 16(b) and (c)).

2.3.4. Spectroscopic Studies of Catalyst Reduction and Reoxidation.

Previous studies using Fourier Transform infrared spectroscopy (FT–IR) have complemented those by XPS and have provided information about the extent of reduction of *surface* metal species on silica–supported iron catalysts. These studies have been extended to include determinations of the influence of potassium promoter and reduction temperature on the susceptibility of reduced 25 wt % Fe/SiO_2 (prepared by impregnation of SiO_2 with $Fe(NO_3)_3$) toward reoxidation by O_2 at ambient temperature. A sample of this material was treated isothermally at 300 °C in flowing H_2 for 15 *h* (Fig. 17), and the resulting "reduced" catalyst subsequently subjected to a typical H_2 TPR experiment. The TPR profile (Fig. 18) shows only a small peak in the region of Fe_3O_4 reduction (~ 400 °C), indicating that reduction of *bulk* iron had been largely completed by the prior treatment

in H_2 at 300 °C. An XPS spectrum in the Fe 2p region (Fig. 19), however, indicated the presence of *both* zero–valent iron (peak at 706.5 eV) and oxidized iron (peak at ~ 710 eV) on the *surface* of the catalyst.

The nature and behavior of surface iron species on this catalyst were further investigated by FT–IR, using nitric oxide (NO) as a probe adsorbate. Adsorption of NO on iron and iron oxide surfaces leads to Fe–NO surface species whose N–O stretching frequencies are characteristic of the valence state and extent of coordination of the metal site. Exposure of a sample of the 25 wt % Fe/SiO_2 catalyst that had been reduced for 16 *h* in highly purified H_2 (containing < 1 ppm of O_2) at 300 °C to gaseous NO for 15 min at 25 °C, followed by evacuation of the NO produced the uppermost spectrum in Fig. 20. The two principal bands at 1735 and 1810 cm^{-1} are due to the N–O stretch of NO adsorbed on Fe^0 and Fe^{n+}, respectively, and are consistent with the XPS data that indicate the presence of both iron species on the surface of the catalyst following treatment in H_2 under these conditions. Since exposure of the freshly calcined catalyst (i.e., Fe_2O_3/SiO_2) to NO generates no observable bands due to NO adsorption, it is likely that the oxidized form of iron is Fe^{2+} in an Fe_3O_4–type structure. Both bands are asymmetric and broad, suggesting that energetically heterogeneous arrays of both types of sites exist on the surface. It should be noted that if the H_2 used for reduction is not rigorously purified of trace amounts of O_2, the band at 1735 cm^{-1}, due to NO adsorbed on Fe^0, is much less intense in comparison to the band at 1810 cm^{-1} than that shown in Fig. 20.

Following acquisition of the uppermost spectrum in Fig. 20, 15 torr of O_2 was admitted to the sample at 25 °C and collection of the next lower spectrum (requiring ~ 5 min) was begun immediately. The remaining six spectra in descending order in the Figure were obtained at 15 min intervals. It is clear that both bands progressively decrease in intensity during exposure to O_2, but that the band at 1735 cm^{-1} diminishes more quickly than the one at 1810 cm^{-1}, corresponding to the loss of NO adsorption sites via the two–step reoxidation process: $Fe \rightarrow Fe_3O_4 \rightarrow Fe_2O_3$. Both

bands become sharper and shift to higher frequencies as they decrease in intensity, reflecting the loss of site heterogeneity during reoxidation. Concomitant with the decrease of the two original bands is the appearance of three new bands at 1550, 1585, and 1615 cm^{-1} that may be due to adsorption of NO_2 (formed by oxidation of NO) on surface metal sites.

The effect of 1 wt % K promoter on the NO adsorption and surface reoxidation processes is shown by the spectra in Fig. 21. The original bands due to adsorption of NO on Fe^{2+} and Fe^0 are somewhat sharper and shifted slightly to lower frequencies than those observed on the unpromoted catalyst. In addition, the rate of reoxidation in O_2 is approximately twice as great in the presence of 1 wt % K, and the bands due to adsorbed NO_2 are not observed. When the potassium content is increased to 5 wt % (Fig. 22) reoxidation occurs about six times faster than for the unpromoted catalyst. In this case, although evidence for the formation of adsorbed NO_2 does not occur, bands due to surface nitrate (NO_3^-) species begin to appear in the frequency range 1300–1450 cm^{-1}.

An increase in the severity of H_2 treatment conditions to 8 *h* and 16 *h* at 730 °C fails to completely reduce surface iron, as demonstrated by the spectra in Figs. 23 and 24, respectively. Following such treatment and subsequent exposure to NO, a band at 1810 cm^{-1}, due to NO adsorbed on Fe^{2+}, is still observed. However, this band is much sharper and more symmetrical than that generated on the same catalyst reduced in H_2 at only 300 °C (Fig. 20), indicating that high temperature reduction leads to an energetically more homogeneous array of oxidized sites than that produced at the lower treatment temperature. Furthermore, *two* closely spaced bands at 1745 and 1760 cm^{-1}, due to NO adsorbed on Fe^0, are observed following reduction in H_2 at 730 °C. These may be due to the presence of structurally dissimilar iron metal sites that result from a phase transition occurring during the high temperature treatment. Although these two bands decrease rapidly upon exposure to O_2, the Fe^{2+} species giving rise to the band at 1810 cm^{-1} appears to decrease to approximately 33 % of its original intensity and then resist further oxidation.

TASK 3 — Process Evaluation Research

3.1. Slurry Reactor Catalyst Study.

3.3.1. Run SA–99–0888 (Ruhrchemie LP 33/81).

Run SA–99–0888 was a long term test of the commercial, state–of–the–art, Ruhrchemie LP 33/81 catalyst. The calcined catalyst was reduced *in situ* with CO at 280 °C for 16 *h* at 0.79 *MPa*, 3.0 *Nl/g*–cat·*h*. 34.6 *g* of the catalyst was charged to the reactor, and purified *n*–octacosane was used as the initial slurry liquid. The run was divided into two portions: during the first part of the run (up to 343 *h* on stream), catalyst stability was evaluated at a fixed set of conditions: 250 °C, 1.48 *MPa*, (H_2/CO) = 0.67, 2.0 *Nl/g*–cat·*h*; during the last part of the run, process conditions were varied to evaluate their effect on catalyst activity and selectivity: 235–265 °C, 1.48–2.96 *MPa*, (H_2/CO) = 0.67–1.0, 1.0–4.0 *Nl/g*–cat·*h*. The major events occurring during run SA–99–0888 are summarized in Table 8, and the wax and solids inventory for the run is shown in Table 9. Five mass balances were performed during the stability portion of the run and 8 mass balances were performed during the process variable studies. The results obtained during these balances are summarized in Table 10.

A stability plot, (H_2+CO) conversion versus time on stream, is shown in Fig. 25 for the stability portion of the run. The catalyst was very stable, and no significant deactivation occurred during 343 *h* on stream. At 46 *h*, the (H_2+CO) conversion was 46.0 %, and at 338 *h*, the conversion was 44.2 %. The conversions obtained during the stability test varied between 42.6–46.4 %, which has a range of 3.8 %. Wax was withdrawn after the catalyst activation and at the end of balances 2, 3, 4, and 5 using the external settling tank system described in the Technical Progress Report for 1 January–31 March 1988, and this procedure did not cause deactivation of the catalyst. The selectivity of the catalyst changed with time on stream, with more gaseous products formed as the catalyst aged. The effect of time on catalyst selectivity is shown in Fig. 26. During balance 1 (49 *h*) the weight % hydrocarbon distribution was 4.3 CH_4, 17.8 C_2–C_4, 22.1 C_5–C_{11}, and 55.8 % C_{12}+

while during balance 5 (336 h) the distribution was 4.6 CH_4, 21.3 C_2–C_4, 29.5 C_5–C_{11}, and 44.6 % C_{12}+. The olefin/paraffin ratios decreased with time, for example, the C_2 ratio decreased from 1.82 in balance 1 to 1.45 in balance 5. A repeat of the conditions was made in balance 11 (619 h), after 5 balances at different process conditions. The (H_2+CO) conversion dropped to 35.9 % in balance 11, showing that the process variable studies had accelerated deactivation of the catalyst. The trends in selectivity seen in balances 1–5 were also evident during balance 11. The weight % of methane increased to 7.0 % and C_{12}+ decreased to 31.5 %. The weak trend in decreasing olefin/paraffin ratios continued as well.

During the process variable studies, the effect of temperature was studied at 2.0 Nl/g–cat·h in balances 8 (235 °C), 5 (250 °C), and 10 (265 °C), and at 1.0 Nl/g–cat·h in balances 9 (235 °C) and 7 (250 °C), with all balances at 1.48 MPa and (H_2/CO) = 0.67. A comparison of catalyst selectivity at these conditions appears in Fig. 27. Conversion increases as expected with temperature: 23.0 (235 °C), 44.4 (250 °C), and 56.9 % (265 °C) at 2.0 Nl/g–cat·h, and 35.8 (235 °C) and 56.1 % (250 °C) at 1.0 Nl/g–cat·h. Temperature had little effect on the weight % hydrocarbon distribution between 235 and 265 °C (2 Nl/g–cat·h) and 235 and 250 °C (1.0 Nl/g–cat·h), which is unexpected since selectivity typically shifts towards lower molecular weight products with increased temperature. Olefin/paraffin ratios decreased with temperature, presumably as hydrogenation activity increases with temperature.

The feed gas space velocity was varied at 235 °C in balances 9 (1.0 Nl/g–cat·h) and 8 (2.0 Nl/g–cat·h), and at 250 °C in balances 7 (1.0 Nl/g–cat·h), 5 (2.0 Nl/g–cat·h) and 6 (4.0 Nl/g–cat·h). Space velocity has a minimal effect on the weight % hydrocarbon distribution, as shown in Fig. 28. A space velocity of 1.0 Nl/g–cat·h at 250 °C tended to produce more lower molecular weight products than at higher space velocities, but this trend was as strong at 235 °C. Olefin/paraffin ratios increased with space velocity at both temperatures. A higher (H_2/CO) feed ratio, 1.0 (balance 12) increased the (H_2+CO) conversion from 35.9 % (H_2/CO = 0.67, balance 11) to 45.4 %. The

(H_2/CO) = 1.0 feed also increased the amount of methane formed from 7.0 to 9.4 % and decreased the percentage of $C_{12}+$ products, as shown in Fig. 29. An increase in pressure to 2.96 *MPa* in balance 13 showed a decrease in (H_2+CO) conversion to 39.8 % which indicates that some catalyst deactivation occurred at the higher pressure. The higher pressure suppressed the formation of gaseous hydrocarbons, and the selectivities at the two pressures are also compared in Fig. 29.

The results obtained in slurry can be compared to the results obtained in the fixed bed reactors at 250 °C, 1.48 *MPa*, 2.0 *Nl/g*-cat-*h*, H_2/CO = 1 in balance 12 and in balances 4 of the fixed bed runs FB-99-1348 and FB-99-3477, and balance 6 of the stability run FB-99-1588 (Sect. 3.2.3 of this report). Comparisons can be made using (H_2/CO) = 0.67 feed between balances 1-5 and 11 of the slurry run and balance 6 of run FB-99-1588. The (H_2+CO) conversion obtained in runs FB-99-1348 and FB-99-3477 was approximately 60 %, and was 56 % in run FB-99-1588, compared to the 45.4 % conversion obtained in slurry (balance 12). The selectivity in the slurry reactor run favored more lighter hydrocarbons than in fixed bed when the higher feed ratio (1.0) was employed. The slurry test produced 9.4 (CH_4), 34.5 (C_2-C_4), 33.2 (C_5-C_{11}), and 23.0 % ($C_{12}+$) at these conditions, compared to 7.5 (CH_4), 32.0 (C_2-C_4), 28.1 (C_5-C_{11}), and 32.4 % ($C_{12}+$) for the uncalcined Ruhrchemie catalyst in run FB-99-3477. The calcined catalyst tested in run FB-99-1348 produced even less gaseous hydrocarbons. With the 0.67 feed gas, the (H_2+CO) conversion declined from 58.6 to 50.2 % between 71 and 426.5 *h* in fixed bed (balances 1-5, run FB-99-1588) while in the slurry run the conversions were lower but more stable, decreasing from 45.9 to 44.4 between 49 and 336 *h* (balances 1-5). The selectivity with the (H_2/CO) = 0.67 feed for fixed bed and slurry were comparable in the first 5 balances of both runs. Comparing balance 2 in fixed bed (FB-99-1588) and balance 3 in the slurry at approximately 170 *h* for both runs, the weight % hydrocarbon distributions were 5.34 (CH_4), 21.1 (C_2-C_4), 18.8 (C_5-C_{11}) and 54.7 % ($C_{12}+$) in fixed bed and 5.09, 20.8, 21.9, and 52.2 %, respectively, in slurry.

3.2. Fixed Bed Catalyst Studies.

3.2.1. Run FA–63–1308 (100 Fe/5 Cu/4.2 K/8 SiO_2).

Run FA–63–1308 was made as a long term fixed bed stability test of the catalyst containing 8 parts SiO_2/100 parts Fe, which is among the most active of the catalysts tested to date and also shows desirable selectivity behavior. This catalyst was previously tested at a variety of process conditions in run FA–63–0418, reported in the Technical Progress Report for 1 January–31 March 1988. The catalyst was reduced *in situ* at 280 °C for 16 h, 3 Nl/g–cat-h with a pure CO reductant. Stability testing was conducted over a 552 h period, at 235 °C, 1.48 MPa, 2.0 Nl/g–cat-h, using (H_2/CO) = 1.0 synthesis gas (up to 271 h) and (H_2/CO) = 0.67 synthesis gas (up to 552 h). Three mass balances were completed with each feed ratio tested. A single mass balance was made at 250 °C during balance 7, and a repeat of the original conditions was made in balance 8. The results obtained during these balances are summarized in Table 11.

A stability plot of the (H_2+CO) conversion versus time on stream is given in Fig. 30. The catalyst deactivated steadily with the (H_2/CO) = 1.0 synthesis gas, with the (H_2+CO) conversion dropping from an initial value of 77.4 % (24.5 h) to a final value of 55.0 % (264 h). Deactivation continued after the switch to (H_2/CO) = 0.67 feed gas, but the rate of deactivation decreased. Between 294.5 and 552 h, the (H_2+CO) conversion dropped from 47.5 to 39.0 %. The average deactivation rates (average change in conversion/unit time) were 0.094 and 0.033 %/h with (H_2/CO) = 1.0 and 0.67, respectively.

The difference in deactivation behavior with feed ratio is difficult to explain as we do not know with any certainty the cause of deactivation in the fixed bed reactors. Decreasing the (H_2/CO) feed ratio from 1.0 to 0.67 between balances 3 and 4 caused the CO partial pressure to increase from 0.36 to 0.64 MPa and the H_2 partial pressure to decrease from 0.63 to 0.49 MPa (exit values). The higher CO partial pressure drives the water–gas shift (WGS) reaction to the right, thus the CO_2 and H_2O partial pressures change from 0.34 and 0.09 MPa to 0.27 and 0.05 MPa, respectively. If

the primary cause of deactivation is carbon fouling, higher CO partial pressure should increase the rate of deactivation (Dry, 1981), which is not what is observed. If the primary cause of deactivation is catalyst reoxidation, the higher CO partial pressures can explain the decreased deactivation in several ways: (1) as we have found that CO is a more effective reductant than H_2 (*e.g.*, Technical Progress Report for 1 July–30 September 1987), a lower feed ratio will lend to a stronger reducing environment in the reactor to offset oxidation, (2) the excess CO consumes oxidizing H_2O via the WGS and decreases the rate of oxidation, or (3) higher CO partial pressures compete more effectively with water for surface sites on the catalyst, inhibiting oxidation.

The effect of time on stream on the selectivity of the silica–containing catalyst is shown in Fig. 31 for both feed ratios. The lower (H_2/CO) feed ratio decreases CH_4 and C_2–C_4 selectivity, increasing the amount of C_{12}+ products formed. The olefin/paraffin ratios using (H_2/CO) = 0.67 synthesis gas are higher than or comparable to those using (H_2/CO) = 1.0 feed. Little change in selectivity with time is seen in the first three balances with (H_2/CO) = 1.0 or the balances using (H_2/CO) = 0.67 feed gas. However, after the catalyst was heavily deactivated at the repeat of the original process conditions (balance 8, 662 *h*, H_2/CO = 1.0), the product distribution shifted towards lighter products (CH_4 and C_2–C_4) at the expense of C_{12}+. The same effect was observed during the slurry reactor stability test of the Ruhrchemie LP 33/81 catalyst. There was no definite trend in the olefin/paraffin ratios with catalyst deactivation.

The ASF plots for active catalyst at 235 °C, (H_2/CO) = 1.0 (balance 1), (H_2/CO) = 0.67 (balance 4), and deactivated catalyst at (H_2/CO) = 1.0 (balance 8) are shown in Figs. 32-34. The feed ratio had little effect on α_{II}, which varied between 0.90 and 0.91 for the three balances. α_I increased from 0.74 to 0.79 and β decreased from 0.80 to 0.62 as the feed ratio decreased from 1.0 to 0.67, which are representative of the higher hydrocarbon selectivity of the lower feed ratio. Deactivation caused a decrease in α_I, from 0.74 to 0.62, with minimal change in either β or α_{II}, thus the gaseous hydrocarbons are the most strongly influenced by deactivation.

In the first balance of the run before deactivation, the catalyst activity and selectivity was similar to the previous test of this catalyst (run FA–63–0418) at the same conditions (235 °C, 1.48 *MPa*, 2.0 *Nl/g*–cat·*h*). The (H_2+CO) conversion at these conditions in the most recent run was 77.9 % as compared to the 76.7 % obtained previously. The weight % hydrocarbon distribution during run FA–63–0418 was 3.47 (CH_4), 16.4 (C_2–C_4), 20.1 (C_5–C_{11}), and 60.0 % (C_{12}+), compared to 4.25, 17.8, 21.4, and 56.5 % obtained in this run. At 250 °C (balance 7) the catalyst was deactivated and the (H_2+CO) conversion was only 46.4 %, while in the previous run the (H_2+CO) conversion at the same temperature and double the space velocity (4 *Nl/g*–cat·*h*, balance 3) was 65.1 %. The hydrocarbon selectivity did not change significantly with deactivation at these conditions.

3.2.2. Runs FA–15–1698/FA–15–1768 (100 Fe/1.0 Cu/0.2 K).

Runs FA–15–1698 and FA–15–1768 were made to evaluate the performance of a precipitated catalyst (100 Fe/1.0 Cu/0.2 K) over the long term in a fixed bed reactor. For both runs, 30/60 mesh catalysts were employed and the catalysts were reduced with CO at 280 °C for 16 *h*. This catalyst was tested previously in a fixed bed reactor during runs FA–15–2097 (Technical Progress Report for 1 July–30 September 1987) and FA–15–0278 (Technical Progress Report for 1 January–31 March 1988).

During run FA–15–1698, the catalyst rapidly deactivated upon reaching the desired synthesis conditions (235 °C, 1.48 *MPa*, 2.0 *Nl/g*–cat·*h*, $H_2/CO = 0.71$), with the (H_2+CO) conversion decreasing from 78.0 % at 0.5 *h* to 51.1 % at 46.0 *h*. During run FA–15–2097 at the same temperature, pressure, and space velocity with an (H_2/CO) = 1.0 feed ratio, the (H_2+CO) conversion was measured at 72.9 %. In run FA–15–0278 the (H_2+CO) conversion was 44.7 % at these conditions but this result was obtained with deactivated catalyst (balance 2). Run FA–15–1698 was terminated voluntarily after the first balance, and a retest was made in run FA–15–1768, which is currently in progress. Catalyst deactivation has also occurred in the most recent run, and the

stability plot for both stability runs is shown in Fig. 35. At approximately 50 h, the (H_2+CO) conversions were 53.7 and 47.5 % in runs FA–15–1698 and FA–15–1768, which are much lower than the conversion obtained in run FA–15–2097.

Based on these results, it appears that the 100 Fe/1.0 Cu/0.2 K catalyst, is not sufficiently stable. While in run FA–15–2097 the catalyst did not deactivate until a high pressure (2.96 MPa) was employed, in all subsequent tests deactivation occurred rapidly during synthesis testing. In the two recent stability tests, the deactivation is apparent from the stability plot (Fig. 35) and in run FA–15–0278 deactivation occurred after the first balance at 250 °C, 1.48 MPa, 2 Nl/g–cat·h. The only difference between runs was the reduction duration, which was 8 h in FA–15–2097 and 16 h in runs FA–15–0278 and the stability runs, although we found that a longer CO reduction duration at 280 °C improves stability during the activation/reduction task of this project (*e.g.*, Technical Progress Report for 1 October–31 December 1987). We have also improved our ability to control reactor temperatures and hot spots since the original test, thus it seems that run FA–15–2097 was an anomaly. The results of the stability tests of the 100 Fe/1.0 Cu/0.2 K catalyst will be discussed in the next quarterly report.

3.2.3. Run FB–99–1588 (Ruhrchemie LP 33/81).

Run FB–99–1588 was a long term stability test of the Ruhrchemie LP 33/81 commercial catalyst, and was made to complement the slurry run SA–99–0888. The initial process conditions for the stability test were 250 °C, 1.48 MPa, (H_2/CO) = 0.67, 2.0 Nl/g–cat·h, which are the same as those during the first five balances of slurry run SA–99–0888. The results of the seven balances of run FB–99–1588 are summarized in Table 12. Balance 7 was made after the end of the reporting period, but was included in the current report for completeness. The calcined Ruhrchemie catalyst was reduced *in situ* at 280 °C, using CO reductant for 12 h, and 30/60 mesh catalyst particles were used. The stability plot of (H_2+CO) conversion versus time is shown in Fig. 36. After an initial rapid decline in catalyst activity, the catalyst was relatively stable, with the conversion dropping

from 58.3 % to 53.6 % between about 100 and 340 *h*. At 382 *h*, a power failure occurred, interrupting the run for approximately 50 *min*, which caused an immediate decrease in the (H_2+CO) conversion to 50 % after the process conditions were reestablished. The catalyst was stable, at lower activity, after the interruption. After the fifth mass balance was completed the feed ratio was changed to 1.0 (nominal) at the same temperature, pressure, and space velocity. The (H_2+CO) conversion increased to 57.2 % at 478.5 *h* and declined slightly to 55.7 % at 629.5 *h*. Catalyst activity was stable with the higher feed ratio.

Catalyst selectivity as a function of time on stream is shown in Fig. 37 for run FB–99–1588. The first five balances are with (H_2/CO) = 0.67 and balances 6 and 7 are with (H_2/CO) = 1.0. The selectivity was not strongly affected by time on stream, and neither the weight % hydrocarbon distribution nor the olefin/paraffin ratios show any specific trends as the catalyst aged. At higher feed ratio, more gaseous hydrocarbons were formed, increasing from 6.38 (CH_4) and 25.0 % (C_2–C_4) in balance 5 (H_2/CO = 0.67) to 8.54 and 29.6 %, respectively, in balance 6 (H_2/CO = 1.0). The olefin/paraffin ratios decreased as well when the concentration of H_2 in the feed was increased.

The fixed bed run shows higher catalyst activity than slurry, with a conversion of 53.2 % in the fixed bed (balance 4) before the power failure compared to the 44.4 % conversion obtained in the slurry reactor (balance 5) at approximately the same time on stream with the (H_2/CO) = 0.67 feed gas. With the (H_2/CO) = 1.0 feed gas, the fixed bed run gave a conversion of 56.0 % in balance 6 (250 °C, 1.48 *MPa*, 2.0 *Nl/g*-cat-*h*) while during balance 12 of run SA–99–0888 at the same conditions, the conversion was 45.4 %, although catalyst deactivation occurred before this measurement was made.

The selectivities of the fixed bed and slurry runs are compared in Fig. 38. The hydrocarbon selectivity of the two runs using (H_2/CO) = 0.67 are similar, with the weight % of hydrocarbons in fixed bed (balance 2) at 5.3 (CH_4), 21.1 (C_2–C_4), 18.8 (C_5–C_{11}), and 54.7 % (C_{12}+) while in slurry (balance 3) the distribution was 5.1, 20.8, 21.9, and 52.2 %, respectively. With (H_2/CO) =

1.0, the slurry reactor produced more CH_4 and C_2–C_4 products than fixed bed. The preference of the slurry run towards lighter products may be due to catalyst deactivation since the catalyst was deactivated during the balance using $(H_2/CO) = 1.0$ in slurry. We observed that the deactivated catalyst produced more lower molecular weight products than fresh catalyst. Also, the differences in the C_5–C_{11} and C_{12}+ fractions may be due to differences in the product collection procedures for the two systems, and the C_5+ fractions are not as dissimilar. The olefin/paraffin ratios, which are also compared in Fig. 38, are lower in slurry than in the fixed bed, which may be due to the different mixing behavior (*i.e.*, plug flow and completely backmixed) of the two reactors.

Task 4 - Economic Evaluation

No work on this task was scheduled during this quarter.

V. LITERATURE REFERENCES

Dry, M. E., "The Fischer–Tropsch Synthesis," in *Catalysis — Science and Technology*, Vol. I, Anderson, J. R. and M. Boudart, Eds., Springer–Verlag, New York (1981) p. 159–255.

Egiebor, N. O., and W. C. Cooper, "Fischer–Tropsch Synthesis on a Precipitated Iron Catalyst: Influence of Silica Support on Product Selectivities," *Can. J. Chem. Eng.*, 63, 81–85 (1985).

Huff, G. A., Jr., and C. N. Satterfield, "Evidence for Two Chain Growth Probabilities on Iron Catalysts in the Fischer–Tropsch Synthesis," *J. Catal.*, 85, 370–379 (1984).

Satterfield, C. N., Huff, G. A., Jr., Stenger, H. G., Carter, J. L., and R. J. Madon, "A Comparison of Fischer–Tropsch Synthesis in a Fixed Bed Reactor and in a Slurry Reactor," *Ind. Eng. Chem. Fundam.*, 24, 450–454 (1985).

Stenger, H. G., "Distributed Chain Growth Probabilities for the Fischer–Tropsch Synthesis," *J. Catal.*, 92, 426–428 (1985).

Table 1. Summary of wax analysis results and hydrocarbon distributions for selected Reduction/Activation study fixed bed runs.

Run/Balance	Reduction Conditions[a]	ASF Results[b]			Wt % of Hydrocarbons[c]				
		α_I	α_{II}	β	CH_4	C_2-C_4	C_5-C_{11}	$C_{12}+$[d]	Wax[e]
FA-25-2737-1	CO, 250 °C, 8 *h*	0.68	0.87	0.92	13.0/13.0	37.0/37.0	34.5/34.6	15.5/15.4	9.9/3.9
FB-25-0098-2	CO, 250 °C, 24 *h*	0.71	0.89	0.81	8.4/8.4	31.5/31.5	35.8/35.9	24.3/24.2	18.3/6.8
FA-25-3077-2	CO, 280 °C, 8 *h*	0.74	0.90	0.84	6.8/6.8	26.8/26.8	32.9/33.2	33.5/33.2	25.4/9.4
FA-25-2967-1	CO, 280 °C, 24 *h*	0.66	0.94	0.85	7.1/7.1	25.8/25.8	22.7/23.0	44.4/44.1	40.8/21.1
FA-25-3517-2	CO, 280 °C, 24 *h*, 1.48 *MPa*	0.70	0.92	0.68	5.8/5.9	26.0/26.1	24.5/24.9	43.7/43.1	40.6/2.6
FB-25-3377-2	H_2+CO = 1, 280 °C, 24 *h*	0.73	0.92	0.92	6.5/6.5	27.0/27.0	32.7/32.8	33.8/33.8	24.3/13.1
FA-25-3237-1	H_2, 250 °C, 24 *h*	0.69	0.84	0.91	12.4/12.4	38.9/38.9	42.0/42.2	6.7/6.5	6.0/3.0
FB-25-3227-2	H_2, 280 °C, 24 *h*	0.66	0.88	0.91	11.7/11.7	38.3/38.4	34.2/34.3	15.8/15.7	12.3/8.6

[a] Atmospheric pressure, 3.0 $Nl/g \cdot cat \cdot h$, except where shown.

[b] $m_n = \beta(1-\alpha_I)\alpha_I^{n-1} + (1-\beta)(1-\alpha_{II})\alpha_{II}^{n-1}$.

[c] (Before wax analysis)/(Following wax analysis).

[d] Includes wax.

[e] Prior to analysis, wax is defined as the unanalyzed products collected in the hot trap. Following analysis, wax is redefined as the weight of sample unrecovered during the analysis.

Table 2. Summary of results for fixed bed run FB-09-1348.

Catalyst: 3.40 g[a], Ruhrchemie LP 33/81 — Diluent: 35.5 g, Glass beads
Catalyst volume: 5.40 cc — Diluent Volume: 23.0 cc

Period	1	2	3	4	5	6
Date	5/15/88	5/16/88	5/16/88	5/18/88	5/19/88	5/20/88
Time on Stream (h)	48.0	48.0	96.0	114.0	144.0	168.5
Balance Duration (h)	6.0	6.0	6.0	6.0	7.0	5.5
Average Temperature (°C)	235.	235.	234.	250.	220.	235.
Maximum Δ Temperature (°C)[b]	3.40	5.00	4.00	4.00	3.00	3.00
Pressure (MPa)	1.48	1.48	1.48	1.48	1.48	2.06
H_2/CO Feed Ratio	.980	.980	.980	.980	.980	.980
Space Velocity (Nl/g-cat·h)[a]	1.00	4.00	1.00	1.00	1.00	3.00
Space Velocity (Nl/g-Fe·h)	3.55	7.24	3.55	3.55	3.55	7.11
GHSV (h^{-1})[c]	238.	484.	238.	238.	238.	476.
CO Conversion (%)	47.0	30.8	46.0	64.5	22.9	33.4
H_2+CO Conversion (%)	49.5	33.8	49.1	60.3	25.9	36.7
H_2/CO Usage	1.05	1.18	1.07	.850	1.24	1.17
STY ($mols$ H_2+CO/g-cat·h)[a]	.044	.061	.044	.054	.023	.005
$P_{CO_2} \cdot P_{H_2} / P_{CO} \cdot P_{H_2O}$	2.21	.704	.800	2.51	.415	.487
Weight % of Outlet						
H_2	3.51	4.26	3.37	3.01	4.85	4.50
H_2O	3.05	5.66	8.46	7.24	5.86	6.51
CO	53.1	66.3	52.0	34.3	74.6	70.7
CO_2	21.5	10.0	20.5	36.5	6.57	8.76
Hydrocarbons	9.36	4.02	10.6	14.2	5.41	3.50
Oxygenates	.731	.575	.787	.895	.617	.613
Wax[d]	8.12	7.30	4.32	3.88	2.10	5.43
Yield (g/Nm^3 H_2 + CO Converted)						
CH_4	8.08	9.36	8.46	10.4	8.00	5.74
C_2–C_4 Hydrocarbons	34.0	34.6	34.3	40.6	35.4	24.7
C_5–C_{11} Hydrocarbons	65.7	40.9	33.2	37.5	37.0	23.3
C_{12}+ Hydrocarbons	109.	155.	120.	107.	107.	91.0
Wax[d]	101.	144.	56.8	41.9	52.7	88.0
Oxygenates	9.14	11.2	10.3	9.67	15.5	9.94
Total	228.	251.	206.	205.	204.	155.
1+2 Olefins/n-Paraffin Ratio						
C_2	1.73	2.18	1.94	1.04	3.13	2.86
C_3	5.76	5.84	5.93	6.13	5.17	4.26
C_4	4.66	4.66	4.76	4.84	4.12	3.26
C_8	4.85	2.08	3.00	2.47	3.31	3.03
C_{10}	4.31	2.59	2.25	1.60	2.30	2.24

[a] Based on unreduced catalyst [b] Maximum axial temperature difference [c] Based on reactor volume
[d] Balances 1,2,6: Unanalyzed products collected from hot trap; balances 3–5: Unrecovered products from wax analysis.

Table 2 (cont'd). Summary of results for fixed bed run FB-00-1348.

Period	1	2	3	4	5	6
Weight % of Hydrocarbons						
CH4	4.11	3.01	4.32	5.33	4.72	3.97
Ethane	1.62	1.30	1.67	2.82	1.30	1.20
Ethylene	2.63	2.05	3.01	2.75	3.07	3.18
Propane	.027	.827	.993	1.16	1.19	1.29
Propylene	5.09	4.01	5.02	6.77	5.88	5.24
n-Butane	.002	.856	1.04	1.20	1.19	1.37
1+2 Butenes	4.32	3.85	4.78	5.50	4.75	4.32
C_4 Isomers	.400	.355	.452	.510	.437	.464
n-Pentane	1.31	1.08	1.37	1.61	1.46	1.54
1+2 Pentenes	4.16	3.55	4.45	5.08	4.48	4.04
C_5 Isomers	.270	.222	.282	.381	.283	.321
n-Hexane	.700	.781	.852	.992	.878	.881
1+2 Hexenes	2.08	2.31	2.51	2.72	3.25	2.83
C_6 Isomers	.386	.349	.435	.480	.521	.506
n-Heptane	.570	.542	.570	.638	.687	.643
1+2 Heptenes	2.02	1.54	1.61	1.64	2.38	1.90
C_7 Isomers	.290	.605	.268	.265	.373	.311
n-Octane	.070	.376	.300	.437	.401	.382
1+2 Octenes	3.10	1.10	.885	1.06	1.50	1.14
C_8 Isomers	.101	.0780	.0394	.105	.118	.0315
n-Nonane	.830	.321	.244	.372	.208	.130
1+2 Nonenes	3.07	.898	.043	.758	.543	.296
C_9 Isomers	.279	.0383	.0372	.0527	.0382	.0252
n-Decane	.815	.442	.362	.441	.324	.163
1+2 Decenes	3.47	1.13	.802	.690	.765	.361
C_{10} Isomers	.392	.0686	.117	.251	.118	.0442
n-Undecane	.600	.484	.372	.487	.387	.169
1+2 Undecenes	2.59	1.08	.768	.691	.795	.334
C_{11} Isomers	.381	.0753	.0606	.0521	.0574	.0500
C_2-C_4	10.0	14.4	17.6	20.8	18.8	17.1
C_5-C_{11}	30.1	17.1	17.0	19.2	19.6	16.1
C_{12}+	49.9	64.6	61.1	54.7	56.9	62.9
Wax[d]	46.5	60.1	29.0	21.5	27.0	60.8

[d] Balances 1,2,6: Unanalysed products collected from hot trap; balances 3-5: Unrecovered products from wax analysis.

Table 3. Comparison of calcined (FB-99-1348) and uncalcined (FB-99-3477) Ruhrchemie LP 33/81 catalyst, $H_2/CO = 1.0$. Catalysts reduced at 280 °C, ambient pressure, using CO at 3 *Nl/g-cat·h* for 12 (FB-99-1348) and 8 (FB-99-3477) *h*.

Conditions	Run/Balance	Conversion			Wt % Hydrocarbons			
		CO	H_2+CO	Usage	CH_4	C_2-C_4	C_5-C_{11}	$C_{12}+$
220 °C, 1.48 *MPa*	FB-99-1348-5[a]	22.9	25.9	1.24	5.5	21.7	19.6	53.2
2 *Nl/g-cat·h*	FB-99-3477-1	37.8	37.9	1.10	4.8	20.8	19.1	55.3
235 °C, 1.48 *MPa*	FB-99-1348-3	46.9	49.1	1.07	4.3	17.6	17.0	61.1
2 *Nl/g-cat·h*	FB-99-3477-2	39.6	43.7	1.31	7.9	36.4	26.3	29.4
235 °C, 1.48 *MPa*	FB-99-1348-2	30.8	33.8	1.18	3.9	14.4	17.1	64.6
4 *Nl/g-cat·h*	FB-99-3477-3	28.6	33.7	1.47	8.2	37.5	27.9	26.4
250 °C, 1.48 *MPa*	FB-99-1348-4	64.5	60.3	0.85	5.3	20.8	19.2	54.7
2 *Nl/g-cat·h*	FB-99-3477-4	64.4	60.6	0.97	7.5	32.0	28.1	32.4
235 °C, 2.96 *MPa*	FB-99-1348-6[a]	33.4	36.7	1.17	3.9	17.1	16.1	62.9
4 *Nl/g-cat·h*	FB-99-3477-8	36.2	42.0	1.43	4.6	25.6	26.0	43.8

[a] Catalyst was deactivated prior to balance.

Table 4. Summary of results for fixed bed run FA-76-0068.

Catalyst: 3.60 g^a, 100 Fe/5 Cu/4.2 K/20.3 Al_2O_3
Catalyst volume: 3.00 *cc*

Diluent: 36.4 *g*, Glass beads
Diluent Volume: 24.0 *cc*

Period	1	2	3	4	5	6
Date	4/07/88	4/08/88	4/09/88	4/10/88	4/11/88	4/11/88
Time on Stream (*h*)	47.5	71.8	95.5	120.0	143.5	168.0
Balance Duration (*h*)	6.5	6.1	6.5	6.5	6.0	5.5
Average Temperature (°C)	235.	235.	250.	220.	235.	235.
Maximum Δ Temperature (°C)[b]	2.80	2.40	3.30	1.40	.900	2.30
Pressure (*MPa*)	1.48	1.48	1.48	1.48	1.48	3.00
H_2/CO Feed Ratio	1.00	1.00	1.00	1.00	1.00	1.03
Space Velocity (*Nl/g-cat·h*)[a]	2.03	4.03	2.03	2.03	2.03	4.03
Space Velocity (*Nl/g-Fe·h*)	3.53	7.04	3.53	3.53	3.53	7.04
GHSV (h^{-1})[c]	270.	538.	270.	270.	270.	538.
CO Conversion (%)	82.2	41.2	88.8	24.7	37.1	33.0
H_2+CO Conversion (%)	68.3	35.3	73.4	22.1	31.5	30.5
H_2/CO Usage	.662	.714	.653	.792	.697	.874
STY (*mole* H_2+CO/*g-cat·h*)[a]	.062	.063	.066	.020	.028	.055
$P_{CO_2} \cdot P_{H_2}/P_{CO} \cdot P_{H_2O}$	16.6	4.96	21.0	2.64	3.70	2.27
Weight % of Outlet						
H_2	3.10	4.76	2.81	5.35	5.01	5.08
H_2O	3.57	2.71	4.41	2.64	3.15	3.69
CO	16.8	55.1	10.4	60.6	50.1	63.8
CO_2	56.7	27.4	62.1	15.0	24.2	18.5
Hydrocarbons	8.00	4.06	9.59	3.07	4.10	4.03
Oxygenates	1.08	.518	.059	.343	.455	.485
Wax[d]	10.8	5.47	9.75	3.03	4.02	4.33
Yield (*g/Nm³* H_2 + CO *Converted*)						
CH_4	6.78	6.75	8.58	7.52	8.62	8.76
C_2-C_4 Hydrocarbons	30.3	30.5	37.1	36.3	36.0	38.8
C_5-C_{11} Hydrocarbons	34.9	31.4	38.1	40.0	34.7	34.0
C_{12}+ Hydrocarbons	110.	112.	93.3	102.	91.3	96.0
Wax[d]	105.	103.	89.3	92.5	85.0	92.0
Oxygenates	10.5	9.79	8.78	10.5	9.61	10.3
Total	193.	190.	186.	197.	181.	188.
1+2 Olefins/*n*-Paraffin Ratio						
C_2	2.92	3.14	2.45	2.22	2.13	1.97
C_3	6.72	6.50	7.86	5.73	6.03	5.11
C_4	5.46	5.27	6.51	4.07	5.52	4.28
C_8	3.77	3.28	4.21	2.78	3.60	2.65
C_{10}	3.58	3.13	4.00	3.36	3.35	2.62

[a] Based on unreduced catalyst
[b] Maximum axial temperature difference
[c] Based on reactor volume
[d] Unanalyzed products collected from hot trap

Table 4 (cont'd). Summary of results for fixed bed run FA-76-0068.

Period	1	2	3	4	5	6
Weight % of Hydrocarbons						
CH_4	3.72	3.74	4.84	4.03	5.02	4.93
Ethane	1.32	1.40	1.93	2.50	2.48	2.52
Ethylene	3.61	4.10	4.41	5.36	4.94	4.63
Propane	.837	.833	.911	.946	1.03	1.34
Propylene	5.36	5.17	6.83	5.17	6.49	6.54
n-Butane	.804	.811	.865	.891	.953	1.21
1+2 Butenes	4.24	4.13	5.44	4.01	5.08	5.00
C_4 Isomers	.469	.465	.569	.470	.553	.610
n-Pentane	1.18	1.20	1.49	1.24	1.37	1.57
1+2 Pentenes	3.83	3.91	5.36	3.69	5.02	4.70
C_5 Isomers	.259	.296	.444	.278	.540	.452
n-Hexane	.591	.696	.617	1.28	.708	1.01
1+2 Hexenes	2.39	2.75	2.70	4.16	3.14	3.00
C_6 Isomers	.540	.687	.660	1.04	.830	.800
n-Heptane	.422	.413	.404	.934	.473	.696
1+2 Heptenes	1.61	1.62	1.76	2.63	1.76	1.88
C_7 Isomers	.356	.572	.401	.750	.557	.533
n-Octane	.360	.274	.334	.395	.274	.393
1+2 Octenes	1.35	.882	1.38	1.08	.969	1.02
C_8 Isomers	.216	.0811	.208	.163	.233	.236
n-Nonane	.384	.244	.345	.209	.242	.203
1+2 Nonenes	1.36	.703	1.39	.663	.773	.481
C_9 Isomers	.286	.122	.246	.0545	.113	.0864
n-Decane	.302	.306	.338	.328	.325	.255
1+2 Decenes	1.38	.945	1.33	1.09	1.07	.659
C_{10} Isomers	.393	.212	.398	.126	.207	.157
n-Undecane	.334	.314	.276	.325	.299	.220
1+2 Undecenes	1.14	.931	1.04	1.17	1.04	.651
C_{11} Isomers	.367	.243	.270	.187	.204	.149
C_2-C_4	16.6	16.9	21.0	19.4	21.5	21.9
C_5-C_{11}	19.2	17.4	21.5	21.8	20.2	19.2
C_{12}+	60.5	61.9	52.7	54.7	53.2	54.1
Wax[d]	57.4	57.4	50.4	40.6	49.5	51.8

[d] Unanalyzed products collected from hot trap

Table 5. Summary of results for fixed bed run FA-31-1118.

Catalyst: 3.40 g^a, 100 Fe/5 Cu/4.2 K
Catalyst volume: 3.00 cc

Diluent: 30.0 g, Glass beads
Diluent Volume: 24.0 cc

Period	1	2	3	4	5	6
Date	4/22/88	4/23/88	4/24/88	4/25/88	4/26/88	4/27/88
Time on Stream (h)	47.5	71.5	94.5	110.8	143.7	168.5
Balance Duration (h)	6.0	5.5	6.0	6.0	6.0	5.5
Average Temperature (°C)	235.	235.	250.	220.	235.	235.
Maximum Δ Temperature (°C)[b]	4.50	3.60	5.00	2.90	1.30	3.80
Pressure (MPa)	1.48	1.48	1.48	1.48	1.48	3.00
H_2/CO Feed Ratio	1.03	1.03	1.03	1.03	1.03	1.03
Space Velocity ($Nl/g\text{-}cat\cdot h$)[a]	2.00	3.99	3.99	1.99	1.99	3.99
Space Velocity ($Nl/g\text{-}Fe\cdot h$)	3.00	6.15	6.15	3.08	3.08	6.15
GHSV (h^{-1})[c]	252.	502.	502.	251.	251.	502.
CO Conversion (%)	93.6	85.6	78.8	37.3	54.7	55.6
H_2+CO Conversion (%)	78.3	54.8	65.4	33.0	47.2	51.3
H_2/CO Usage	.697	.694	.685	.795	.749	.873
STY ($mols\ H_2+CO/g\text{-}cat\cdot h$)[a]	.070	.097	.110	.029	.042	.001
$P_{CO_2}\cdot P_{H_2}/P_{CO}\cdot P_{H_2O}$	34.8	6.83	8.25	2.77	4.18	3.18
Weight % of Outlet						
H_2	2.62	3.86	3.28	5.03	4.21	3.73
H_2O	4.41	4.34	5.07	3.96	4.67	5.26
CO	6.18	32.2	10.8	59.9	42.9	42.4
CO_2	63.8	43.5	52.3	22.9	34.9	33.6
Hydrocarbons	11.3	6.94	9.15	4.30	7.09	6.98
Oxygenates	1.50	1.02	1.32	.578	1.03	.759
Wax[d]	10.2	8.09	8.10	3.30	5.25	7.34
Yield ($g/Nm^3\ H_2 + CO\ Converted$)						
CH_4	11.1	8.73	10.0	8.52	10.2	8.32
C_2–C_4 Hydrocarbons	38.2	34.6	39.1	35.2	40.2	41.6
C_5–C_{11} Hydrocarbons	38.9	34.7	38.5	34.7	41.6	35.0
C_{12}+ Hydrocarbons	86.8	102.	87.4	71.0	78.4	95.2
Wax[d]	83.1	97.1	82.7	64.4	72.5	92.3
Oxygenates	12.2	12.2	13.4	11.3	14.2	9.55
Total	187.	193.	188.	161.	185.	190.
1+2 Olefins/n-Paraffin Ratio						
C_2	1.86	2.51	2.19	1.91	1.62	1.94
C_3	6.34	6.32	7.05	5.36	6.17	4.50
C_4	5.19	5.18	5.87	4.46	5.22	3.56
C_8	3.75	3.50	3.04	3.08	3.51	3.08
C_{10}	3.50	3.50	3.86	2.87	3.19	3.26

[a] Based on unreduced catalyst
[b] Maximum axial temperature difference
[c] Based on reactor volume
[d] Unanalyzed products collected from hot trap

Table 5 (cont'd). Summary of results for fixed bed run FA-31-1118.

Period	1	2	3	4	5	6
Weight % of Hydrocarbons						
CH_4	6.37	4.84	5.74	5.70	5.96	4.02
Ethane	2.48	1.89	2.24	3.04	3.11	2.44
Ethylene	4.30	4.43	4.56	5.42	4.68	4.41
Propane	1.16	.982	1.06	1.33	1.24	1.55
Propylene	7.00	5.02	7.13	6.79	7.20	6.80
n-Butane	1.05	.908	1.01	1.21	1.10	1.58
1+2 Butenes	5.27	4.54	5.70	5.21	5.56	5.44
C_4 Isomers	.572	.511	.643	.600	.599	.862
n-Pentane	1.41	1.25	1.44	1.61	1.55	1.58
1+2 Pentenes	5.13	4.77	5.35	6.07	5.93	5.10
C_5 Isomers	.434	.477	.420	.703	.608	.588
n-Hexane	.753	.738	.670	1.34	.919	.953
1+2 Hexenes	2.94	2.80	3.15	3.76	3.37	2.86
C_6 Isomers	.563	.570	.691	.755	.720	.642
n- Heptane	.517	.488	.509	.839	.594	.577
1+2 Heptenes	1.96	1.70	2.09	2.23	2.15	1.63
C_7 Isomers	.370	.401	.494	.576	.578	.424
n-Octane	.410	.334	.381	.342	.410	.301
1+2 Octenes	1.51	1.15	1.36	1.04	1.41	.909
C_8 Isomers	.244	.195	.288	.176	.261	.147
n-Nonane	.415	.260	.310	.183	.300	.275
1+2 Nonenes	1.44	.870	1.16	.493	1.24	.844
C_9 Isomers	.354	.198	.333	.0745	.236	.0972
n-Decane	.388	.283	.309	.316	.445	.296
1+2 Decenes	1.34	.979	1.18	.892	1.40	.952
C_{10} Isomers	.392	.271	.376	.181	.342	.148
n-Undecane	.310	.257	.262	.340	.399	.227
1+2 Undecenes	1.02	.884	.981	1.01	1.20	.761
C_{11} Isomers	.301	.249	.270	.202	.277	.139
C_2-C_4	21.8	19.2	22.3	23.6	23.6	23.1
C_5-C_{11}	22.2	19.2	22.0	23.2	24.4	19.5
C_{12}+	49.6	56.8	49.9	47.5	46.0	52.8
Wax[d]	47.5	53.8	47.2	43.1	42.5	51.3

[d] Unanalyzed products collected from hot trap

Table 6. Summary of Binder/Support catalyst tests.

Catalyst	Run	Bal	TOS (h)	Conditions T (°C)	P (MPa)	SV[a]	H_2/CO	STY[b]	% Conversion CO	H_2+CO	Usage	Wt % Hydrocarbons CH_4	C_2-C_4	C_5-C_{11}	$C_{12}+$
100 Fe/5 Cu/4.2 K	FA-31-1118	1	47.5	235	1.48	2.00	1.03	0.070	93.6	78.3	0.70	6.4	21.8	22.2	49.6
		2	71.5	235	1.48	3.99	1.03	0.097	65.6	54.8	0.69	4.8	19.2	19.2	56.8
		3	94.5	250	1.48	3.00	1.03	0.110	78.8	65.4	0.69	5.8	22.3	22.0	49.9
		4[c]	119.8	220	1.48	1.99	1.03	0.020	37.3	33.0	0.80	5.7	23.6	23.2	47.5
		5[c]	143.7	235	1.48	1.99	1.03	0.042	54.7	47.2	0.75	6.0	23.6	24.4	46.0
		6[c]	168.5	235	3.00	3.99	1.03	0.091	55.6	51.3	0.87	4.6	23.1	19.5	52.8
100 Fe/5 Cu/4.2 K/8 SiO_2	FA-63-0418	1	48.0	235	1.48	2.00	1.10	0.069	93.8	76.7	0.71	3.5	16.4	20.1	60.0
		2	72.0	235	1.48	4.01	1.10	0.094	64.5	52.8	0.71	3.2	16.9	20.3	59.6
		3	96.0	250	1.48	4.01	1.10	0.116	80.5	65.1	0.70	3.7	16.0	12.4	67.9
		4	121.0	220	1.48	2.00	1.10	0.055	73.6	62.1	0.77	2.8	16.0	15.4	65.8
		5[c]	145.0	235	3.00	4.01	1.10	0.076	46.4	42.7	0.93	2.8	17.5	16.7	63.0
		6[c]	169.0	235	1.48	2.00	1.10	0.040	52.9	44.8	0.78	3.4	18.8	16.5	61.3
100 Fe/5 Cu/4.2 K/25 SiO_2	FA-66-0548	1	48.0	234	1.48	2.00	1.00	0.049	59.0	55.0	0.85	5.7	22.7	15.2	56.4
		2	72.5	235	1.48	4.01	1.00	0.069	39.4	38.5	0.95	5.0	22.4	17.7	54.9
		3	95.5	250	1.48	2.01	1.00	0.061	78.2	67.6	0.73	8.1	30.0	19.9	42.0
		4	120.0	220	1.48	2.01	1.00	0.028	20.7	31.1	1.09	4.8	23.2	20.7	51.3
		5	144.5	235	2.96	4.01	1.00	0.086	49.5	48.1	0.94	4.0	22.8	16.5	57.7
100 Fe/5 Cu/4.2 K/100 SiO_2	FA-69-0668	1	48.5	234	1.48	1.00	1.00	0.026	24.3	20.1	1.39	5.2	17.2	20.4	57.2
		2	72.0	235	1.48	3.99	1.00	0.039	17.5	22.0	1.61	4.4	14.9	16.5	64.2
		3	96.0	250	1.48	1.99	1.00	0.031	30.8	35.2	1.29	5.8	18.6	25.9	49.7
		4	119.0	220	1.48	2.01	1.00	0.014	11.3	15.8	1.79	4.5	15.8	18.3	61.4
		5	143.0	235	1.48	1.99	1.00	0.023	20.1	26.7	1.56	5.2	16.8	18.5	59.5
		6	169.0	235	2.96	3.99	1.00	0.052	22.4	29.4	1.63	4.5	15.6	15.5	64.4
100 Fe/5 Cu/4.2 K/8 Al_2O_3	FA-73-0828	1	47.5	235	1.48	2.01	1.00	0.067	90.3	75.1	0.66	4.8	18.4	19.3	57.5
		2	72.0	234	1.48	4.02	1.00	0.084	56.0	47.0	0.68	4.2	17.4	18.4	60.0
		3	96.0	250	1.48	4.02	1.00	0.104	69.8	57.8	0.66	4.9	19.2	20.2	55.7
		4	118.5	220	1.48	2.01	1.00	0.028	36.9	31.7	0.72	4.1	17.0	18.9	59.1
		5[c]	143.5	235	1.48	2.01	1.00	0.038	50.8	42.9	0.69	4.0	19.6	18.3	57.2
		6[c]	168.0	235	2.96	4.01	1.00	0.071	42.2	40.0	0.90	4.6	21.9	19.3	54.2
100 Fe/5 Cu/4.2 K/20 Al_2O_3	FA-76-0968	1	47.5	235	1.48	2.03	1.00	0.062	82.2	68.3	0.66	3.6	16.7	19.2	60.5
		2	71.8	235	1.48	4.03	1.00	0.063	41.2	35.3	0.71	3.7	16.9	17.4	62.0
		3	95.5	250	1.48	2.03	1.00	0.066	88.8	73.4	0.65	4.8	21.0	21.5	52.7
		4	120.0	220	1.48	2.03	1.00	0.020	24.7	22.1	0.79	4.0	19.5	21.8	54.7
		5[c]	143.5	235	1.48	2.03	1.00	0.028	37.1	31.5	0.70	5.1	21.5	20.2	53.2
		6[c]	168.0	235	3.00	4.03	1.00	0.055	33.0	30.5	0.87	4.8	21.9	19.2	54.1
Ruhrchemie LP 33/81 (100 Fe/5 Cu/4.2 K/24 SiO_2)	FB-90-1348	2	48.0	235	1.48	4.06	0.98	0.061	30.6	33.8	1.18	3.8	14.5	17.1	64.6
		3	96.0	234	1.48	1.99	0.98	0.044	46.9	49.1	1.07	4.3	17.6	17.0	61.1
		4	120.0	250	1.48	1.99	0.98	0.054	64.5	60.3	0.85	5.3	20.8	19.2	54.7
		5[c]	144.0	220	1.48	1.99	0.98	0.023	22.9	25.9	1.24	4.7	18.8	19.6	56.9
		6[c]	168.5	235	2.96	3.99	0.98	0.065	33.4	36.7	1.17	3.9	17.1	16.1	62.9

[a]Space Velocity (SV) [=] $Nl/g\text{-cat}\cdot h$

[b]Space Time Yield (STY) [=] $mols(H_2 + CO)/g\text{-cat}\cdot h$

[c]Balance made with partially deactivated catalyst

Table 7. Fractional metal exposures for selected H_2 and CO reduced cataltysts.

	Fractional Metal Exposures	
	Reductant	
Nominal Catalyst Composition	H_2	CO
100 Fe	0.036	0.064
100 Fe/1 Cu	0.015	—
100 Fe/3 Cu	0.022	0.077
100 Fe/0.2 K	0.035	—
100 Fe/2 K	0.035	0.020
100 Fe/1 Cu/0.05 K	0.020	0.023
100 Fe/1 Cu/0.2 K	0.020	0.023
100 Fe/5 Cu/4.2 K	0.022	0.023
100 Fe/5 Cu/4.2 K/8 SiO_2	0.034	0.022
100 Fe/5 Cu/4.2 K/25 SiO_2	0.036	0.021
100 Fe/5 Cu/4.2 K/8 Al_2O_3	0.023	0.040
100 Fe/5 Cu/4.2 K/25 Al_2O_3	0.022	0.051

Table 8. Major events occurring in run SA-99-0888.

TOS (h)	Event
− 17	Catalyst pretreatment: CO, 280 °C, 0.79 MPa, 16 h.
0	Initiated synthesis gas.
4.0	Achieved desired operating conditions: 250 °C, 1.48 MPa, (H_2/CO) = 0.67, 2.0 Nl/g-cat·h
49.0	Conditions stable, (H_2+CO) conversion = 45.9 %.
94.5	Conditions stable, (H_2+CO) conversion = 46.1 %.
166.5	Conditions stable, (H_2+CO) conversion = 43.1 %.
264.0	Conditions stable, (H_2+CO) conversion = 43.8 %.
336.0	Conditions stable, (H_2+CO) conversion = 44.4 %.
343.0	Changed process conditions: 250 °C, 1.48 MPa, (H_2/CO) = 0.67, 4.0 Nl/g-cat·h
391.0	Changed process conditions: 250 °C, 1.48 MPa, (H_2/CO) = 0.65, 1.0 Nl/g-cat·h
439.0	Changed process conditions: 235 °C, 1.48 MPa, (H_2/CO) = 0.65, 2.0 Nl/g-cat·h
488.0	Changed process conditions: 235 °C, 1.48 MPa, (H_2/CO) = 0.67, 1.0 Nl/g-cat·h
531.0	Changed process conditions: 265 °C, 1.48 MPa, (H_2/CO) = 0.67, 2.0 Nl/g-cat·h
584.0	Changed process conditions: 250 °C, 1.48 MPa, (H_2/CO) = 0.67, 2.0 Nl/g-cat·h
619.0	Replication of initial process conditions: (H_2+CO) conversion = 36.0 %.
627.0	Changed process conditions: 250 °C, 1.48 MPa, (H_2/CO) = 1.0, 2.0 Nl/g-cat·h
699.0	Changed process conditions: 250 °C, 2.96 MPa, (H_2/CO) = 1.0, 4.0 Nl/g-cat·h
721.5	Voluntary termination of run SA-99-0888.

Table 9. Wax and solids inventory for run SA-99-0888.

TOS (*h*)	Description
− 42	Reactor charged with 301 *g*-wax, 34.6 *g*-cat
− 1	5.2 *g*-wax, 0 *g*-cat removed after reduction
101	269 *g*-wax, 1.5 *g*-cat removed
173	176 *g*-wax, 0.3 *g*-cat removed
266	231 *g*-wax, 0.1 *g*-cat removed
342	168 *g*-wax, 0.5 *g*-cat removed
390	101 *g*-wax, 0.4 *g*-cat removed
438	49 *g*-wax, 0.2 *g*-cat removed
488	27 *g*-wax, 0.1 *g*-cat removed
534	23 *g*-wax, 0.1 *g*-cat removed
577	61 *g*-wax, 0.3 *g*-cat removed
607	47 *g*-wax, 0.3 *g*-cat removed
650	36 *g*-wax, 0.2 *g*-cat removed
722	69 *g*-wax, 0.4 *g*-cat removed
722	315 *g*-wax, 24.4 *g*-cat removed at end of run, 106 % wax recovery, 83 % solids recovery

Table 10. Summary of results for slurry run SA-00-0888.

Catalyst: 34.0 g[a], LP 33/81 Slurry liquid: 270 g, Purified n-octacosane

Reactor volume: 385 cc[b]

Period	1	2	3	4	5	6	7
Date	3/30/88	4/1/88	4/4/88	4/7/88	4/10/88	4/13/88	4/15/88
Time on Stream (*h*)	49.0	94.5	166.5	264.0	336.0	386.0	385.0
Balance Duration (*h*)	7.0	6.0	6.0	6.0	6.0	6.0	6.0
Average Temperature (°C)	250.	250.	250.	250.	250.	250.	250.
Pressure (*MPa*)	1.48	1.48	1.48	1.48	1.48	1.48	1.48
H_2/CO Feed Ratio	.667	.667	.667	.667	.667	.667	.652
Space Velocity (*Nl/g-cat·h*)[a]	2.00	2.00	2.00	2.00	2.01	4.00	1.00
Space Velocity (*Nl/g-Fe·h*)	3.81	3.81	3.81	3.81	3.82	7.62	1.91
GHSV (h^{-1})[b]	180.	180.	172.	171.	171.	336.	82.9
CO Conversion (%)	42.7	43.2	41.2	41.1	40.4	25.7	56.0
H_2+CO Conversion (%)	45.0	46.1	43.1	43.8	44.4	28.3	56.1
H_2/CO Usage	.790	.770	.740	.774	.835	.835	.655
STY (*mols* H_2+CO/*g-cat·h*)[a]	.041	.041	.038	.030	.040	.050	.025
$P_{CO_2} \cdot P_{H_2}/P_{CO} \cdot P_{H_2O}$	1.21	1.26	1.19	1.35	1.20	.706	2.54
Weight % of Outlet							
H_2	2.33	2.34	2.52	2.45	2.28	3.21	2.01
H_2O	4.86	4.86	5.13	4.31	4.48	4.16	3.69
CO	56.3	55.8	56.0	57.7	57.2	73.2	43.1
CO_2	25.0	25.7	24.2	24.0	23.7	11.8	35.4
Hydrocarbons	5.85	5.03	5.81	6.18	7.34	5.23	10.0
Oxygenates	.505	.407	.552	.643	.366	.252	.676
Wax[c]	5.24	5.24	4.83	4.78	4.61	2.14	4.23
Yield (*g/Nm³ H_2 + CO Converted*)							
CH_4	7.86	8.33	9.73	9.86	9.67	10.5	12.0
C_2-C_4 Hydrocarbons	32.9	37.5	30.7	42.8	44.9	43.6	55.3
C_5-C_{11} Hydrocarbons	40.7	35.0	41.9	43.8	62.0	61.0	67.4
C_{12}+ Hydrocarbons	103.	98.8	99.8	95.3	93.8	82.8	72.9
Wax[c]	87.1	86.6	86.8	83.6	81.1	57.6	58.2
Oxygenates	6.40	6.72	9.02	11.2	6.44	6.79	9.30
Total	193.	186.	201.	203.	217.	205.	217.
1+2 Olefins/n-Paraffin Ratio							
C_2	1.82	1.68	1.64	1.52	1.45	2.21	.843
C_3	7.51	6.61	7.33	7.02	6.91	7.32	5.73
C_4	6.21	5.61	5.96	5.82	5.58	6.00	4.07
C_8	3.32	3.30	2.89	2.95	2.85	3.39	2.28
C_{10}	2.80	2.77	2.63	2.44	2.36	2.78	1.85

[a] Based on unreduced catalyst [b] Based on static slurry volume

[c] Unanalyzed wax withdrawn from reactor

Table 10 (cont'd). Summary of results for slurry run SA-99-0888.

Period	8	9	10	11	12	13
Date	4/17/88	4/19/88	4/21/88	4/23/88	4/25/88	4/27/88
Time on Stream (h)	451.5	528.0	571.0	619.0	667.5	715.5
Balance Duration (h)	6.0	6.0	6.0	6.0	6.0	6.0
Average Temperature (°C)	245.	235.	265.	250.	250.	250.
Pressure (MPa)	1.48	1.48	1.48	1.48	1.48	2.96
H_2/CO Feed Ratio	.652	.667	.667	.669	1.00	1.02
Space Velocity ($Nl/g\text{-cat}\cdot h$)[a]	2.01	1.00	2.00	2.02	2.02	4.03
Space Velocity ($Nl/g\text{-Fe}\cdot h$)	3.83	1.91	3.82	3.85	3.85	7.68
GHSV (h^{-1})[b]	165.	82.3	164.	163.	162.	321.
CO Conversion (%)	18.8	30.6	57.3	32.8	48.5	36.6
H_2+CO Conversion (%)	23.0	35.8	56.9	35.0	45.4	30.8
H_2/CO Usage	1.01	.946	.653	.829	.869	1.20
STY ($mols\ H_2+CO/g\text{-cat}\cdot h$)[a]	.021	.016	.051	.032	.041	.071
$P_{CO_2}\cdot P_{H_2}/P_{CO}\cdot P_{H_2O}$	.418	.706	4.38	1.13	1.05	.590
Weight % of Outlet						
H_2	3.23	2.60	2.06	2.80	4.04	4.11
H_2O	4.20	5.19	2.52	3.07	6.35	8.53
CO	78.9	66.6	41.9	65.7	50.0	62.2
CO_2	7.66	16.5	30.4	18.5	27.0	13.4
Hydrocarbons	4.54	6.65	11.0	6.53	10.0	9.01
Oxygenates	.318	.479	.420	.527	.070	.835
Wax[c]	1.10	2.02	2.03	2.05	1.90	1.91
Yield ($g/Nm^3\ H_2+CO\ Converted$)						
CH_4	11.1	10.7	15.0	12.8	15.8	11.6
C_2-C_4 Hydrocarbons	57.4	51.1	54.0	52.6	58.3	50.8
C_5-C_{11} Hydrocarbons	70.8	67.9	64.9	59.8	56.1	60.4
C_{12}+ Hydrocarbons	51.8	59.6	40.6	57.6	39.0	50.3
Wax[c]	37.3	44.1	35.3	43.6	27.0	30.3
Oxygenates	10.8	10.5	5.73	11.2	9.49	13.2
Total	202.	200.	189.	194.	179.	186.
1+2 Olefins/n-Paraffin Ratio						
C_2	2.19	1.70	.700	1.47	.865	1.44
C_3	6.61	6.58	5.12	6.59	4.85	4.62
C_4	5.33	5.01	4.08	5.43	4.16	3.81
C_8	2.98	2.85	2.23	2.53	2.13	2.50
C_{10}	2.30	2.34	1.71	2.05	1.03	1.92

[a] Based on unreduced catalyst [b] Based on static slurry volume
[c] Unanalyzed wax withdrawn from reactor

Table 10 (cont'd). Summary of results for slurry run SA-00-0888.

Period	1	2	3	4	5	6	7
Weight % of Hydrocarbons							
CH_4	4.26	4.64	5.00	5.14	4.60	5.30	5.78
Ethane	1.89	2.30	2.46	2.66	2.60	1.07	4.51
Ethylene	3.22	3.70	3.76	3.78	3.62	4.00	3.55
Propane	.700	1.00	.950	1.06	.990	1.02	1.56
Propylene	5.73	6.33	6.71	7.08	6.57	7.14	8.54
n-Butane	.818	1.06	.943	1.09	1.09	1.07	1.35
1+2 Butenes	4.90	5.70	5.42	6.10	5.86	6.17	6.47
C_4 Isomers	.480	.652	.533	.556	.511	.522	.652
n-Pentane	1.18	1.22	1.28	1.49	1.30	1.41	1.70
1+2 Pentenes	4.46	4.61	4.62	5.45	5.12	5.41	5.50
C_5 Isomers	.297	.310	.351	.431	.410	.326	.801
n-Hexane	.881	.580	1.12	.944	1.34	1.00	1.40
1+2 Hexenes	2.64	1.91	2.02	2.75	4.02	3.96	3.94
C_6 Isomers	.506	.446	.473	.415	.549	.580	.627
n-Heptane	.537	.446	.394	.502	1.00	1.01	1.26
1+2 Heptenes	1.74	1.35	1.62	1.69	2.71	2.97	2.75
C_7 Isomers	.333	.281	.367	.250	.383	.459	.442
n-Octane	.478	.357	.459	.477	.816	.703	1.09
1+2 Octenes	1.56	1.19	1.30	1.38	2.29	2.54	2.44
C_8 Isomers	.242	.111	.558	.159	.281	.230	.419
n-Nonane	.452	.430	.438	.498	.745	.707	1.05
1+2 Nonenes	1.46	1.35	1.28	1.34	2.02	2.28	2.16
C_9 Isomers	.0022	.166	.252	.168	.208	.209	.376
n-Decane	.630	.573	.505	.628	.870	.883	1.05
1+2 Decenes	1.77	1.57	1.46	1.51	2.02	2.42	1.90
C_{10} Isomers	.135	.149	.335	.232	.301	.257	.457
n-Undecane	.721	.654	.637	.687	.878	.946	1.02
1+2 Undecenes	1.78	1.56	1.43	1.42	1.73	2.22	1.58
C_{11} Isomers	.196	.204	.362	.308	.315	.348	.420
C_3-C_4	17.8	20.9	20.8	22.3	21.3	22.0	20.6
C_5-C_{11}	22.1	19.5	21.9	22.8	29.5	31.0	32.5
C_{12}+	55.8	55.0	52.2	49.7	44.6	41.7	35.1
Wax[c]	47.2	48.2	45.4	43.6	38.6	29.0	28.1

[c] Unanalyzed wax withdrawn from reactor

Table 10 (cont'd). Summary of results for slurry run SA-09-0888.

Period	8	9	10	11	12	13
Weight % of Hydrocarbons						
CH_4	5.83	5.03	8.15	7.00	9.35	6.68
Ethane	3.30	3.31	5.35	3.86	5.78	3.82
Ethylene	6.03	5.26	3.50	5.29	4.66	5.15
Propane	1.42	1.34	1.87	1.42	2.28	2.01
Propylene	8.03	8.38	9.14	8.04	10.5	8.86
n-Butane	1.42	1.38	1.61	1.38	2.07	1.87
1+2 Butenes	7.30	6.70	7.28	7.23	8.31	6.87
C_4 Isomers	.664	.637	.681	.603	.841	.752
n-Pentane	1.85	1.69	2.17	1.92	2.45	2.13
1+2 Pentenes	8.32	6.53	6.58	7.54	7.23	6.80
C_5 Isomers	.078	.670	1.14	.880	1.02	.823
n-Hexane	2.80	1.76	1.70	1.57	1.66	1.53
1+2 Hexenes	5.03	4.24	3.63	4.43	4.07	4.86
C_6 Isomers	.903	.694	.787	.803	.784	.852
n-Heptane	1.05	1.53	1.43	1.06	1.14	1.15
1+2 Heptenes	2.85	3.07	2.52	2.67	2.41	3.02
C_7 Isomers	1.03	.442	.679	.647	.515	.626
n-Octane	.724	1.04	1.05	.770	.804	.902
1+2 Octenes	2.12	2.92	2.29	1.93	1.87	2.36
C_8 Isomers	.283	.288	.507	.334	.303	.398
n-Nonane	.698	.911	1.06	.643	.848	.860
1+2 Nonenes	1.88	2.46	2.03	1.47	1.52	1.82
C_9 Isomers	.280	.310	.535	.256	.383	.308
n-Decane	.809	1.03	1.18	.806	1.000	.983
1+2 Decenes	1.01	2.38	1.98	1.63	1.60	1.86
C_{10} Isomers	.473	.409	.648	.386	.463	.385
n-Undecane	.823	1.05	1.10	.880	1.02	1.04
1+2 Undecenes	1.66	2.01	1.68	1.52	1.39	1.71
C_{11} Isomers	.488	.418	.624	.459	.509	.437
C_2-C_4	30.0	27.0	29.4	28.8	34.5	29.3
C_5-C_{11}	37.0	35.0	35.4	32.7	33.2	34.9
C_{12}+	27.1	31.5	27.0	31.5	23.0	29.1
Wax[c]	19.5	23.3	19.2	23.0	15.0	17.5

[c] Unanalyzed wax withdrawn from reactor

Table 11. Summary of results for fixed bed run FA-63-1308.

Catalyst: 3.40 g^a, 100 Fe/5 Cu/4.2 K/8 SiO2
Catalyst volume: 3.60 cc

Diluent: 35.1 g, Glass beads
Diluent Volume: 23.0 cc

Period	1	2	3	4	5	6	7	8
Date	5/11	5/15	5/19	5/23	5/27	5/31	6/3	6/6/88
Time on Stream (h)	48.0	144.0	240.0	336.5	432.0	528.0	600.0	662.0
Balance Duration (h)	6.0	6.0	6.0	6.0	6.5	7.5	6.5	7.2
Average Temperature (°C)	235.	235.	235.	235.	235.	235.	250.	235.
Maximum Δ Temperature (°C)[b]	2.30	1.50	1.40	2.00	1.40	1.50	1.50	2.40
Pressure (MPa)	1.48	1.48	1.48	1.48	1.48	1.48	1.48	1.48
H_2/CO Feed Ratio	1.03	1.03	1.03	.689	.689	.689	.689	1.03
Space Velocity (Nl/g-cat·h)[a]	1.09	1.09	1.09	1.09	1.09	1.09	1.09	1.09
Space Velocity (Nl/g-Fe·h)	3.24	3.24	3.24	3.24	3.24	3.24	3.24	3.24
GHSV (h^{-1})[c]	251.	251.	251.	251.	251.	251.	251.	251.
CO Conversion (%)	94.6	87.5	68.1	48.6	43.7	41.2	48.7	37.1
H_2+CO Conversion (%)	77.9	71.8	56.0	46.0	42.1	40.1	46.4	31.7
H_2/CO Usage	.660	.664	.693	.598	.630	.647	.609	.740
STY ($mols$ H_2+CO/g-cat·h)[a]	.069	.064	.051	.041	.037	.036	.041	.028
$P_{CO_2} \cdot P_{H_2}/P_{CO} \cdot P_{H_2O}$	34.1	13.7	6.63	4.52	3.71	3.56	4.48	2.99
Weight % of Outlet								
H_2	2.70	3.04	3.76	2.75	2.88	2.92	2.71	5.11
H_2O	5.53	6.01	4.60	2.20	2.34	2.32	2.36	3.71
CO	5.11	11.8	20.0	49.3	54.4	56.5	49.1	59.0
CO_2	62.7	55.8	43.6	32.6	28.9	28.1	33.8	22.5
Hydrocarbons	15.0	15.6	11.2	8.10	7.20	6.80	8.00	6.05
Oxygenates	1.33	1.58	1.11	.519	.427	.346	.416	.002
Wax[d]	7.58	6.17	5.75	4.39	3.84	2.96	2.97	2.10
Yield (g/Nm^3 H_2 + CO $Converted$)								
CH_4	8.01	6.91	7.88	6.67	7.46	8.10	12.0	13.1
C_2–C_4 Hydrocarbons	33.6	32.4	32.4	27.4	29.4	30.3	38.3	40.2
C_5–C_{11} Hydrocarbons	40.3	38.7	36.8	34.5	31.2	27.3	30.0	33.9
C_{12}+ Hydrocarbons	106.	120.	118.	141.	133.	123.	113.	94.1
Wax[d]	63.1	56.1	66.4	73.6	69.8	56.8	49.6	43.4
Oxygenates	11.1	14.3	12.9	8.70	7.70	6.64	8.93	12.5
Total	199.	212.	208.	218.	208.	195.	200.	200.
1+2 Olefins/n-Paraffin Ratio								
C_2	2.68	2.84	2.70	2.50	2.27	2.08	1.62	1.94
C_3	6.49	6.59	6.44	7.52	7.35	7.40	7.78	6.28
C_4	5.23	5.28	5.28	6.17	6.05	6.12	6.56	5.16
C_6	5.00	4.17	3.72	4.62	5.59	4.20	4.08	3.86
C_{10}	3.99	3.33	3.35	3.79	3.87	3.48	2.91	2.92

[a] Based on unreduced catalyst
[b] Maximum axial temperature difference
[c] Based on reactor volume
[d] Unrecovered products from wax analysis

Table 11 (cont'd). Summary of results for fixed bed run FA-63-1308.

Period	1	2	3	4	5	6	7	8
Weight % of Hydrocarbons								
CH_4	4.25	3.40	4.03	3.10	3.72	4.34	6.19	6.00
Ethane	1.48	1.33	1.49	1.24	1.55	1.78	2.74	2.04
Ethylene	3.71	3.53	3.73	2.09	3.27	3.45	4.14	5.32
Propane	.940	.847	.869	.501	.674	.739	.873	1.30
Propylene	5.82	5.32	5.35	4.24	4.73	5.21	6.48	7.80
n-Butane	.896	.790	.773	.533	.507	.655	.700	1.12
1+2 Butenes	4.52	4.07	3.94	3.18	3.40	3.87	4.49	5.60
C_4 Isomers	.471	.432	.414	.309	.342	.375	.436	.575
n-Pentane	1.23	1.10	1.05	.779	.810	.937	1.03	1.42
1+2 Pentenes	4.00	3.57	3.39	2.74	2.93	3.27	3.59	4.41
C_5 Isomers	.270	.249	.240	.167	.185	.210	.235	.356
n-Hexane	.552	.454	.433	.458	.362	.477	.415	.674
1+2 Hexenes	2.29	1.97	2.17	1.73	1.76	1.92	1.91	2.32
C_6 Isomers	.448	.381	.463	.390	.416	.464	.504	.555
n-Heptane	.373	.347	.480	.328	.231	.299	.247	.414
1+2 Heptenes	1.75	1.52	1.46	1.28	1.28	1.20	1.18	1.43
C_7 Isomers	.267	.235	.304	.270	.205	.252	.299	.272
n-Octane	.366	.307	.376	.255	.189	.194	.182	.223
1+2 Octenes	1.80	1.62	1.37	1.16	1.04	.800	.888	.847
C_8 Isomers	.250	.130	.164	.0542	.0987	.0371	.0651	.0980
n-Nonane	.462	.457	.415	.326	.282	.214	.212	.241
1+2 Nonenes	2.02	1.70	1.46	1.38	1.17	.839	.883	.822
C_9 Isomers	.154	.197	.147	.110	.0802	.0760	.106	.0837
n-Decane	.522	.561	.504	.475	.412	.321	.424	.437
1+2 Decenes	2.05	1.84	1.67	1.77	1.57	1.10	1.22	1.26
C_{10} Isomers	.290	.365	.257	.267	.215	.190	.243	.184
n-Undecane	.422	.517	.489	.479	.452	.348	.390	.442
1+2 Undecenes	1.65	1.69	1.57	1.79	1.65	1.14	1.32	1.36
C_{11} Isomers	.232	.222	.223	.243	.205	.210	.222	.264
C_2-C_4	17.8	16.3	16.6	13.1	14.7	16.1	19.9	24.7
C_5-C_{11}	21.4	19.5	18.8	16.5	15.5	14.5	15.6	18.1
C_{12}+	56.5	60.7	60.6	67.3	66.1	65.1	58.4	50.2
Wax[d]	33.5	28.3	34.0	35.2	34.8	30.1	25.7	23.2

[d] Unrecovered products from wax analysis

Table 12. Summary of results for fixed bed run FB-09-1588.

Catalyst: 3.40 g[a], Ruhrchemie LP 33/81
Catalyst volume: 5.40 cc

Diluent: 35.6 g, Glass beads
Diluent Volume: 23.0 cc

Period	1	2	3	4	5	6	7
Date	6/9/88	6/13/88	6/17/88	6/21/88	6/25/88	6/28/88	7/2/88
Time on Stream (h)	71.0	167.0	262.5	300.0	426.5	528.0	622.5
Balance Duration (h)	7.0	7.2	7.0	6.8	7.0	7.1	7.5
Average Temperature (°C)	250.	250.	250.	250.	250.	250.	250.
Maximum Δ Temperature (°C)[b]	4.00	4.00	5.00	6.00	6.00	6.00	6.00
Pressure (MPa)	1.48	1.48	1.48	1.48	1.48	1.48	1.48
H_2/CO Feed Ratio	.680	.680	.686	.686	.686	.980	.980
Space Velocity (Nl/g-cat·h)[a]	2.00	2.00	2.00	2.00	2.00	2.00	2.00
Space Velocity (Nl/g-Fe·h)	3.81	3.81	3.81	3.81	3.81	3.81	3.81
GHSV (h^{-1})[c]	239.	239.	239.	239.	239.	239.	239.
CO Conversion (%)	56.4	52.4	51.6	50.1	46.9	59.1	59.1
H_2+CO Conversion (%)	58.6	55.3	54.4	53.2	50.2	56.0	55.5
H_2/CO Usage	.757	.780	.778	.700	.803	.878	.859
STY (mols H_2+CO/g-cat·h)[a]	.052	.049	.049	.048	.045	.050	.050
$P_{CO_2} \cdot P_{H_2} / P_{CO} \cdot P_{H_2O}$	2.22	2.03	2.05	2.14	1.97	2.97	2.83
Weight % of Outlet							
H_2	1.88	1.99	1.99	2.01	2.14	3.16	3.24
H_2O	3.97	3.86	3.81	3.48	3.62	5.50	5.76
CO	43.4	47.0	47.0	48.1	51.1	39.0	39.0
CO_2	35.8	32.5	32.4	31.2	29.9	35.5	34.5
Hydrocarbons	11.4	9.26	9.43	9.43	8.06	13.0	12.9
Oxygenates	.645	.545	.503	.396	.421	.988	.906
Wax[d]	2.88	4.82	4.01	5.36	3.87	2.92	3.63
Yield (g/Nm³ H_2 + CO Converted)							
CH_4	10.1	10.2	11.2	11.5	12.6	16.1	15.5
C_2-C_4 Hydrocarbons	41.2	40.3	45.8	46.2	49.1	55.8	54.7
C_5-C_{11} Hydrocarbons	33.6	35.8	40.7	42.8	46.4	47.6	46.9
C_{12}+ Hydrocarbons	96.2	104.	103.	113.	88.7	69.0	81.2
Wax[d]	36.5	65.2	68.8	77.3	59.4	34.6	43.2
Oxygenates	8.18	7.37	7.05	5.72	6.46	11.7	10.8
Total	180.	198.	208.	219.	203.	200.	208.
1+2 Olefins/n-Paraffin Ratio							
C_2	1.68	1.02	1.99	2.09	2.10	1.44	1.54
C_3	7.65	7.83	7.80	7.75	7.74	6.44	6.50
C_4	6.22	6.35	6.33	6.23	6.22	5.13	5.20
C_8	3.80	4.06	3.71	4.03	4.15	3.25	3.19
C_{10}	2.62	2.66	2.78	2.81	3.00	2.27	2.31

[a] Based on unreduced catalyst
[b] Maximum axial temperature difference
[c] Based on reactor volume
[d] Unrecovered products from wax analysis

Table 12 (cont'd). Summary of results for fixed bed run FB-99-1588.

Period	1	2	3	4	5	6	7
Weight % of Hydrocarbons							
CH_4	5.55	5.34	5.58	5.41	6.38	8.54	7.87
Ethane	2.48	2.18	2.25	2.00	2.33	3.50	3.12
Ethylene	3.87	3.02	4.18	3.90	4.56	4.70	4.49
Propane	1.05	.975	1.04	.983	1.13	1.50	1.48
Propylene	7.70	7.29	7.76	7.27	8.35	9.70	9.20
n-Butane	1.01	.878	.984	.906	1.14	1.57	1.46
1+2 Butenes	6.05	5.39	6.01	5.99	6.85	7.78	7.35
C_4 Isomers	.580	.509	.543	.524	.598	.670	.624
n-Pentane	1.43	1.15	1.35	1.46	1.65	2.04	1.87
1+2 Pentenes	5.11	4.18	5.10	5.51	6.21	6.85	6.38
C_5 Isomers	.333	.263	.305	.325	.372	.499	.450
n-Hexane	.634	.709	.605	.665	.701	.826	.755
1+2 Hexenes	2.56	2.66	2.87	2.72	3.50	3.30	3.00
C_6 Isomers	.578	.536	.583	.594	.632	.595	.517
n-Heptane	.372	.392	.401	.469	.469	.550	.497
1+2 Heptenes	1.51	1.60	1.60	1.93	2.02	1.93	1.76
C_7 Isomers	.343	.323	.347	.377	.442	.389	.306
n-Octane	.202	.311	.324	.295	.363	.465	.422
1+2 Octenes	1.09	1.24	1.18	1.17	1.48	1.48	1.32
C_8 Isomers	.165	.102	.174	.258	.146	.163	.152
n-Nonane	.280	.383	.370	.288	.377	.553	.475
1+2 Nonenes	.872	1.16	1.14	.913	1.20	1.38	1.22
C_9 Isomers	.0098	.107	.110	.0676	.0631	.102	.126
n-Decane	.359	.457	.450	.360	.472	.621	.564
1+2 Decenes	.927	1.20	1.23	1.02	1.40	1.39	1.28
C_{10} Isomers	.174	.181	.224	.121	.119	.190	.173
n-Undecane	.418	.475	.473	.408	.502	.602	.603
1+2 Undecenes	.892	1.01	1.09	.959	1.26	1.16	1.15
C_{11} Isomers	.150	.185	.195	.124	.158	.175	.202
C_2-C_4	22.7	21.1	22.8	21.7	25.0	20.6	27.7
C_5-C_{11}	18.6	18.8	20.2	20.0	23.6	25.3	23.2
C_{12}+	53.1	54.7	51.4	52.9	45.1	36.6	41.2
Wax[d]	20.2	34.2	34.2	30.2	30.2	18.4	21.9

[d] Unrecovered products from wax analysis

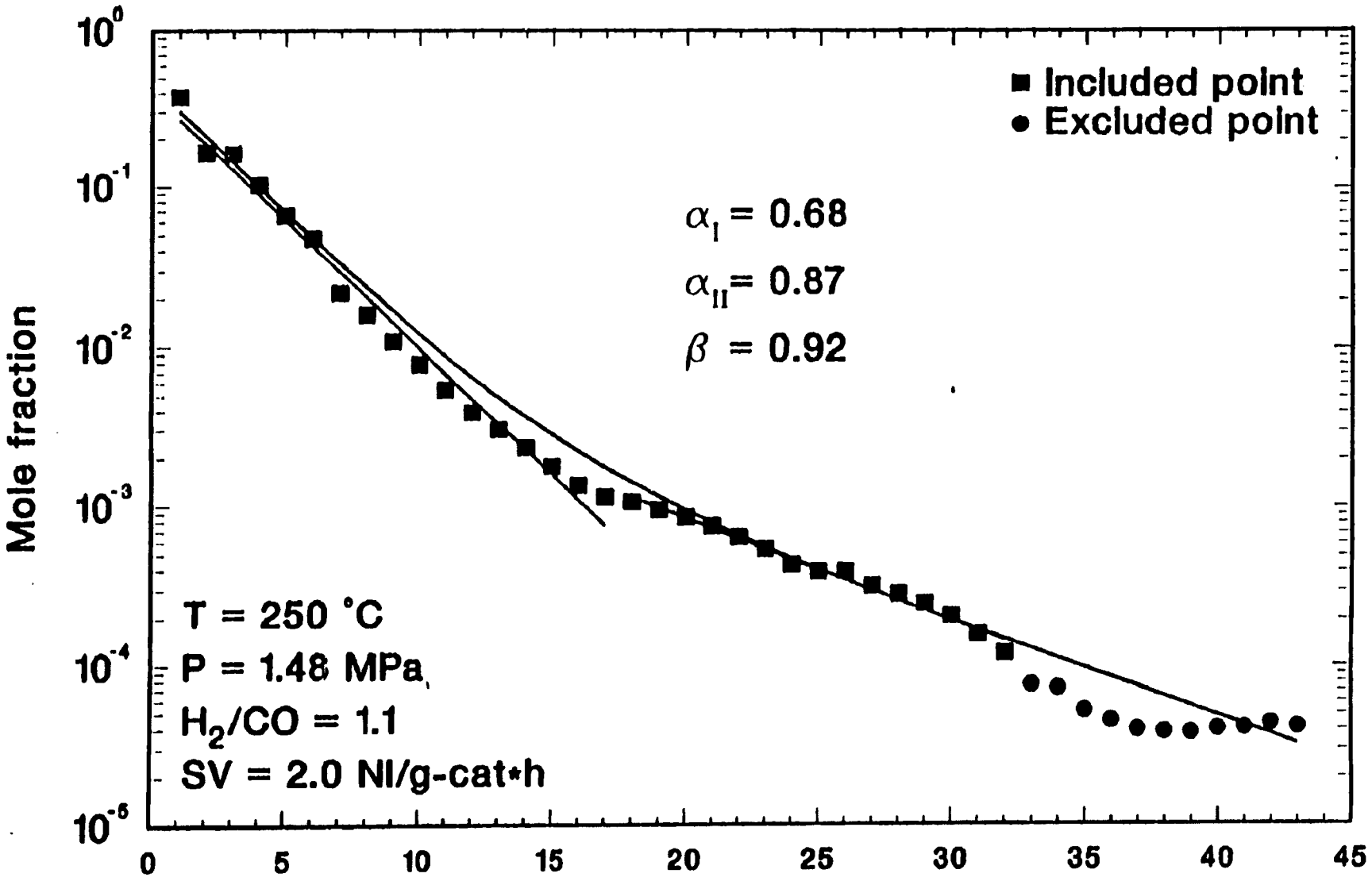

Figure 1. Anderson-Schulz-Flory plot for run FA-25-2737-1, total products excluding unrecovered wax.

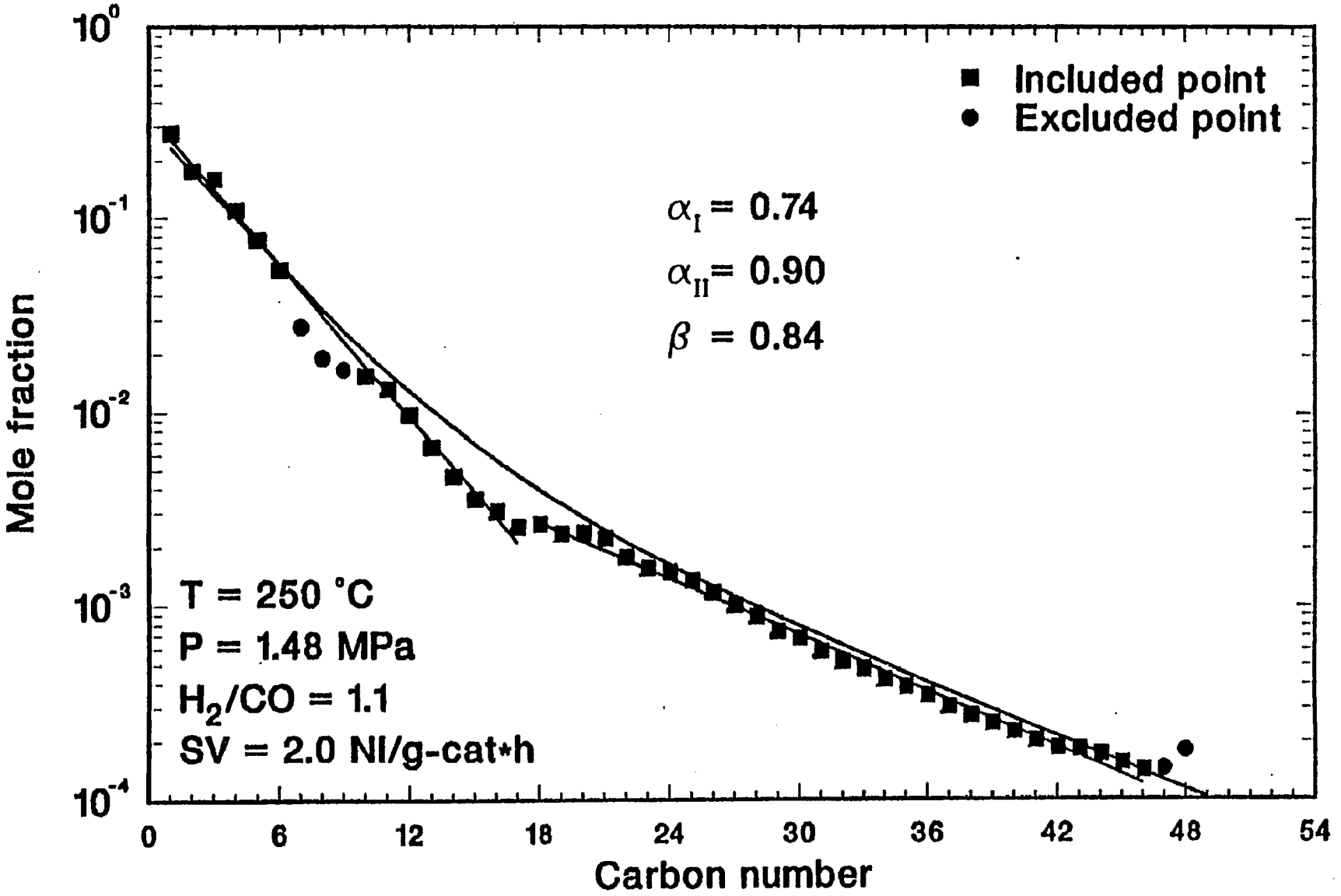

Figure 2. Anderson-Schulz-Flory plot for run FA-25-3077-2, total products excluding unrecovered wax.

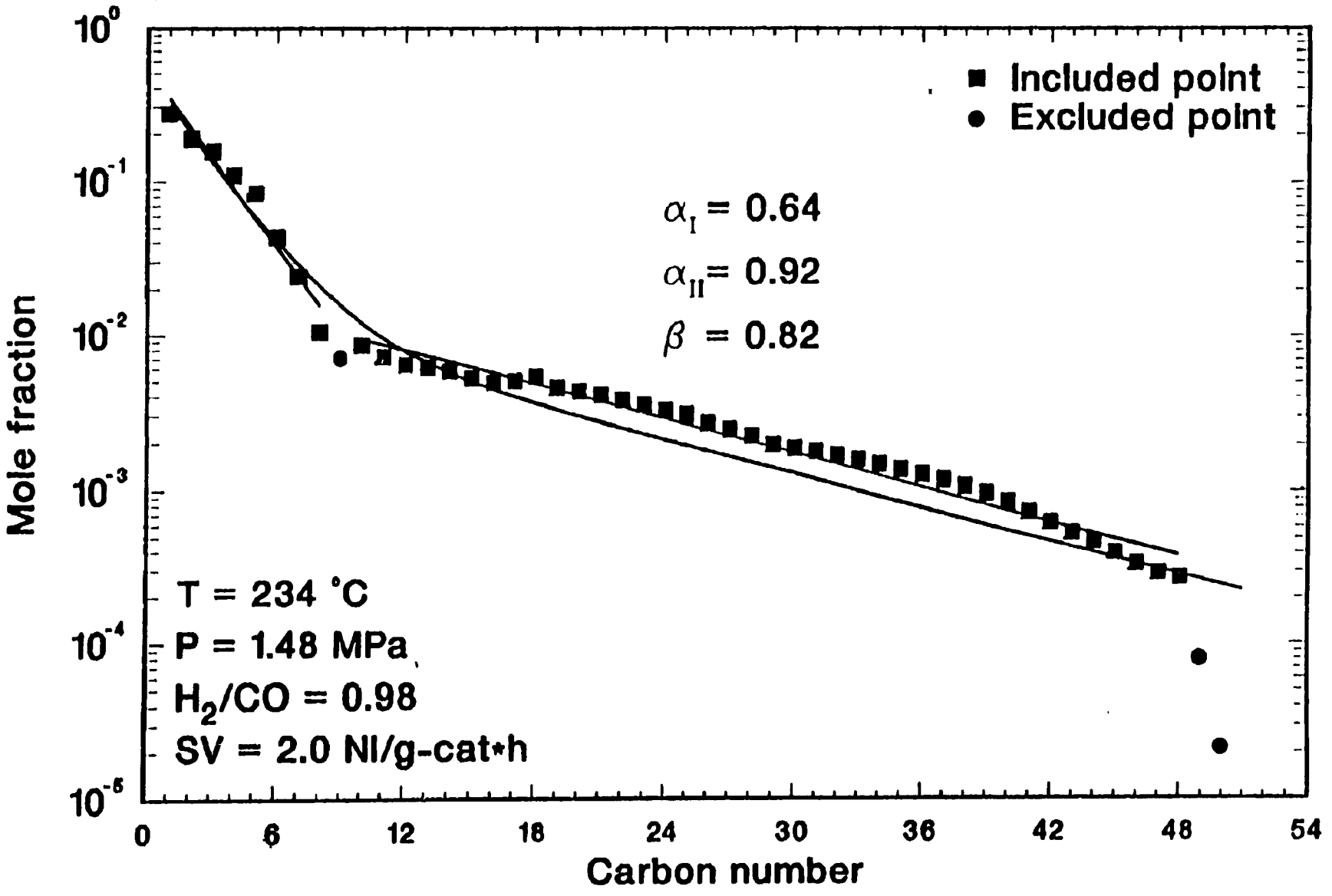

Figure 3. Anderson-Schulz-Flory plot for run FD-00-1348-3 (calcined Ruhrchemie LP 33/81), total products excluding unrecovered wax.

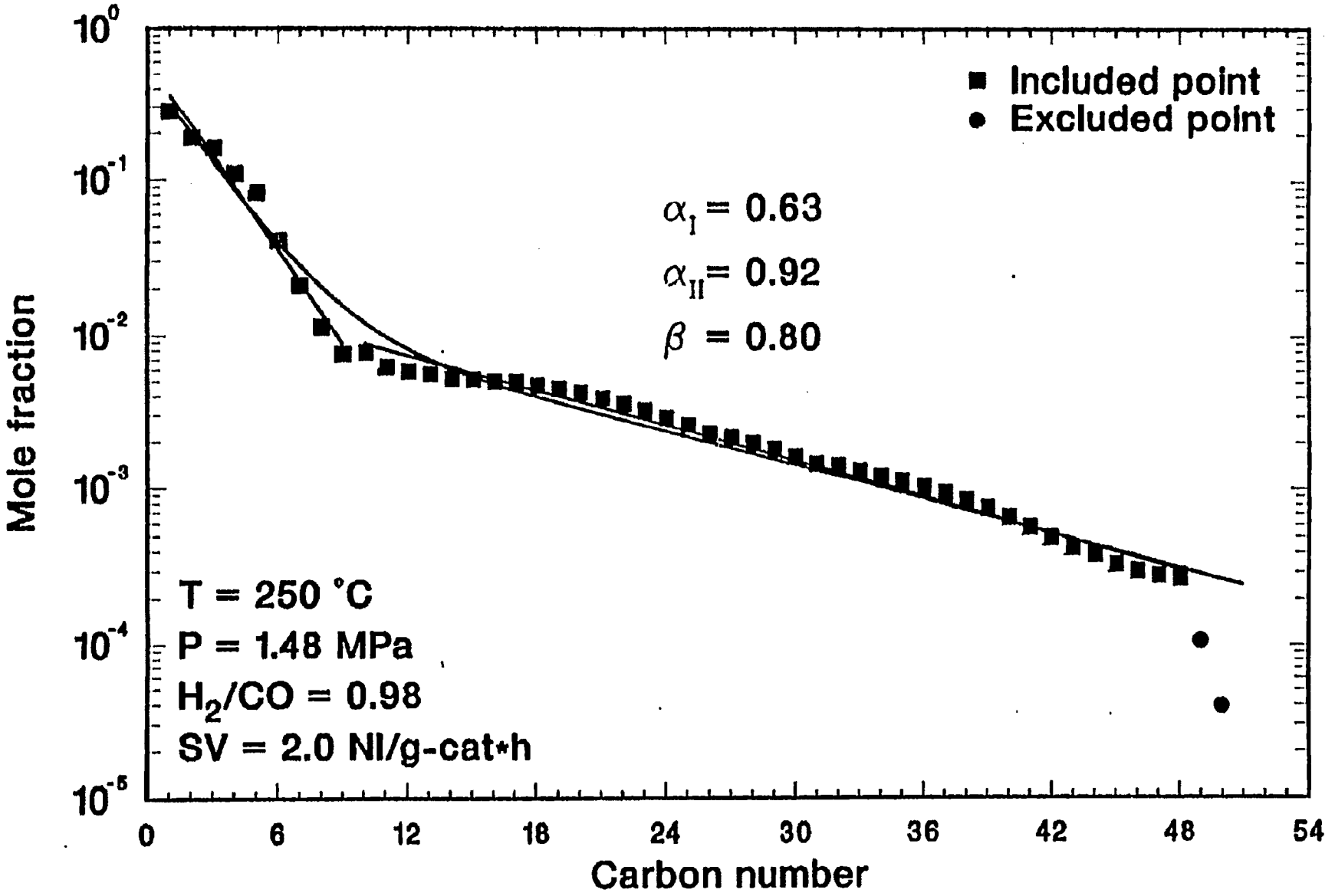

Figure 4. Anderson-Schulz-Flory plot for run FB-00-1348-4 (Ruhrchemie LP 33/81), total products excluding unrecovered wax.

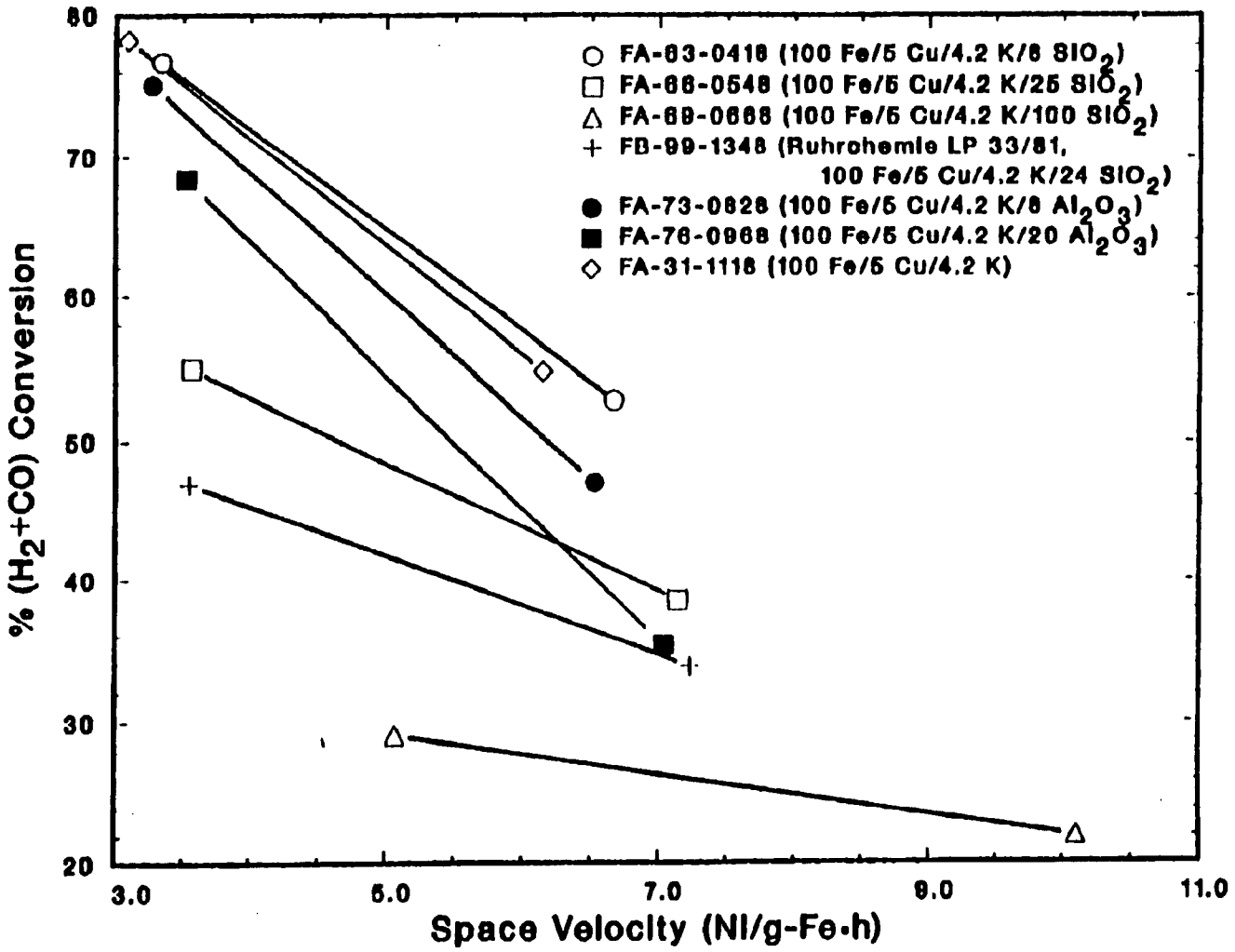

Figure 5. Comparison of (H_2+CO) conversions for the binder/support catalysts and Ruhrchemie LP 33/81: 250 °C, 1.48 *MPa*, (H_2/CO) = 1.0.

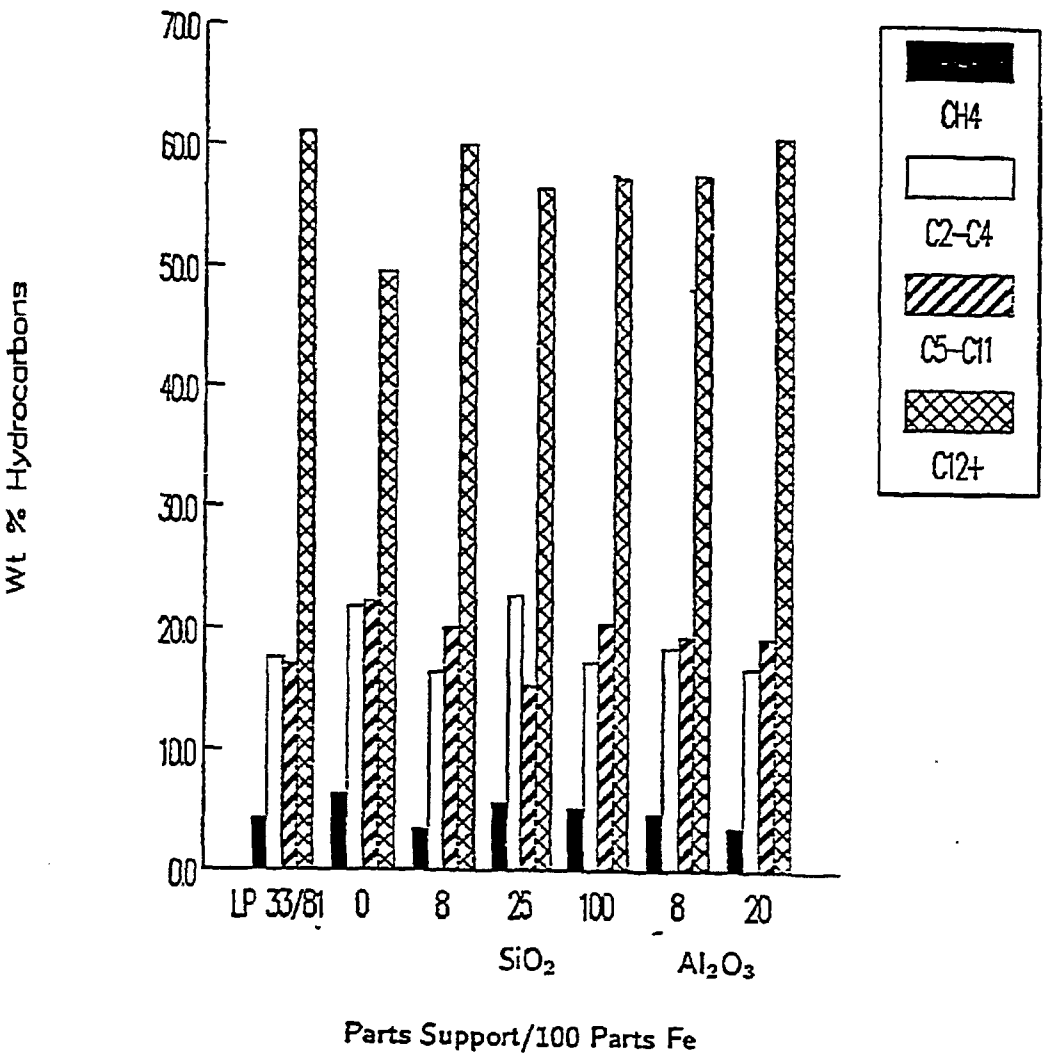

Figure 6. Weight percent hydrocarbon distribution of binder/support catalysts and Ruhrchemie LP 33/81: 235 °C, 1.48 MPa, 2 Nl/g-cat-h, (H_2/CO) = 1.0.

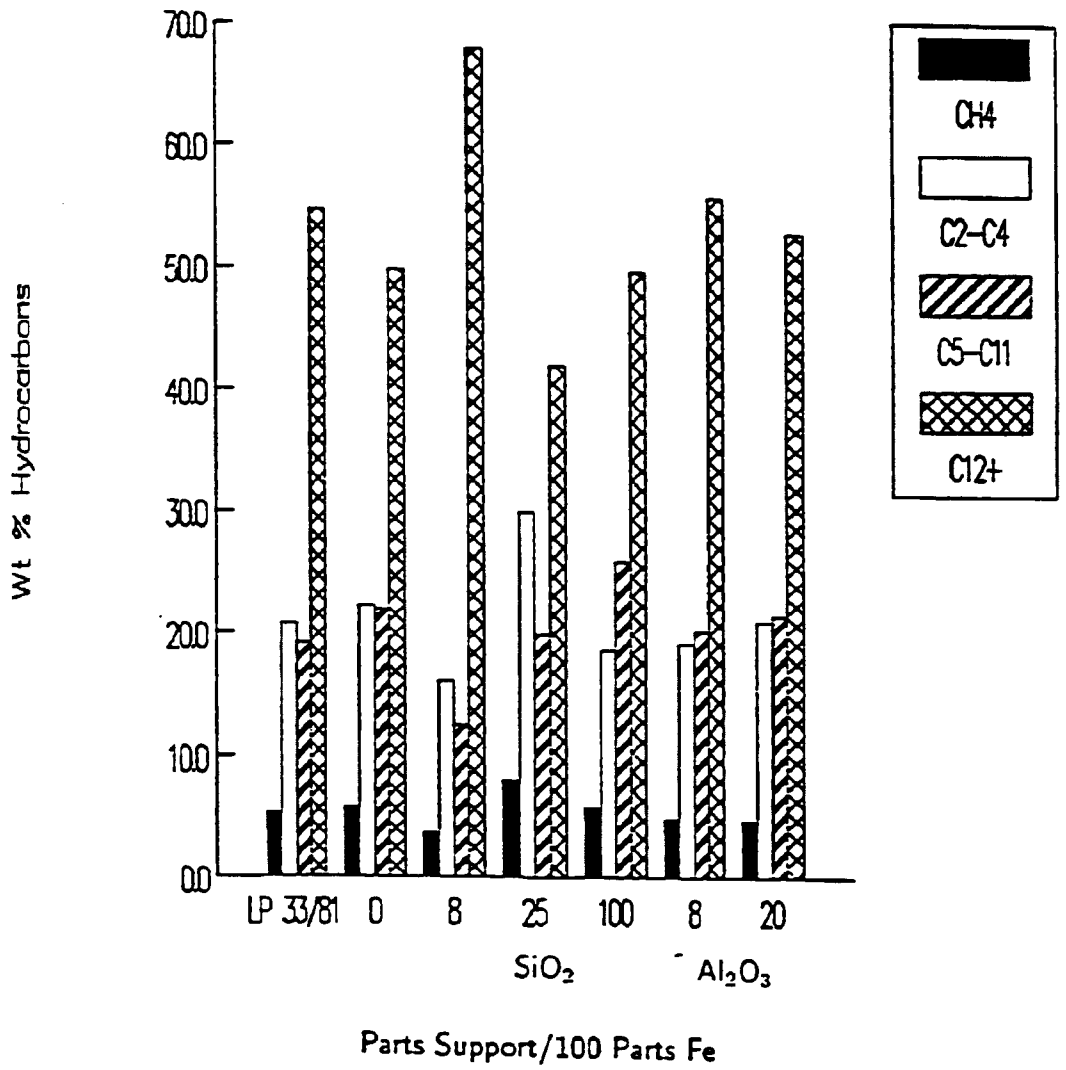

Figure 7. Weight percent hydrocarbon distribution of binder/support catalysts and Ruhrchemie LP 33/81: 250 °C, 1.48 *MPa*. 2 Nl/g–cat·h, (H_2/CO) = 1.0.

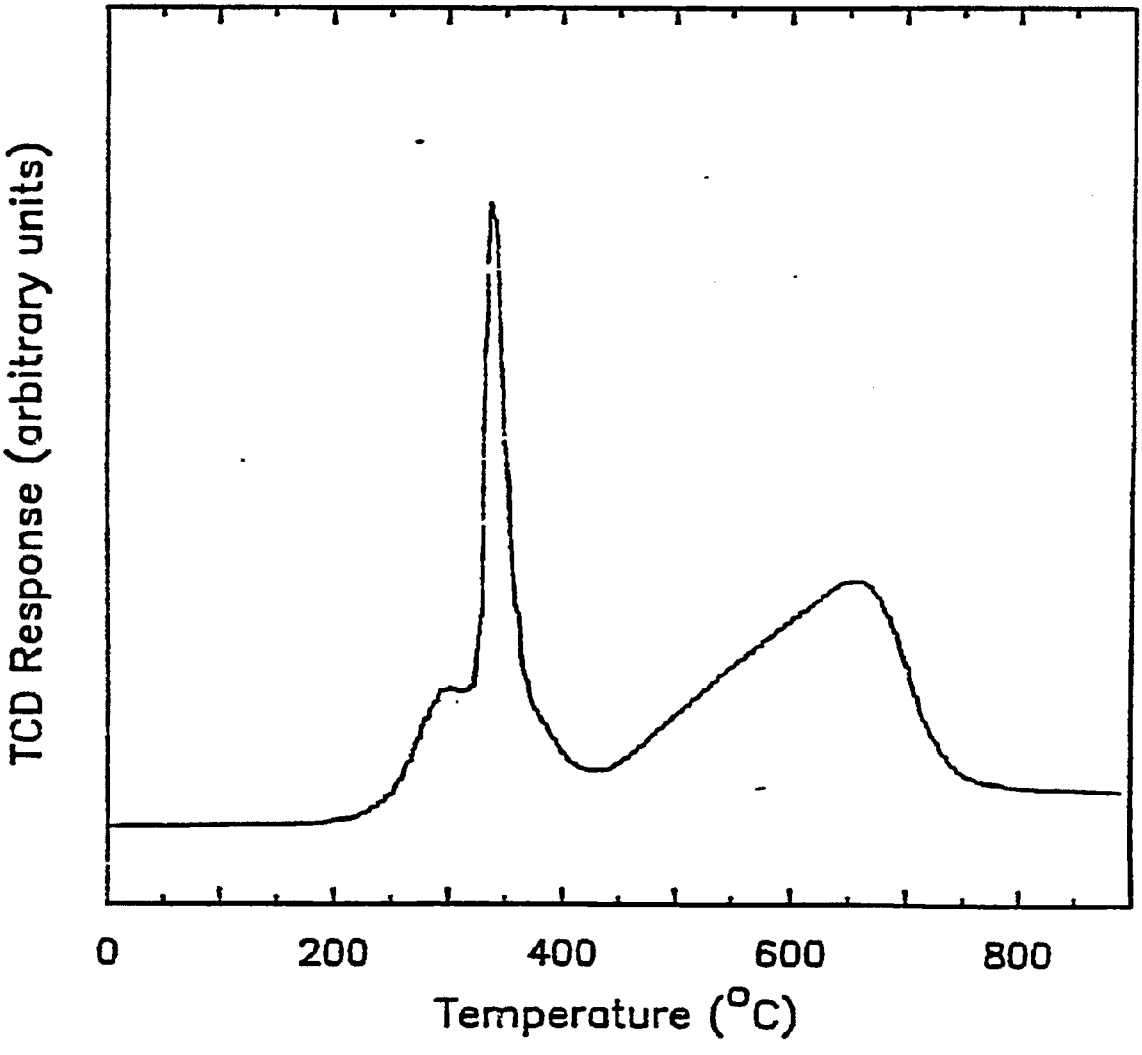

Figure 8. TPR profile in H_2 at 20 °C/min for calcined (16 hrs in air at 300 °C) sample of commercial Ruhrchemie catalyst.

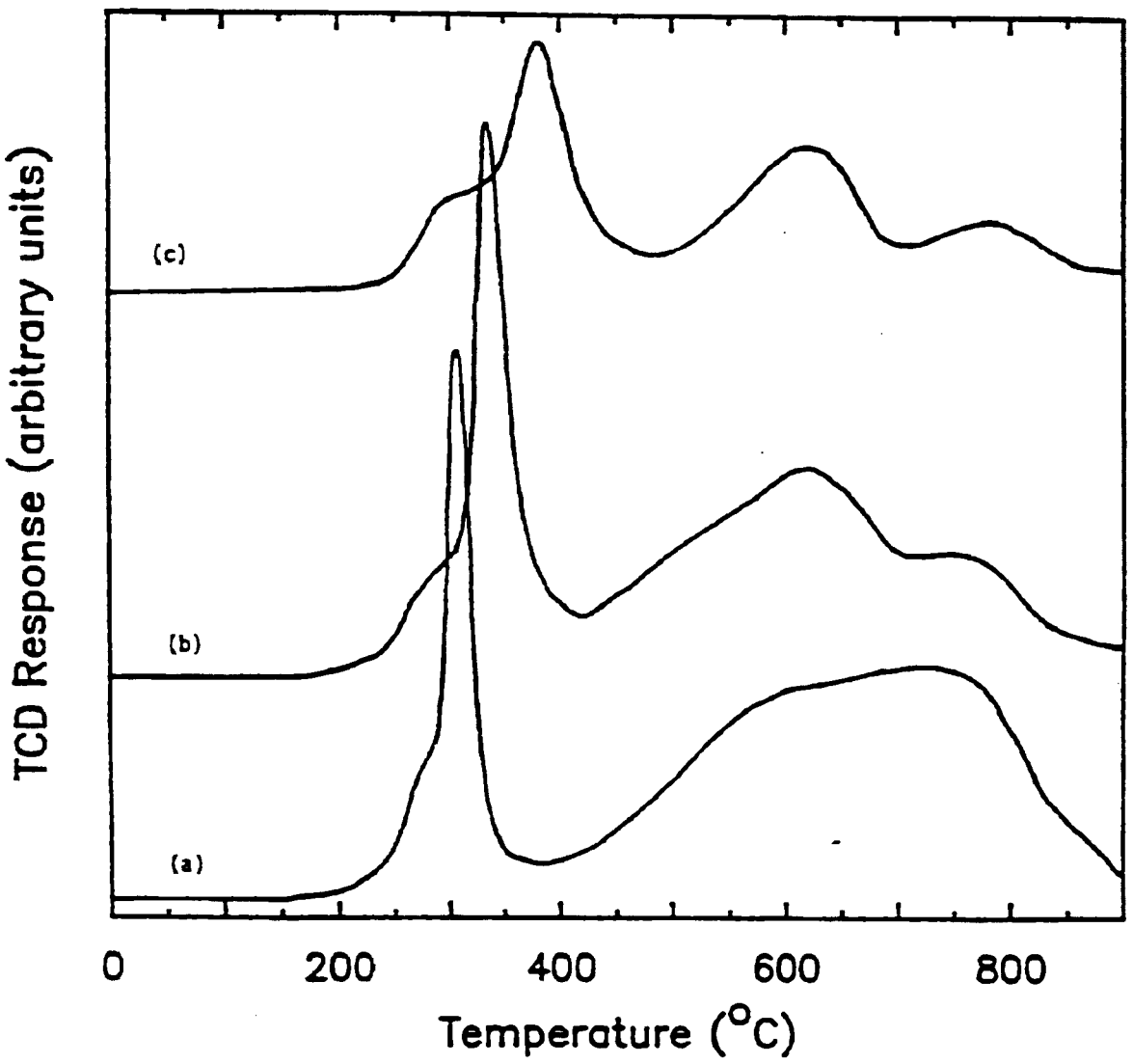

Figure 9. TPR profiles in H_2 at 20 °C/min for calcined (16 hrs in air at 300 °C) samples of: (a) 100 Fe/5 Cu/4.2 K/8 SiO_2; (b) 100 Fe/5 Cu/4.2 K/25 SiO_2; (c) 100 Fe/5 Cu/4.2 K/100 SiO_2

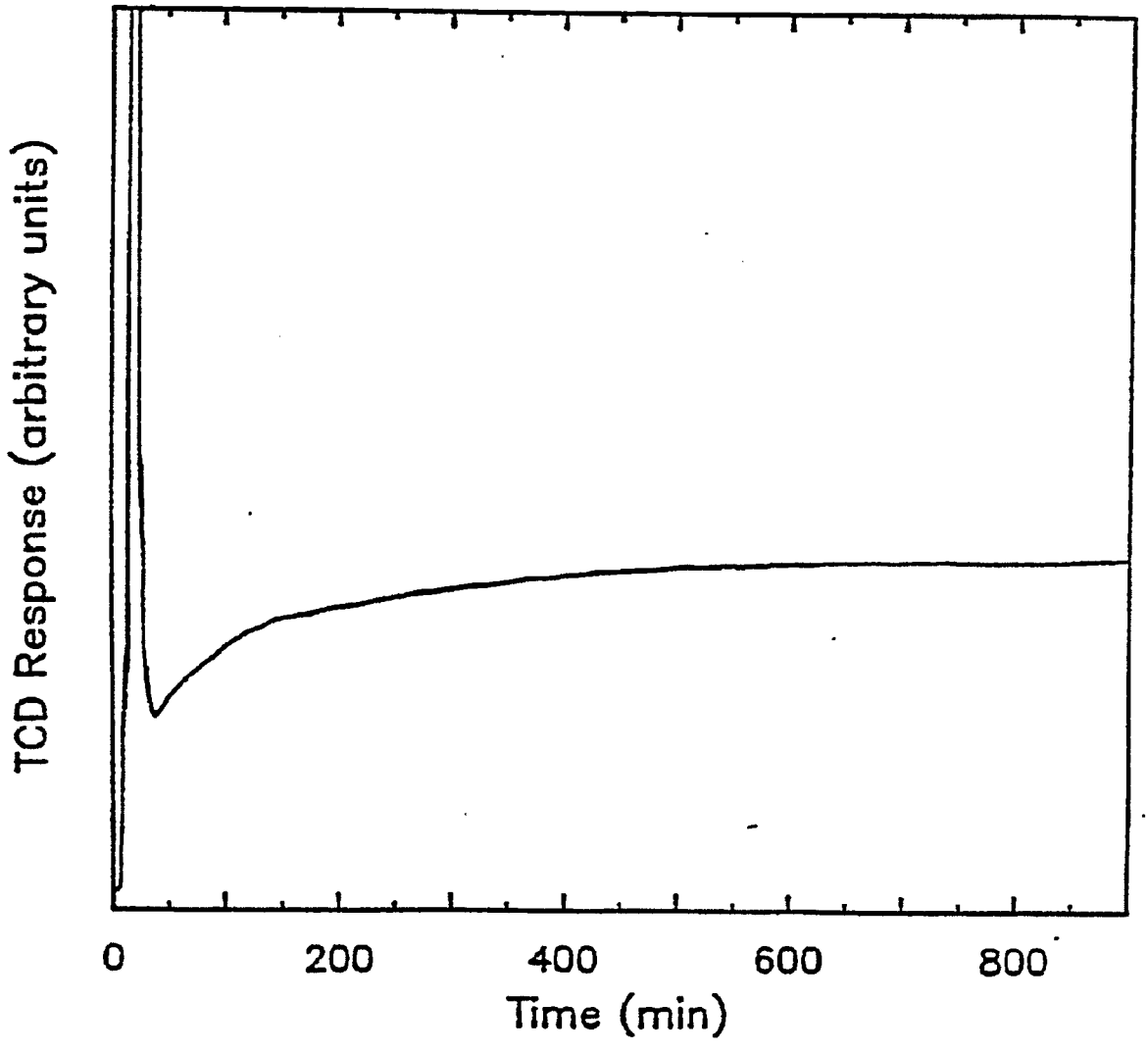

Figure 10. Isothermal reduction profile in H_2 for calcined (16 hrs in air at 300 °C) sample of commercial Ruhrchemie catalyst.

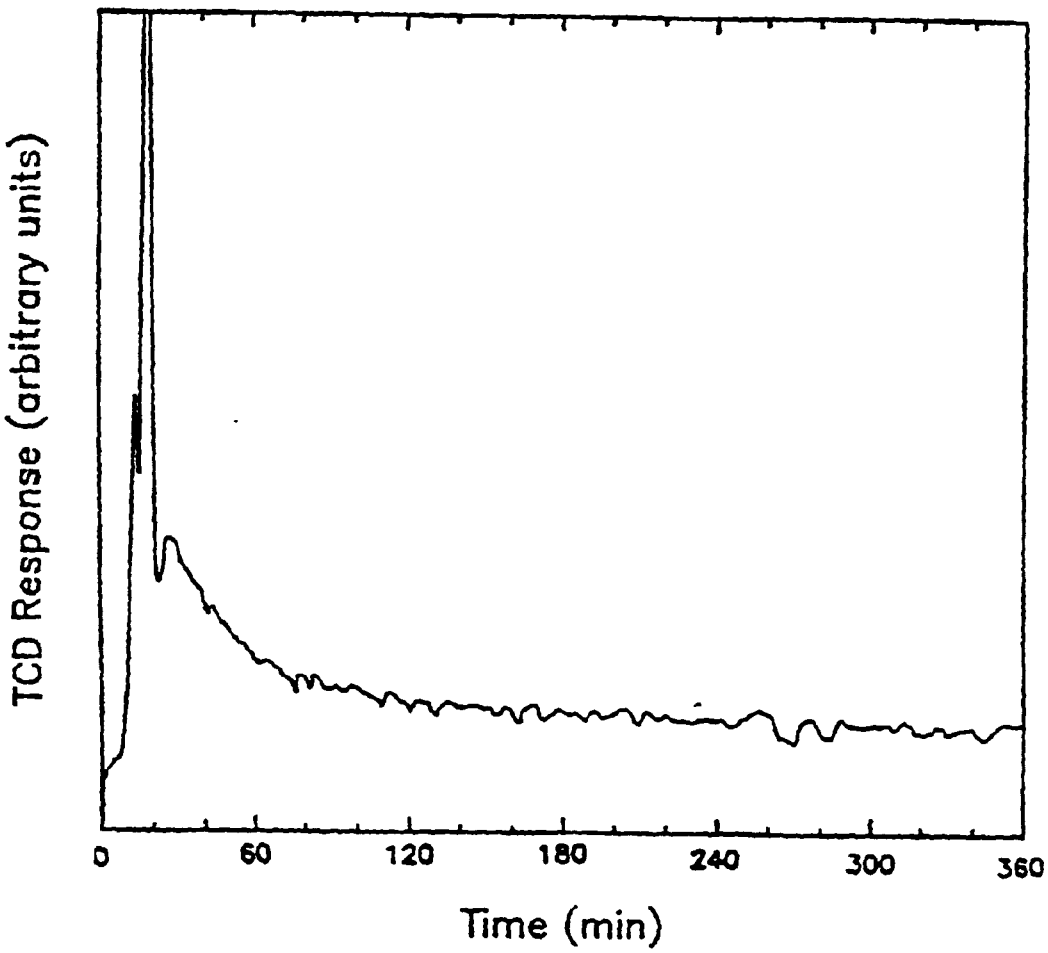

Figure 11. Isothermal reduction profile in CO for calcined (16 hrs in air at 300 °C) sample of commercial Ruhrchemie catalyst.

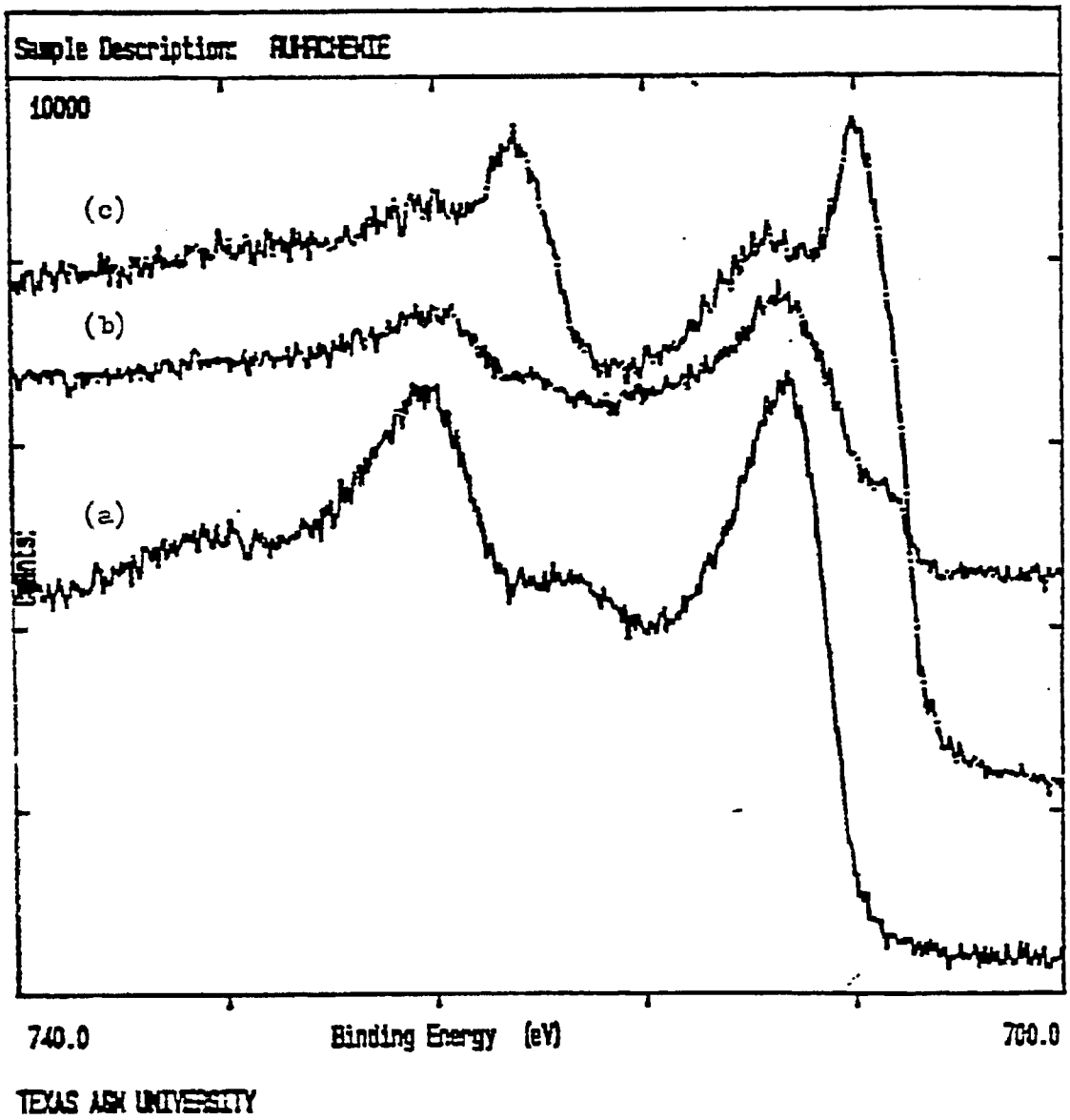

Figure 12. XPS spectra of commercial Ruhrchemie catalyst in Fe 2p region. (a) following calcination for 16 hrs at 300 °C; (b) following exposure of (a) to CO at 300 °C; (c) following exposure of (a) to H_2 at 300 °C.

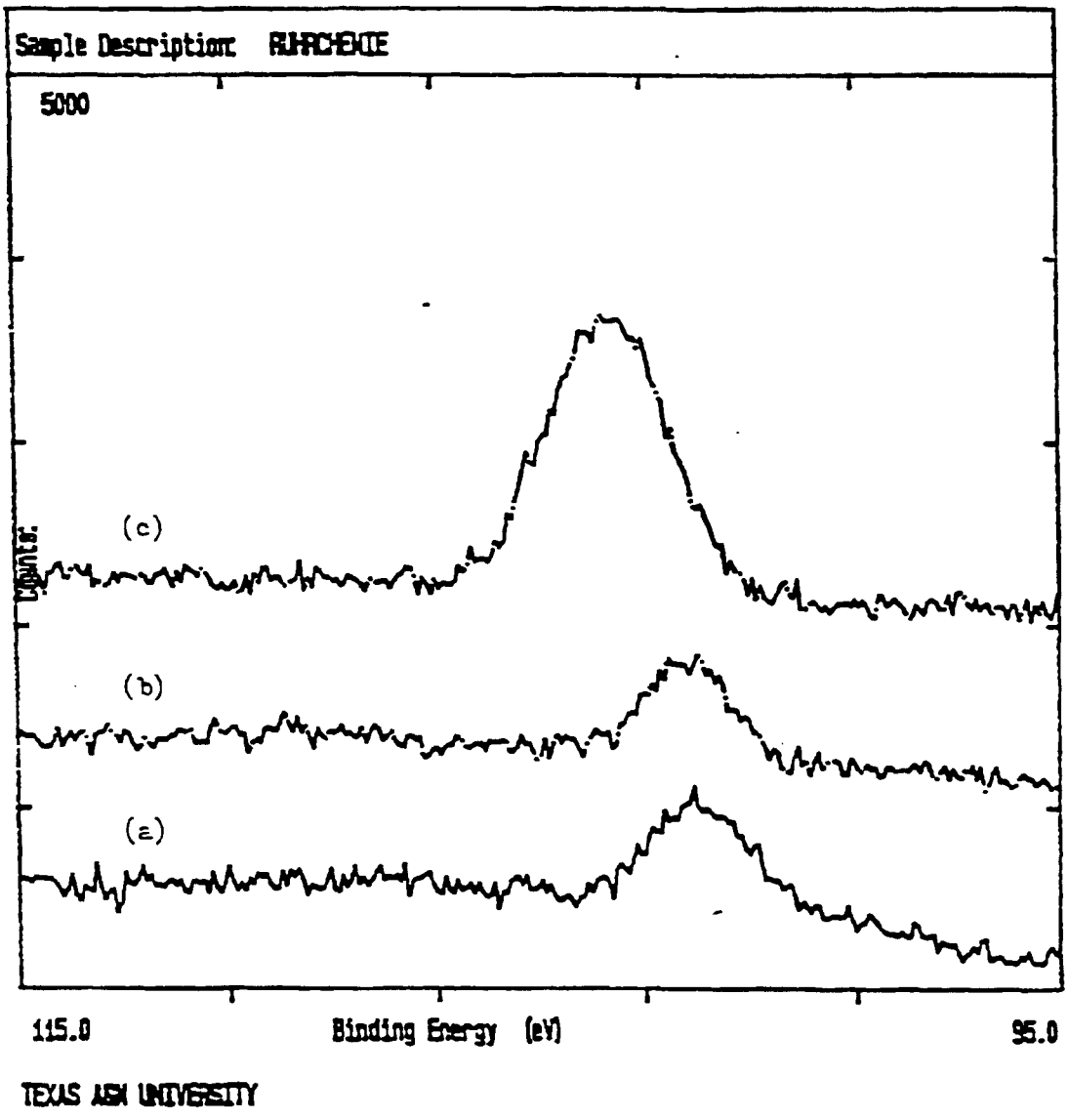

Figure 13. XPS spectra of commercial Ruhrchemie catalyst in Si 2p region. (a) following calcination for 16 hrs at 300 °C; (b) following exposure of (a) to CO at 300 °C; (c) following exposure of (a) to H_2 at 300 °C.

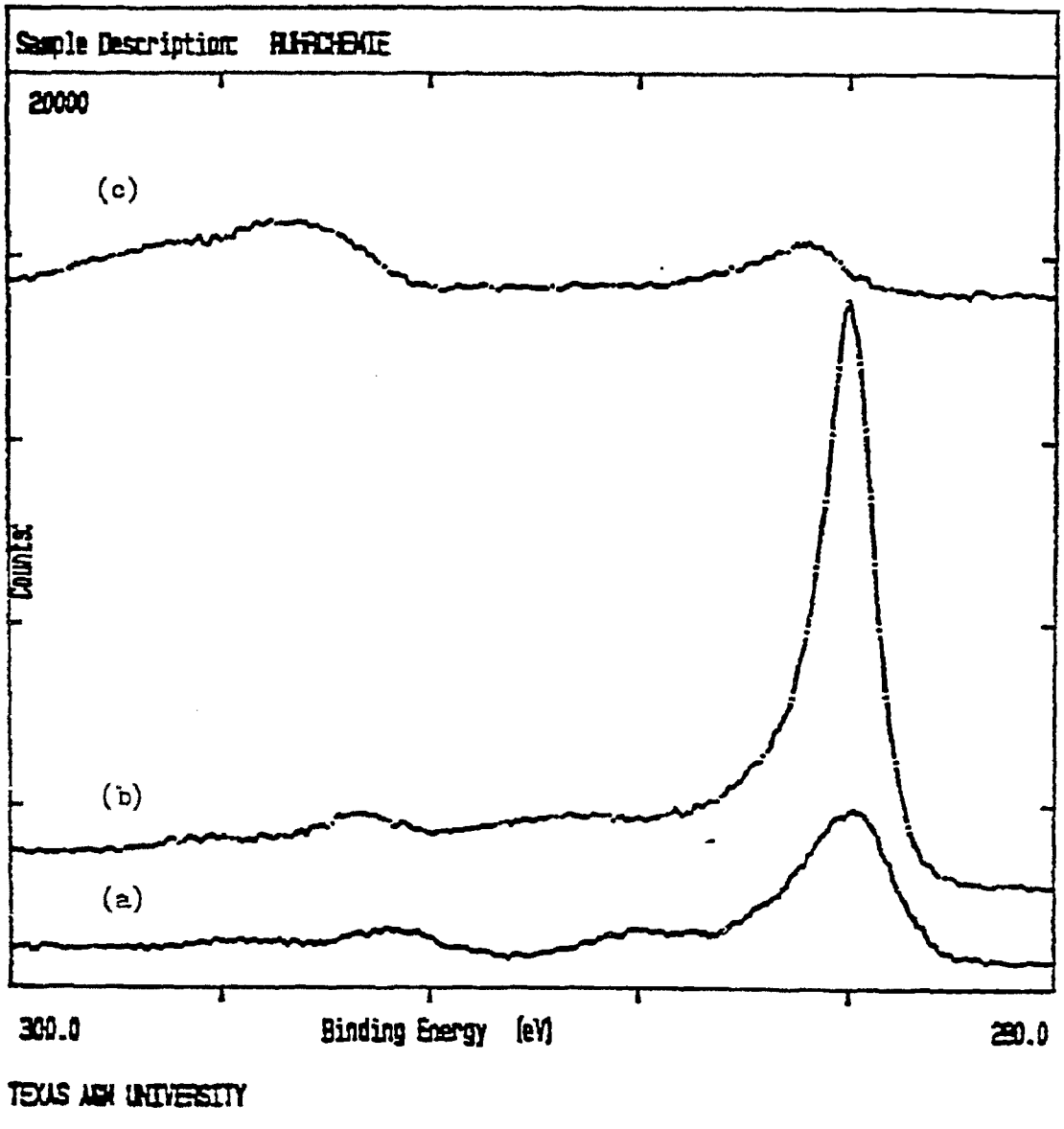

Figure 14. XPS spectra of commercial Ruhrchemie catalyst in K 2p and C 1s regions. (a) following calcination for 16 hrs at 300 °C; (b) following exposure of (a) to CO at 300 °C; (c) following exposure of (a) to H_2 at 300 °C.

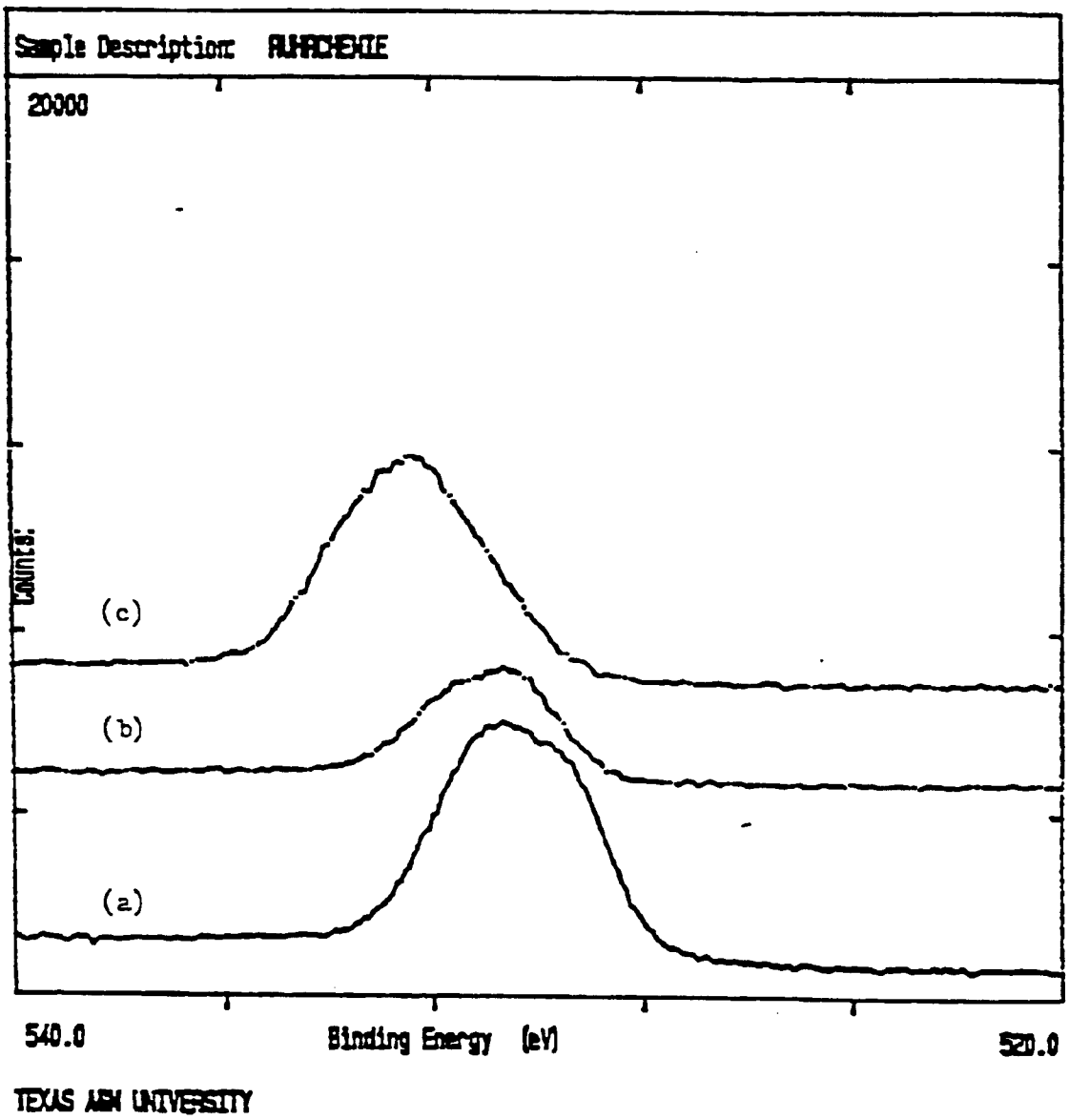

Figure 15. XPS spectra of commercial Ruhrchemie catalyst in O 1s region. (a) following calcination for 16 hrs at 300 °C; (b) following exposure of (a) to CO at 300 °C; (c) following exposure of (a) to H_2 at 300 °C.

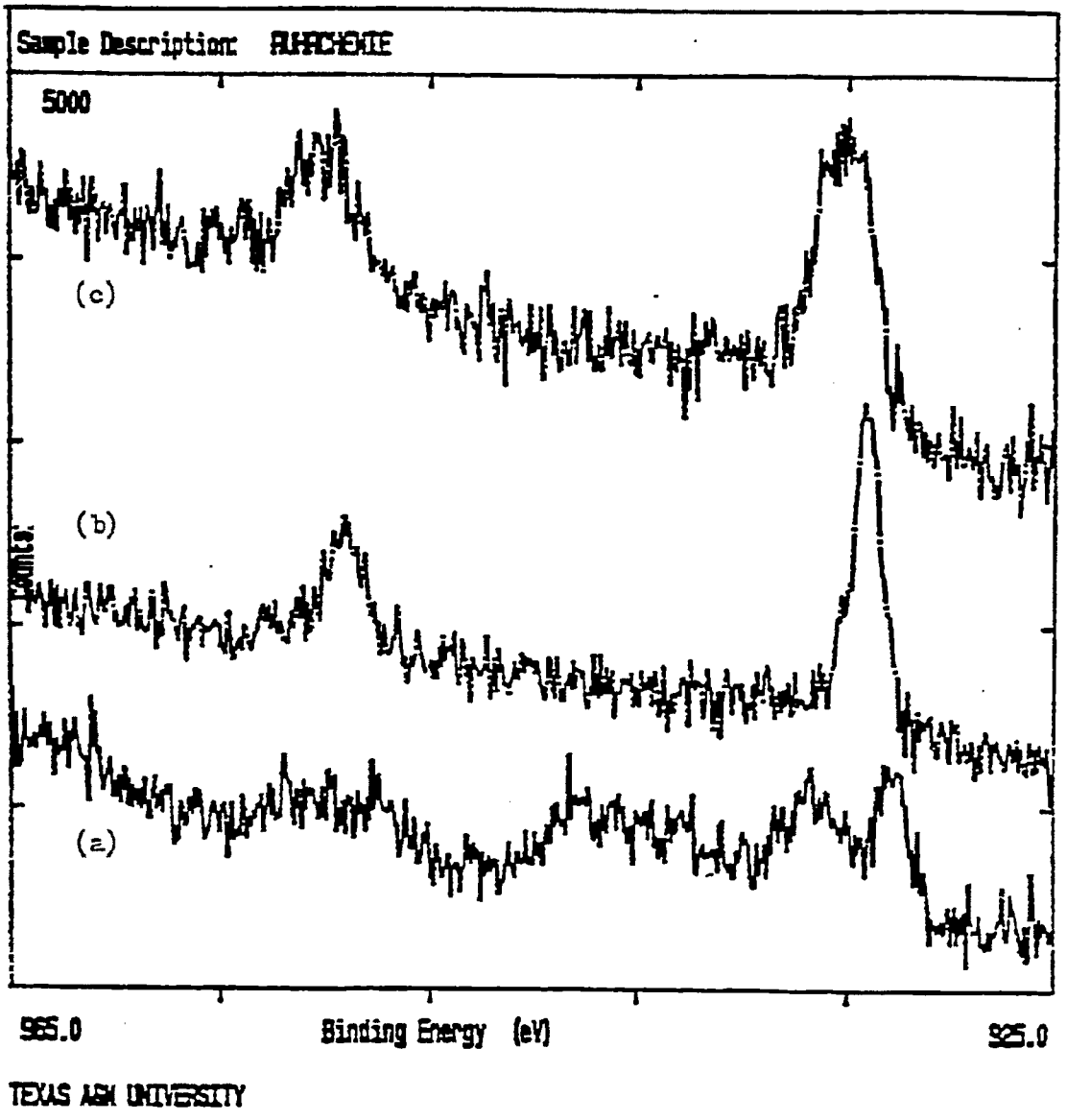

Figure 16. XPS spectra of commercial Ruhrchemie catalyst in Cu 2p region. (a) following calcination for 16 hrs at 300 °C; (b) following exposure of (a) to CO at 300 °C; (c) following exposure of (a) to H_2 at 300 °C.

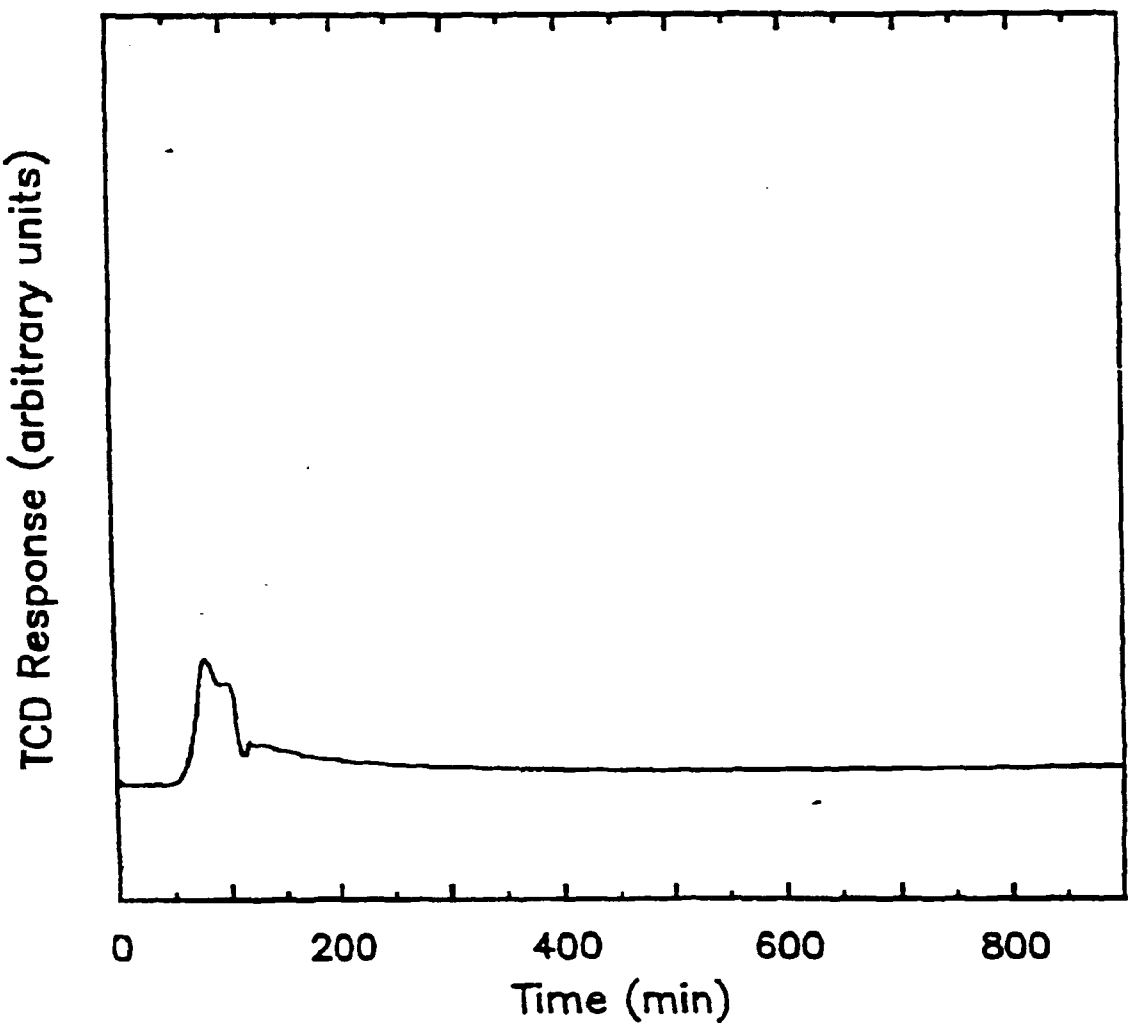

Figure 17. Isothermal reduction profile in H_2 for calcined (16 hrs in O_2 at 300 °C) sample of 25 wt % Fe/SiO_2.

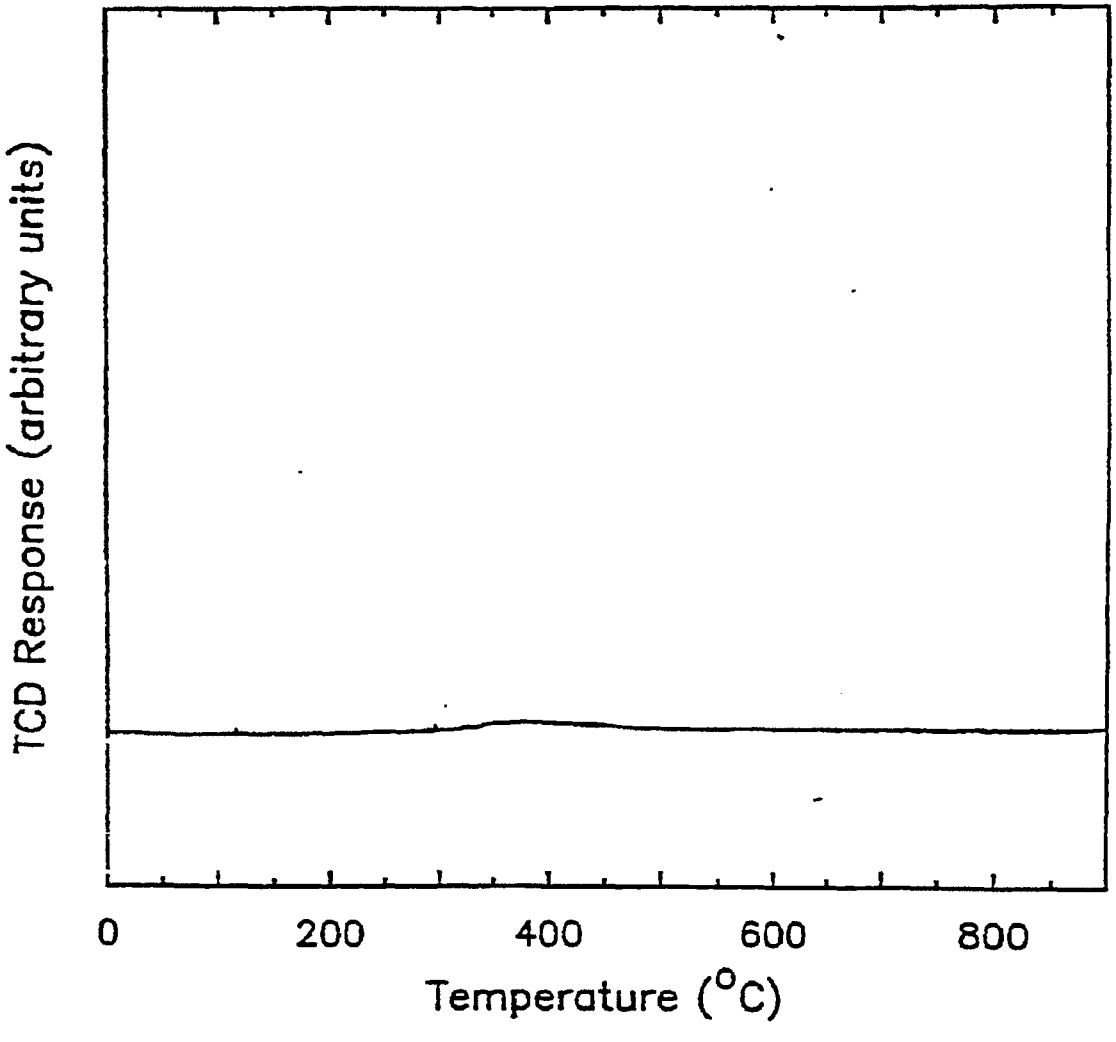

Figure 18. TPR profile in H_2 at 20 °C/min for sample of 25 wt % Fe/SiO_2 that had been previously treated for 15 hrs in H_2 at 300 °C.

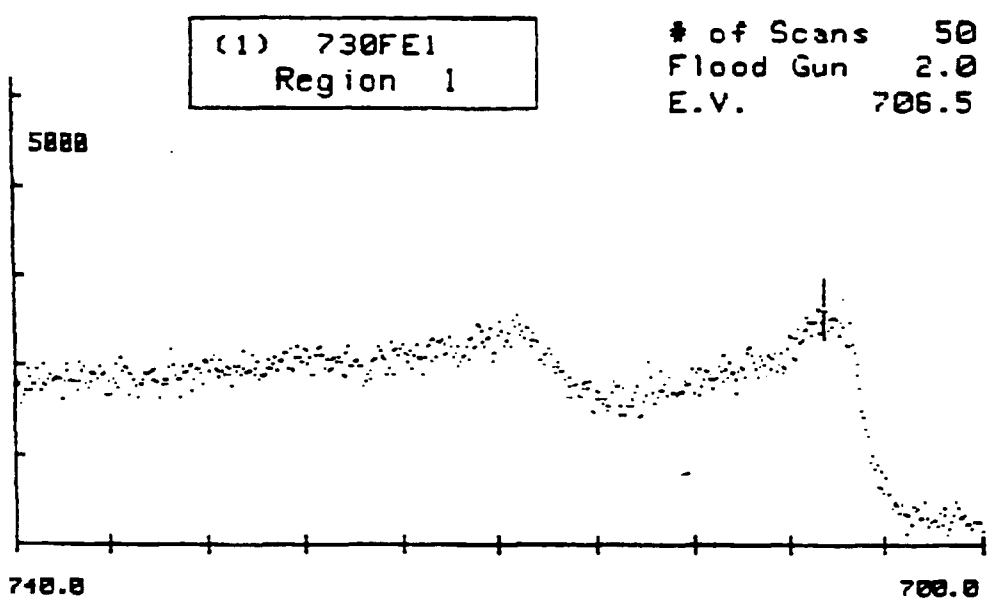

Figure 19. XPS spectra of 25 wt % Fe/SiO_2 in Fe 2p region following calcination for 16 hrs at 300 °C and subsequent treatment in H_2 for 16 hrs at 300 °C.

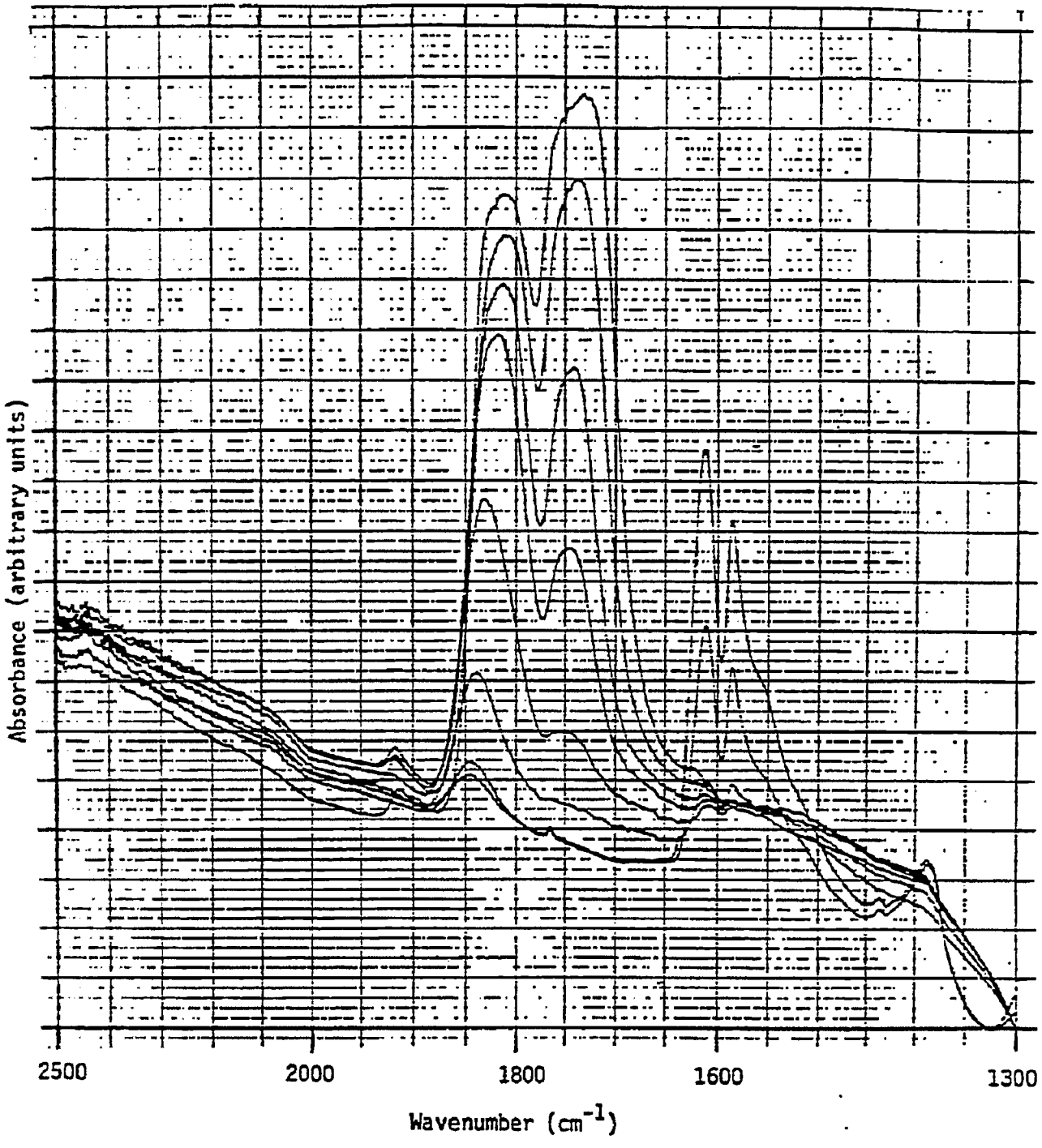

Figure 20. FT-IR spectra of NO adsorbed at 25 °C on 25 wt % Fe/SiO_2 that had been calcined for 16 hrs at 300 °C and subsequently treated in H_2 for 16 hrs at 300 °C. The uppermost spectrum was obtained following exposure of the sample to 10 torr of NO for 15 min, followed by evacuation. The second spectrum was obtained immediately after admission of 10 torr of O_2 at 25 °C. The remaining spectra were then obtained at 15 min intervals in the continuing presence of gaseous O_2.

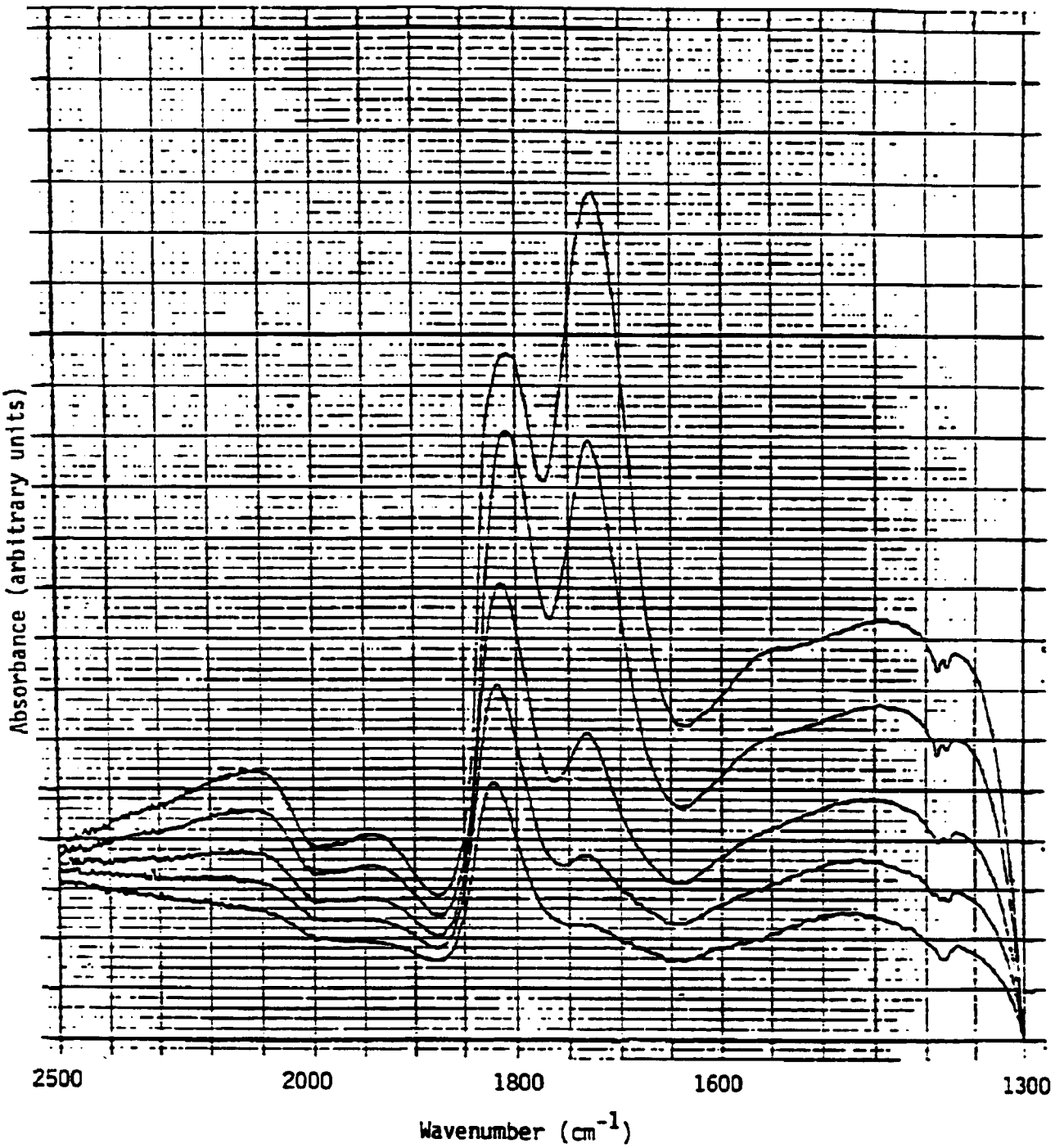

Figure 21. FT-IR spectra of NO adsorbed at 25 °C on 25 wt % Fe/SiO_2 containing 1 wt % K that had been calcined for 16 hrs at 300 °C and subsequently treated in H_2 for 16 hrs at 300 °C. The uppermost spectrum was obtained following exposure of the sample to 10 torr of NO for 15 min, followed by evacuation. The second spectrum was obtained immediately after admission of 10 torr of O_2 at 25 °C. The remaining spectra were then obtained at 15 min intervals in the continuing presence of gaseous O_2.

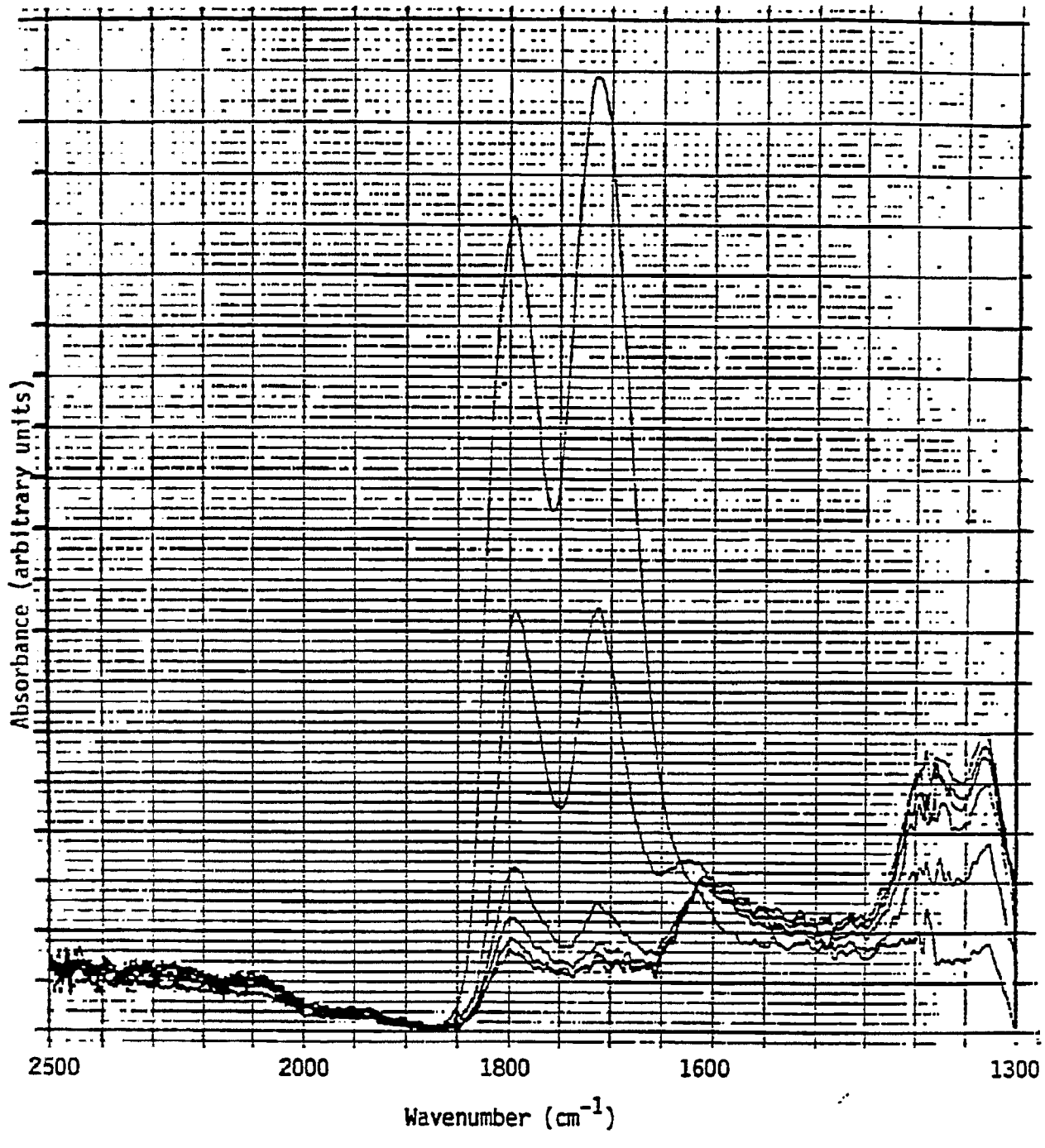

Figure 22. FT-IR spectra of NO adsorbed at 25 °C on 25 wt % Fe/SiO_2 containing 5 wt % K that had been calcined for 16 hrs at 300 °C and subsequently treated in H_2 for 16 hrs at 300 °C. The uppermost spectrum was obtained following exposure of the sample to 10 torr of NO for 15 min, followed by evacuation. The second spectrum was obtained immediately after admission of 10 torr of O_2 at 25 °C. The remaining spectra were then obtained at 15 min intervals in the continuing presence of gaseous O_2.

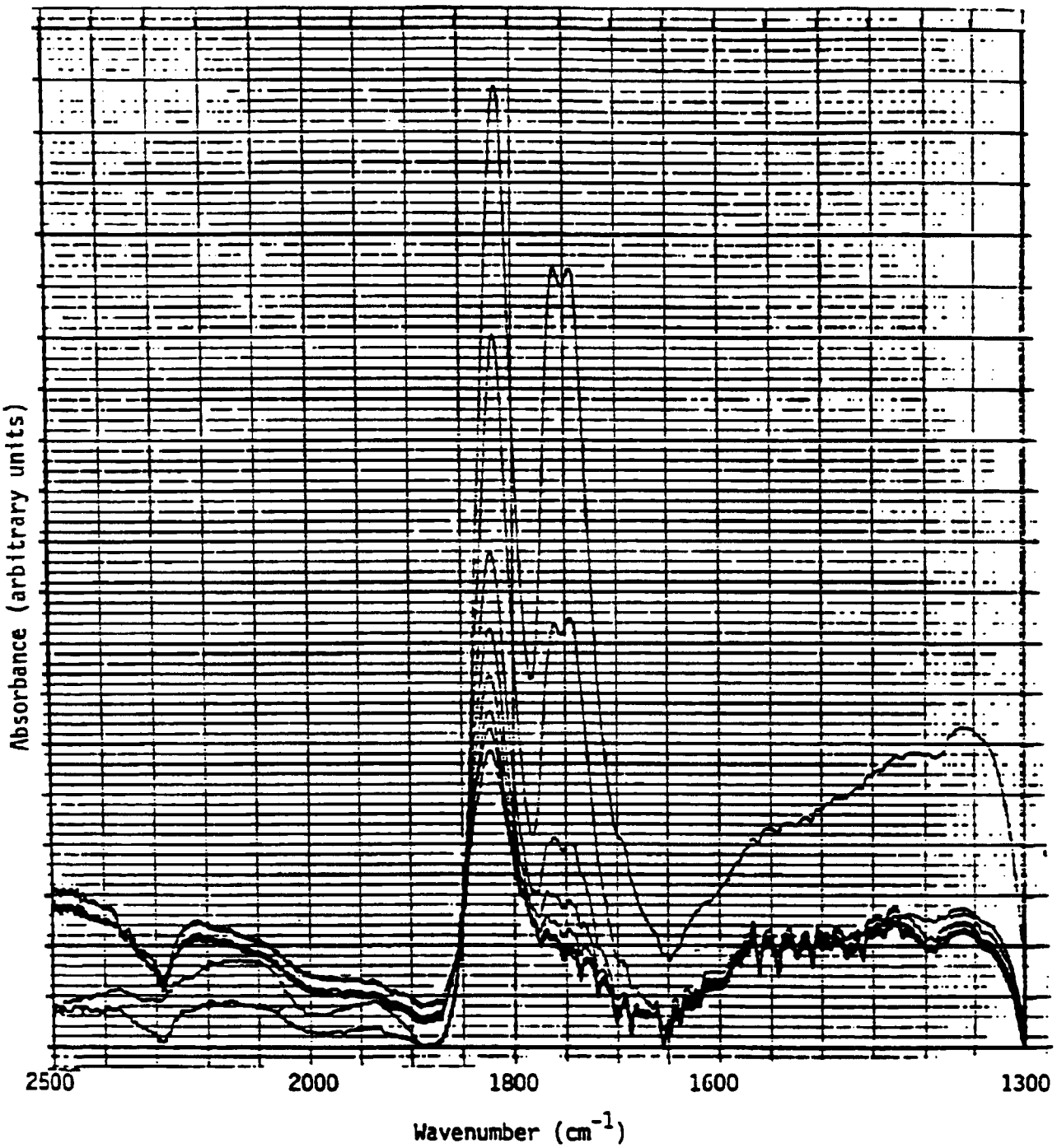

Figure 23. FT-IR spectra of NO adsorbed at 25 °C on 25 wt % Fe/SiO_2 that had been calcined for 16 hrs at 300 °C and subsequently treated in H_2 for 8 hrs at 730 °C. The uppermost spectrum was obtained following exposure of the sample to 10 torr of NO for 15 min, followed by evacuation. The second spectrum was obtained immediately after admission of 10 torr of O_2 at 25 °C. The remaining spectra were then obtained at 15 min intervals in the continuing presence of gaseous O_2.

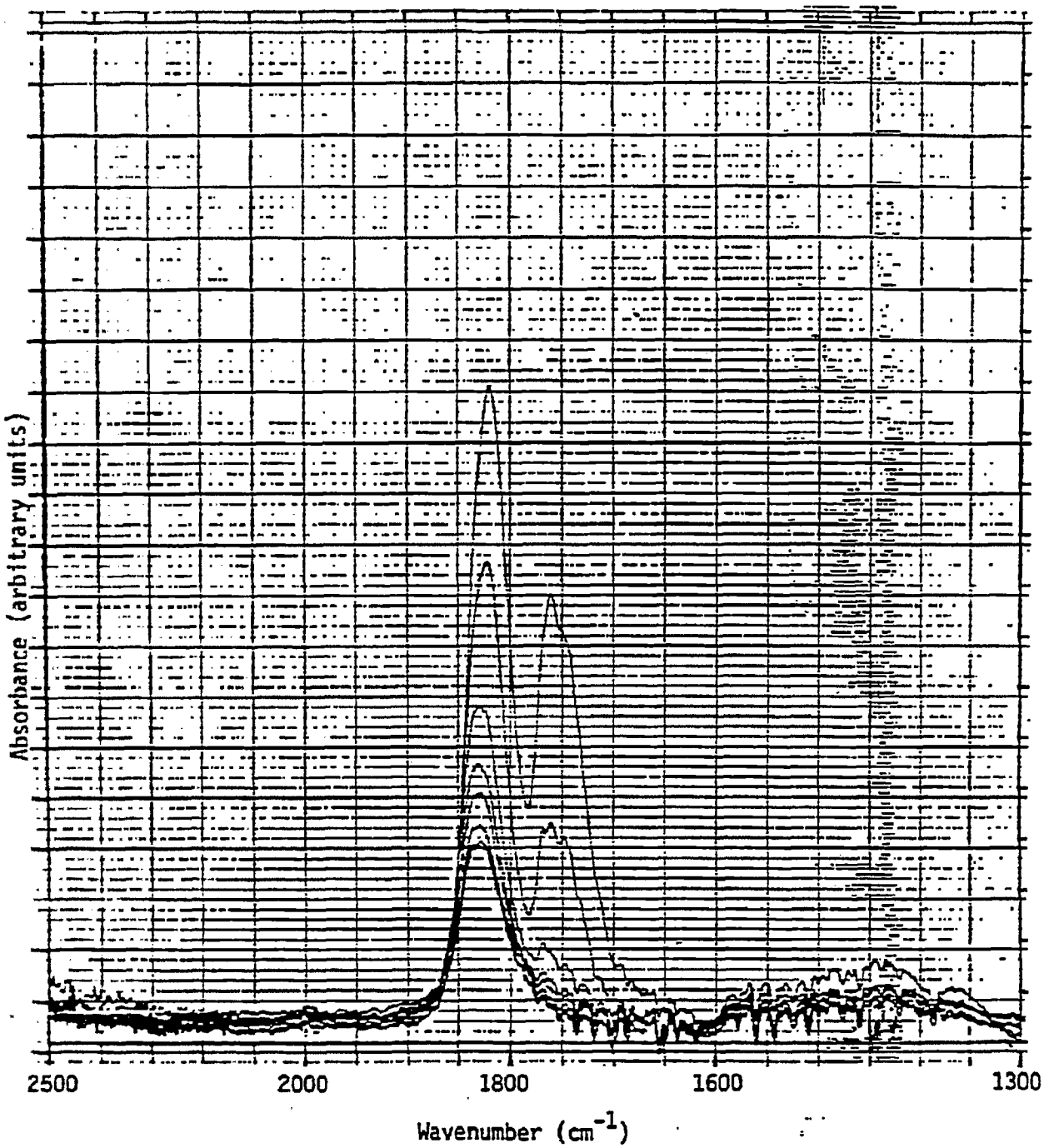

Figure 24. FT-IR spectra of NO adsorbed at 25 °C on 25 wt % Fe/SiO_2 that had been calcined for 16 hrs at 300 °C and subsequently treated in H_2 for 16 hrs at 730 °C. The uppermost spectrum was obtained following exposure of the sample to 10 torr of NO for 15 min, followed by evacuation. The second spectrum was obtained immediately after admission of 10 torr of O_2 at 25 °C. The remaining spectra were then obtained at 15 min intervals in the continuing presence of gaseous O_2.

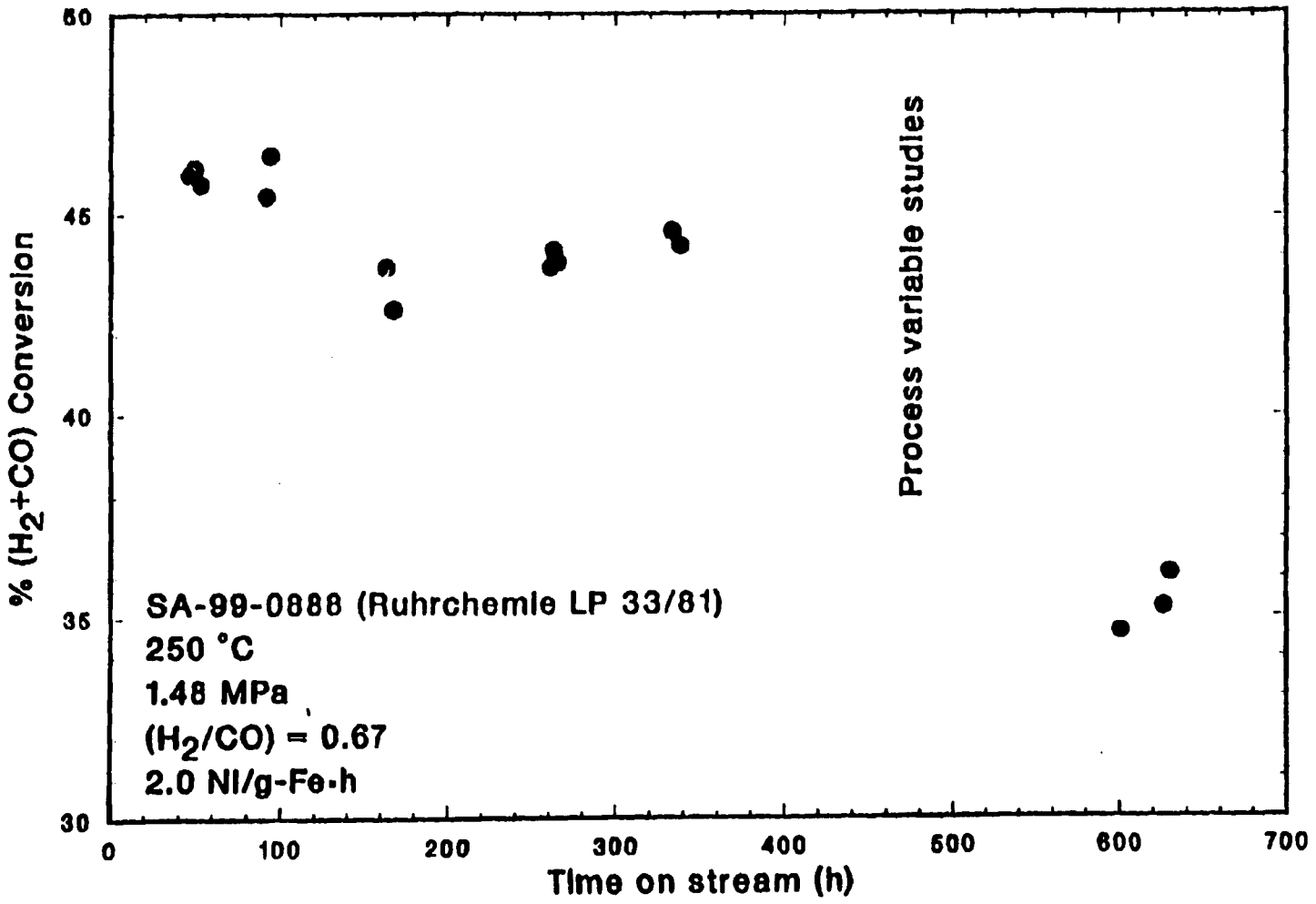

Figure 25. Stability plot, (H_2+CO) conversion versus time on stream, for run SA-99-0888.

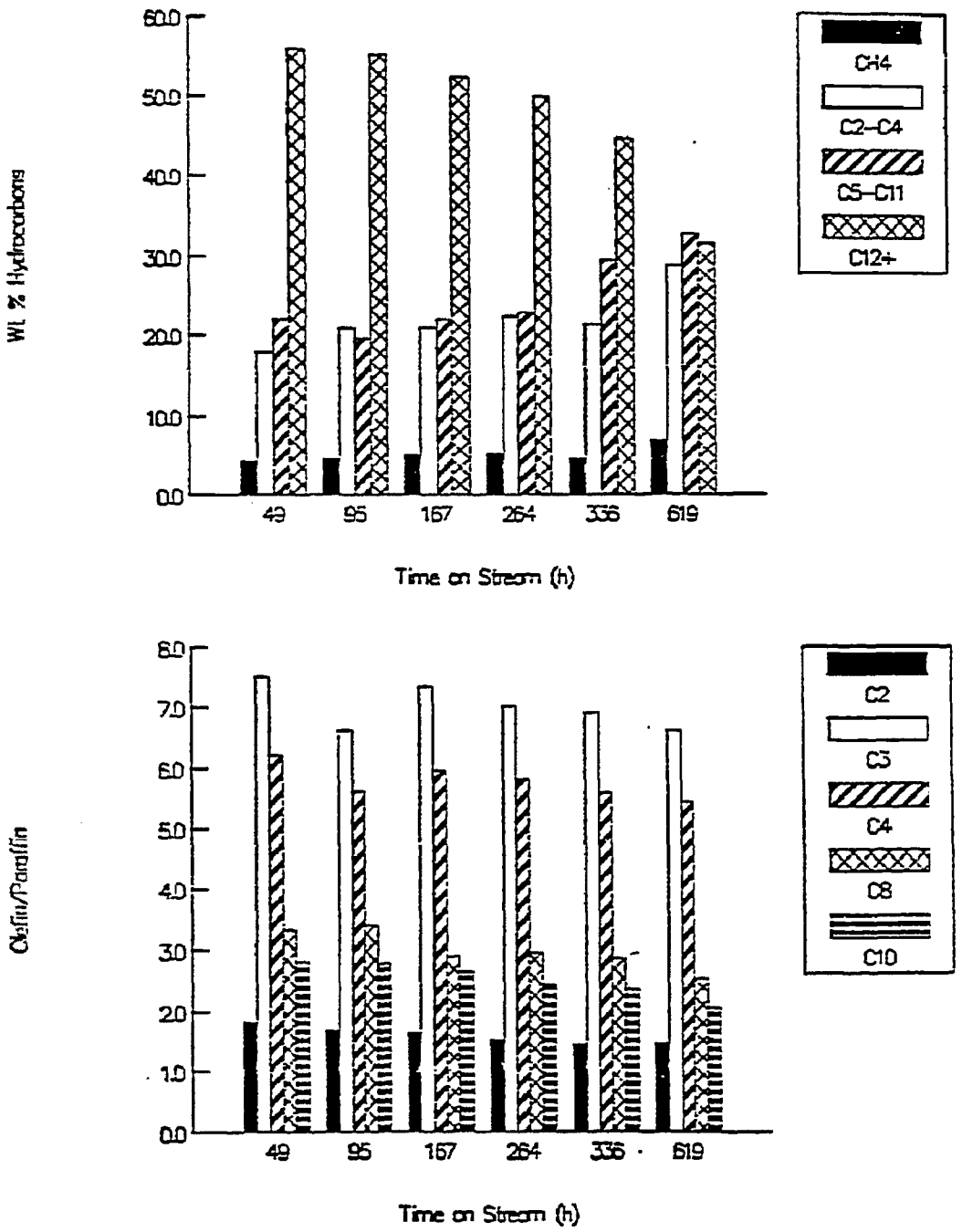

Figure 26. Effect of time on stream on Ruhrchemie LP 33/81 selectivity for run SA-99-08SS: 250 °C, 1.48 MPa, 2 Nl/g-cat-h, $(H_2/CO) = 0.67$.

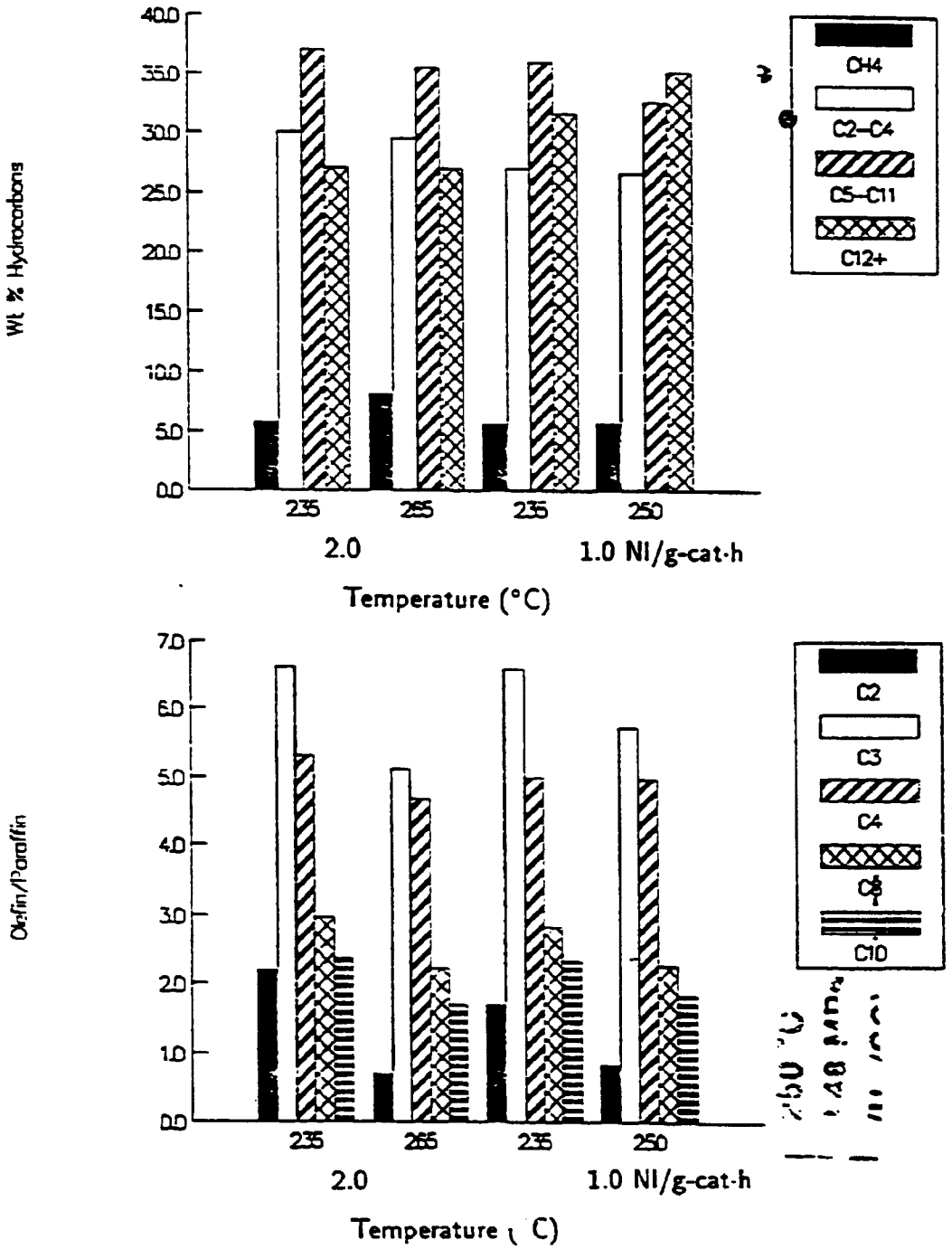

Figure 27. Effect of temperature on Ruhrchemie LP 33/81 selectivity for run SA–99–08SS: 1.48 MPa, $(H_2/CO) = 0.67$.

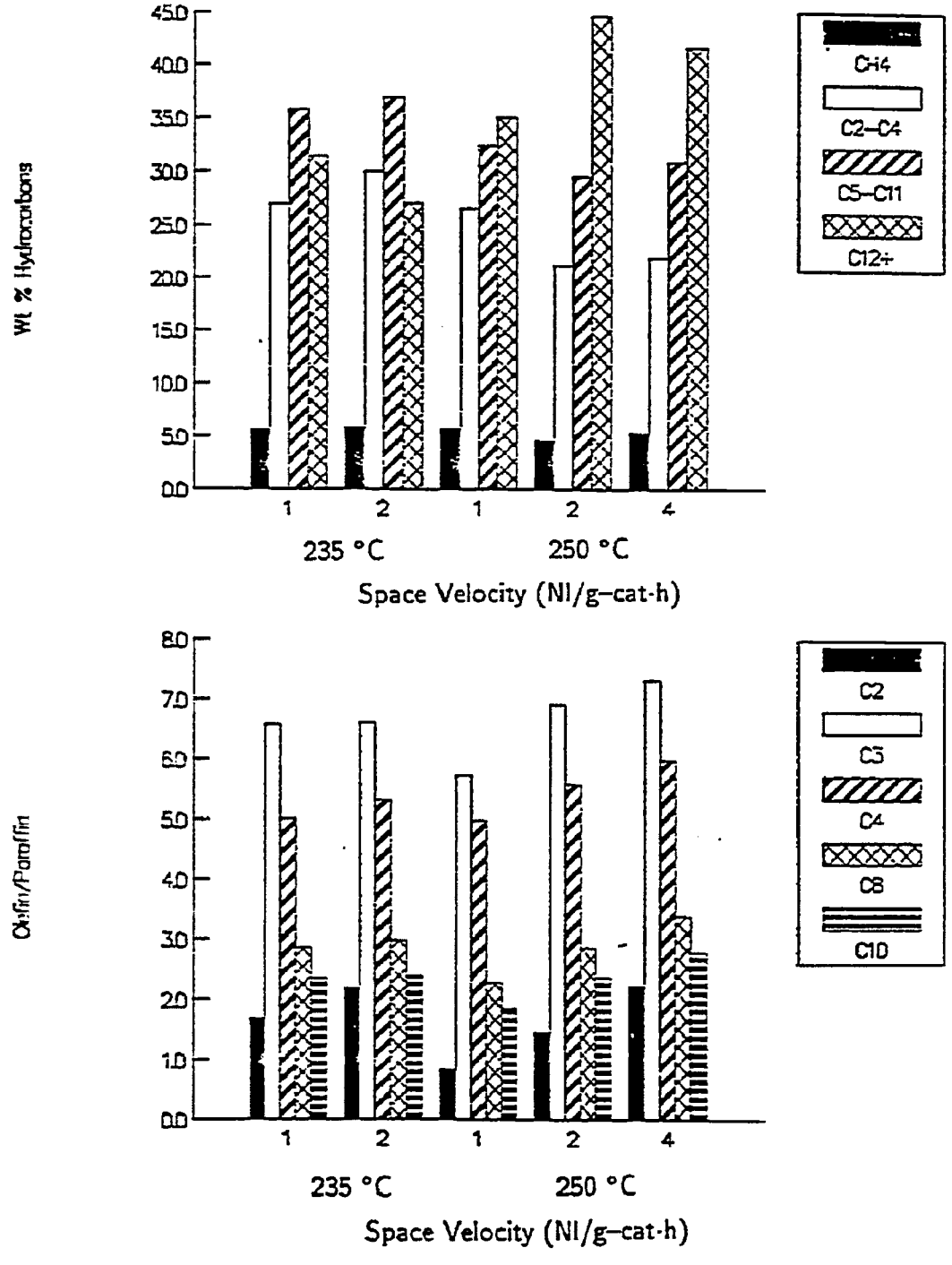

Figure 28. Effect of space velocity on Ruhrchemie LP 33/81 selectivity for run SA–99–0888: 1.48 MPa, $(H_2/CO) = 0.67$.

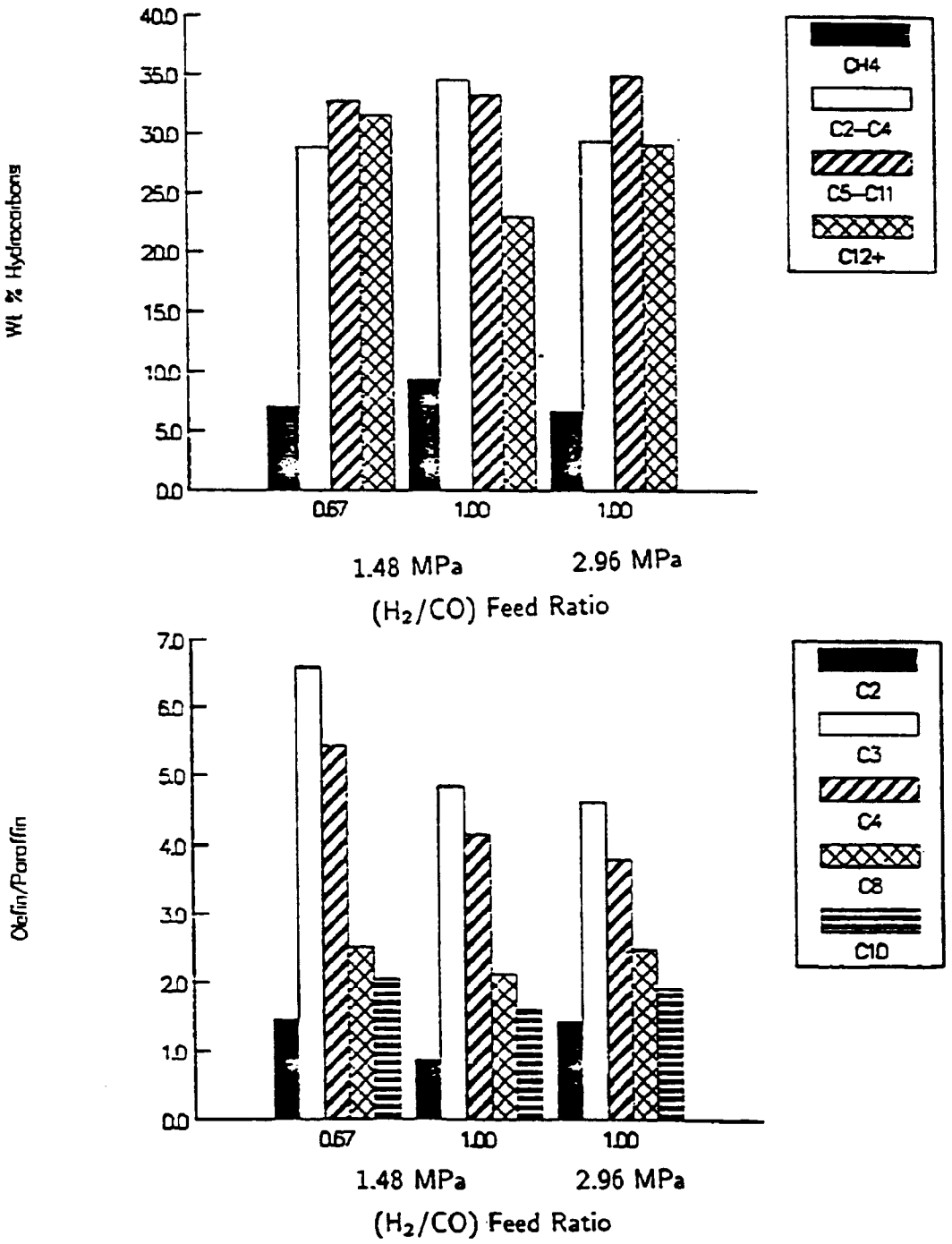

Figure 29. Effect of feed ratio and pressure on Ruhrchemie LP 33/81 selectivity for run SA-99-0888: 250 °C.

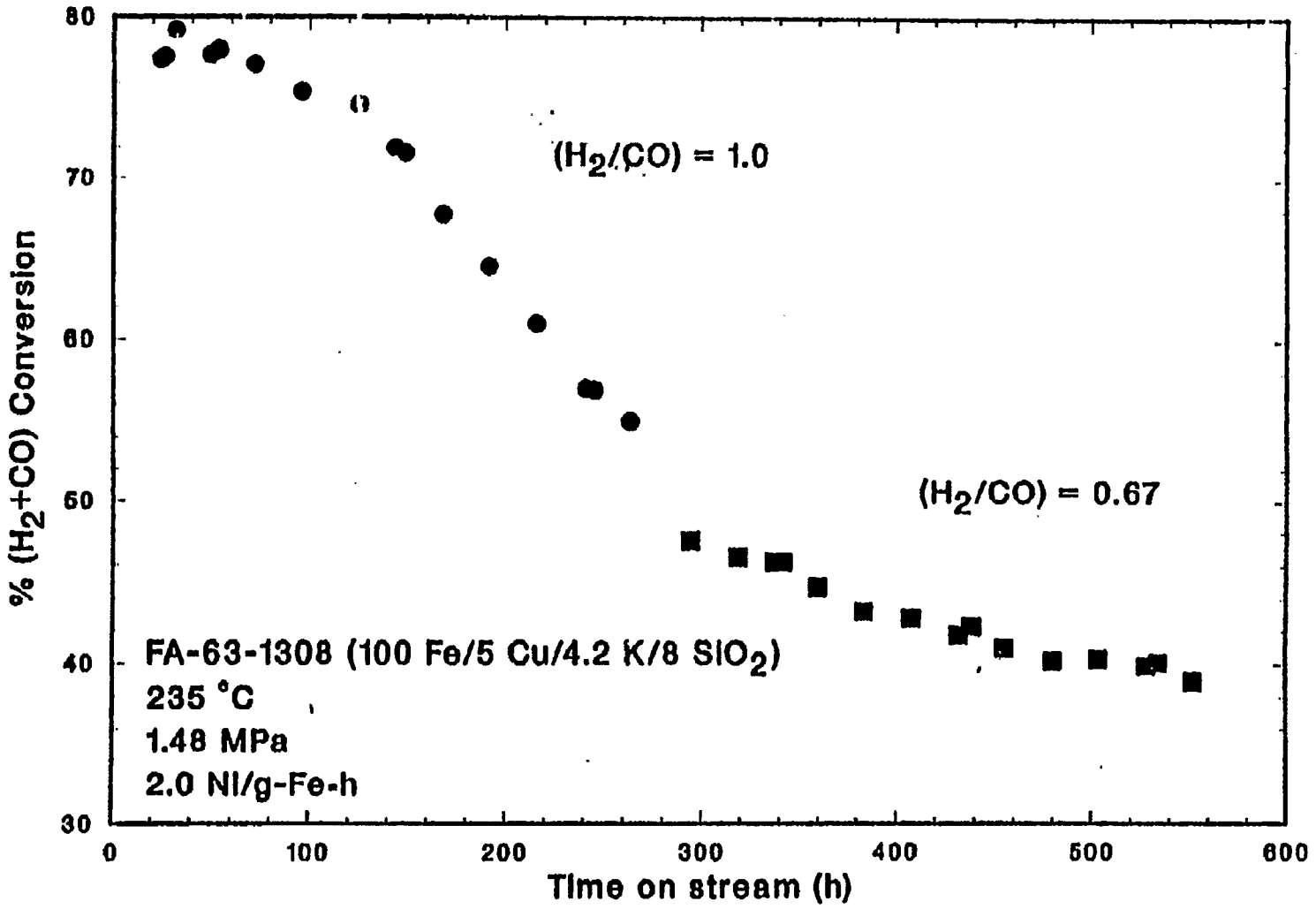

Figure 30. Stability plot, (H_2+CO) conversion versus time on stream, for run FA-63-1308.

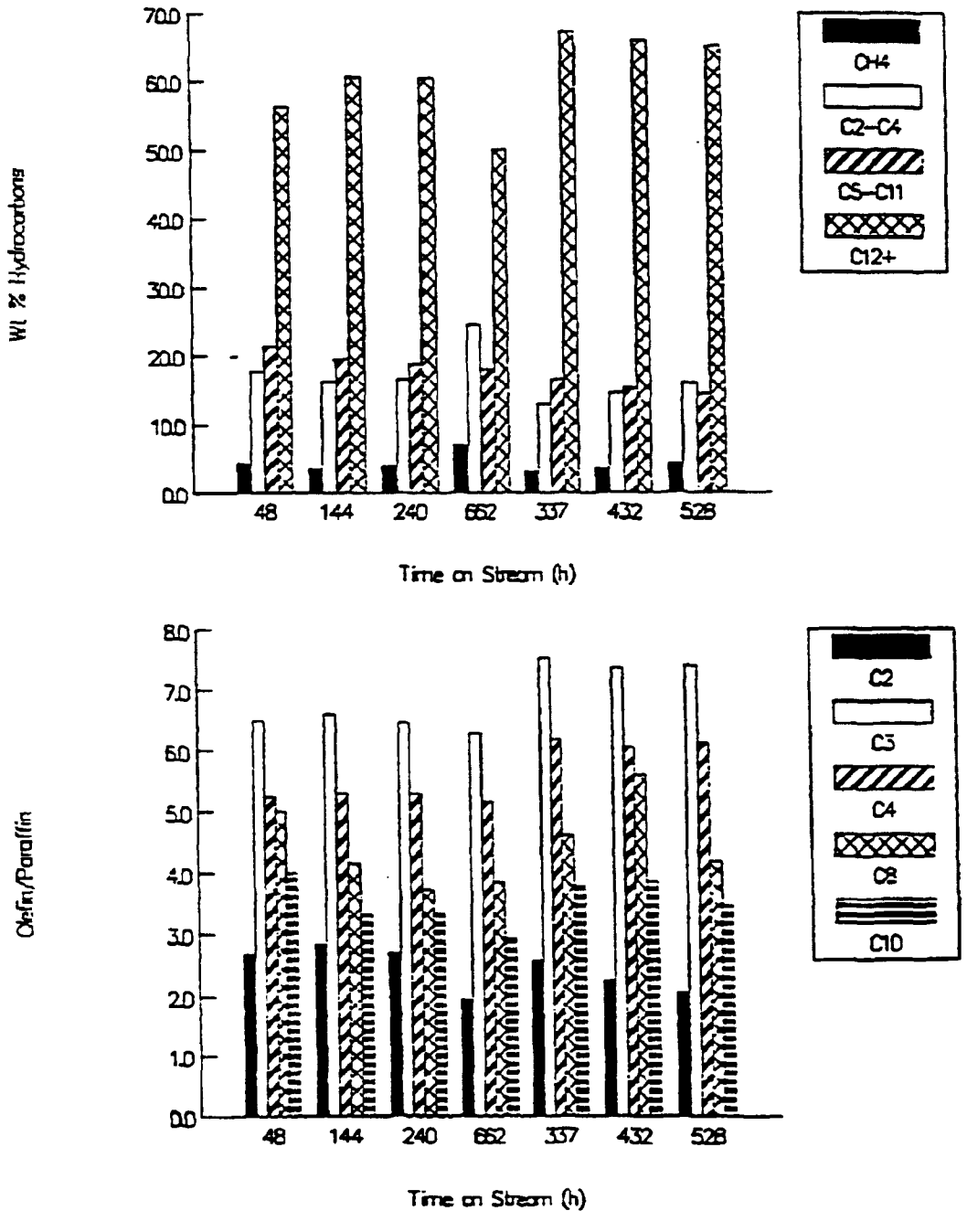

Figure 31. Effect of time on stream on 100 Fe/5 Cu/4.2 K/8 SiO_2 catalyst selectivity for run FA-63-1308: 235 °C, 1.48 *MPa*, 2 *Nl/g*-cat·*h*, (H_2/CO) = 1.0 (48–240, 662 *h*) and 0.67 (337–528 *h*).

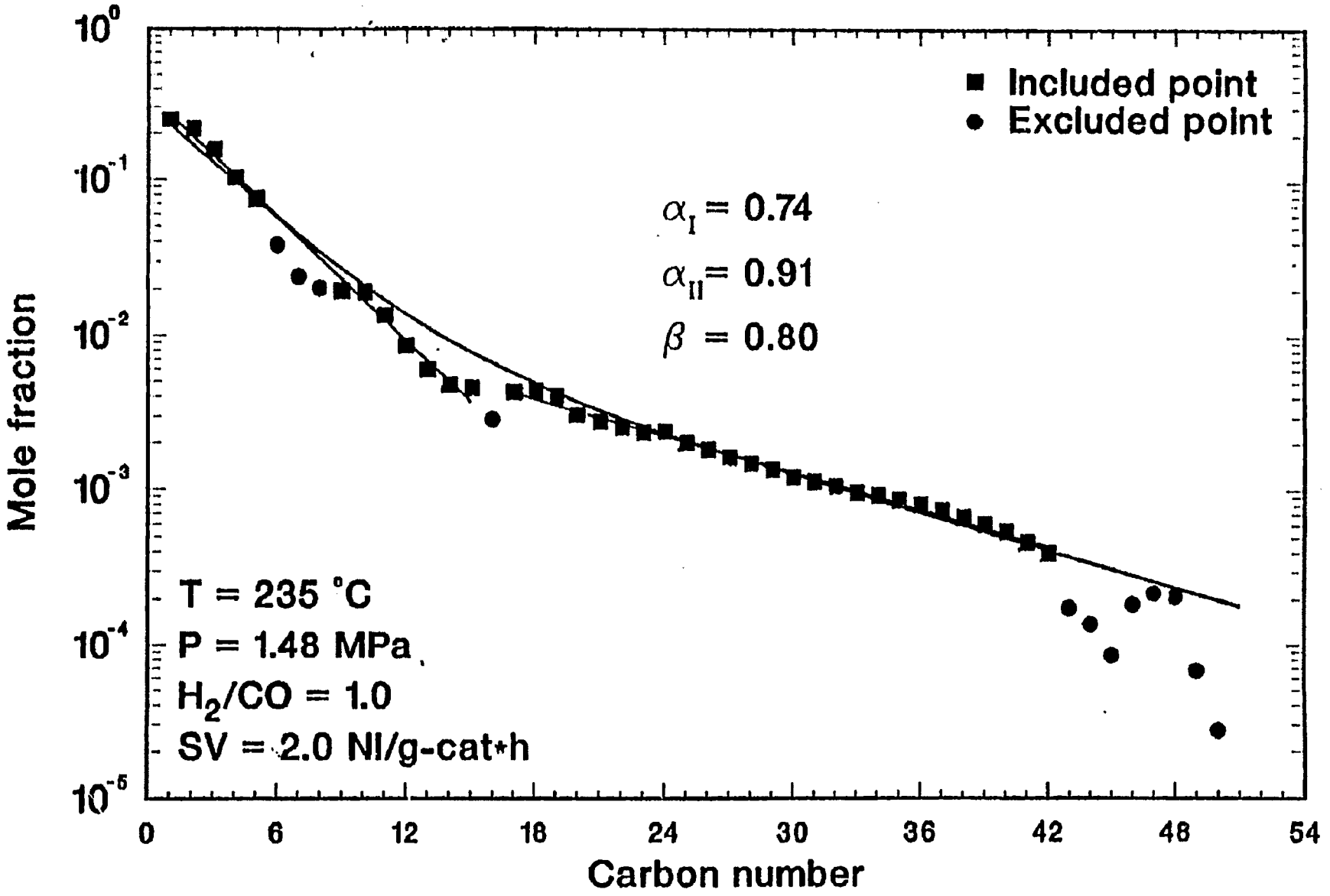

Figure 32. Anderson-Schulz-Flory plot for run FA-03-1308-1, total products excluding unrecovered wax.

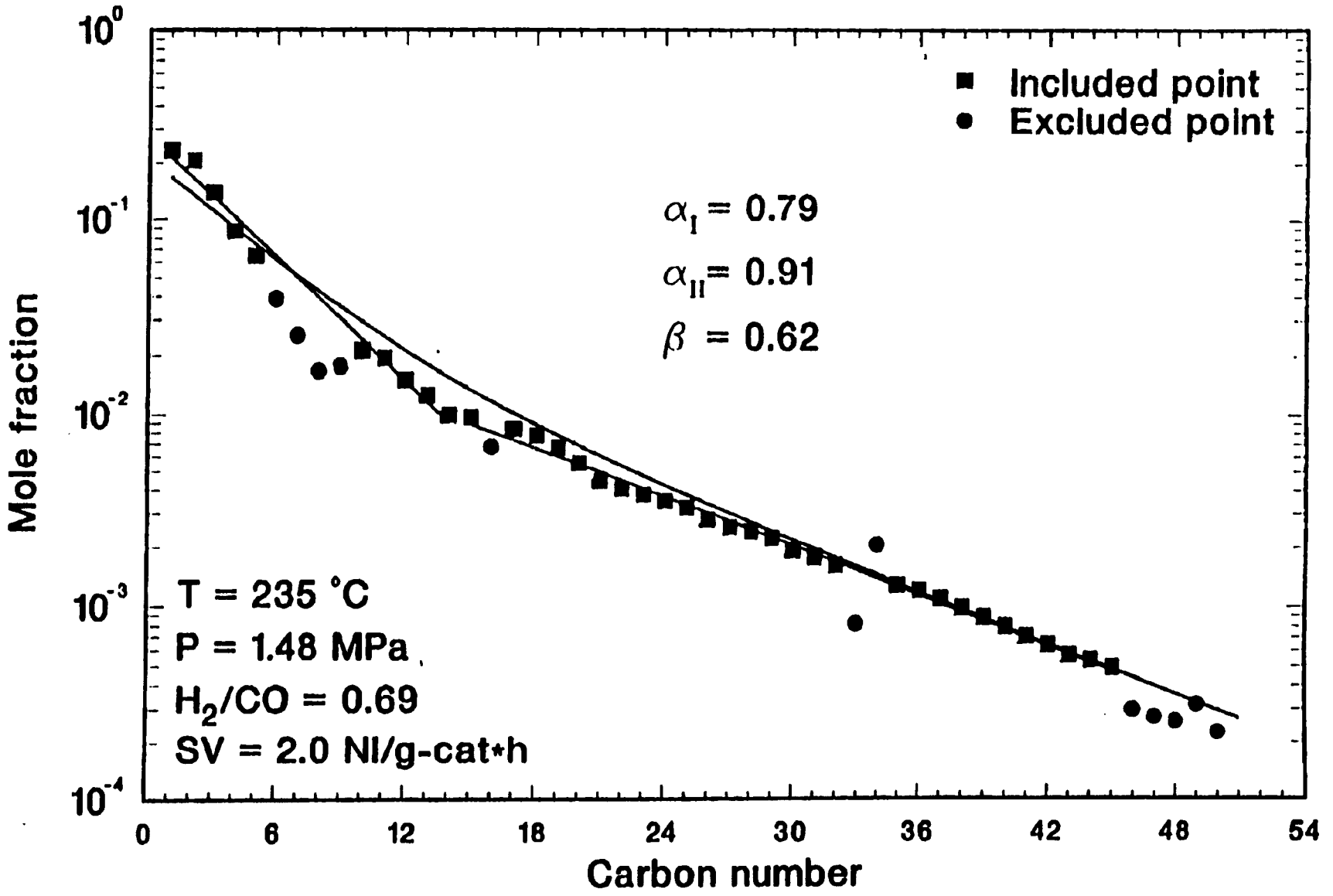

Figure 33. Anderson-Schulz-Flory plot for run PA-03-1308-4, total products excluding unrecovered wax.

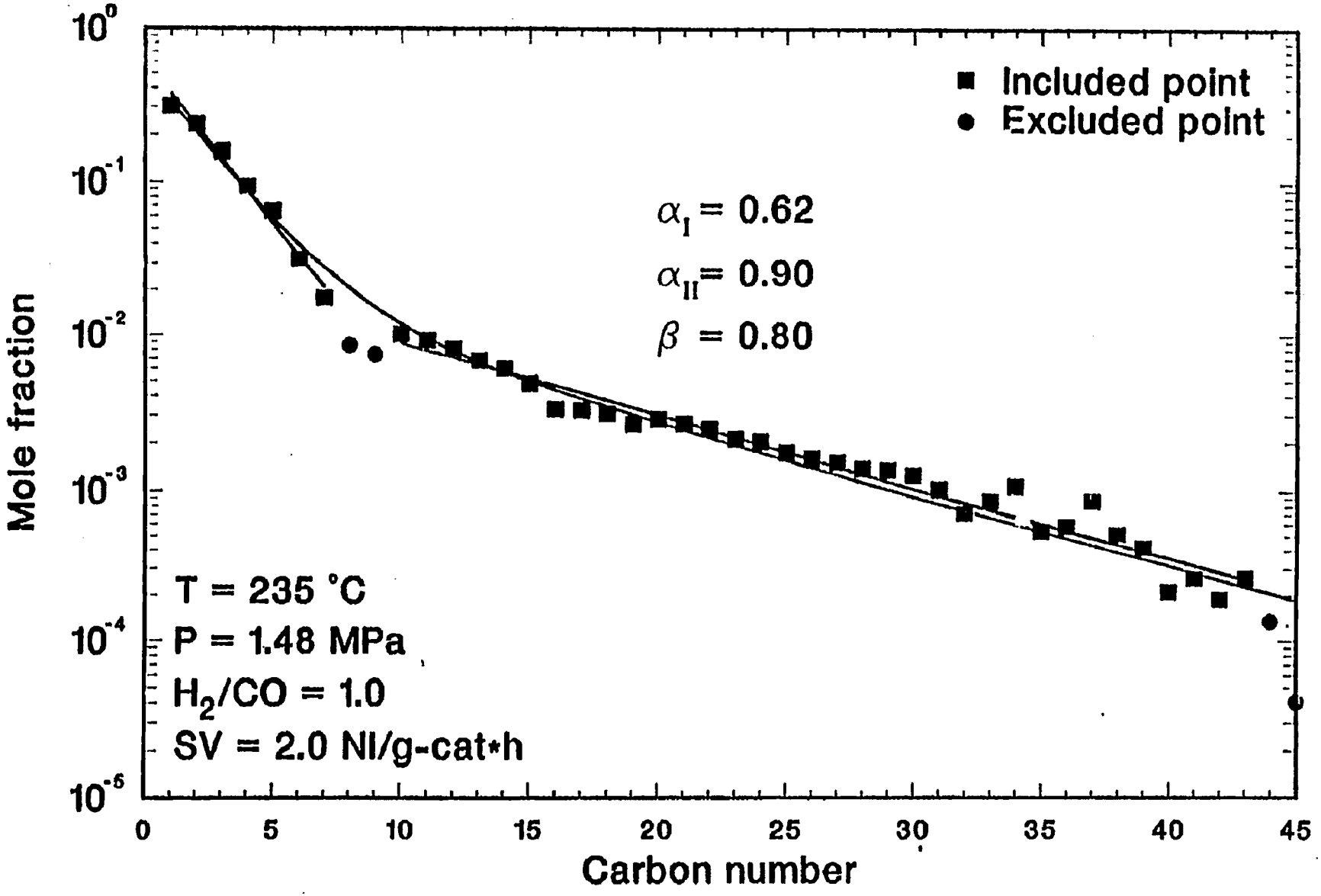

Figure 34. Anderson-Schulz-Flory plot for run FA-63-1308-8, total products excluding unrecovered wax.

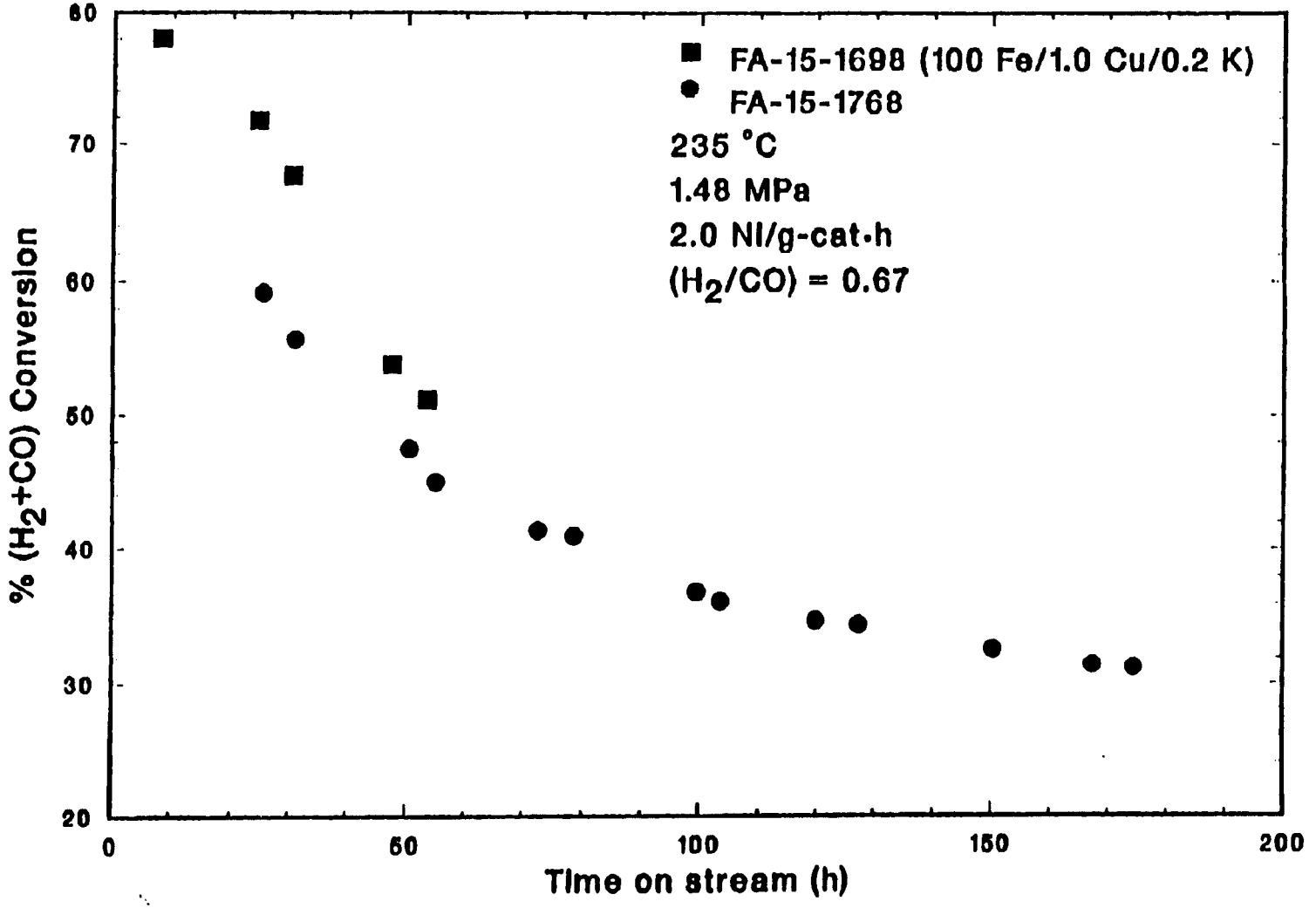

Figure 35. Stability plot, (H_2+CO) conversion versus time on stream, for runs FA-15-1698 and FA-15-1768.

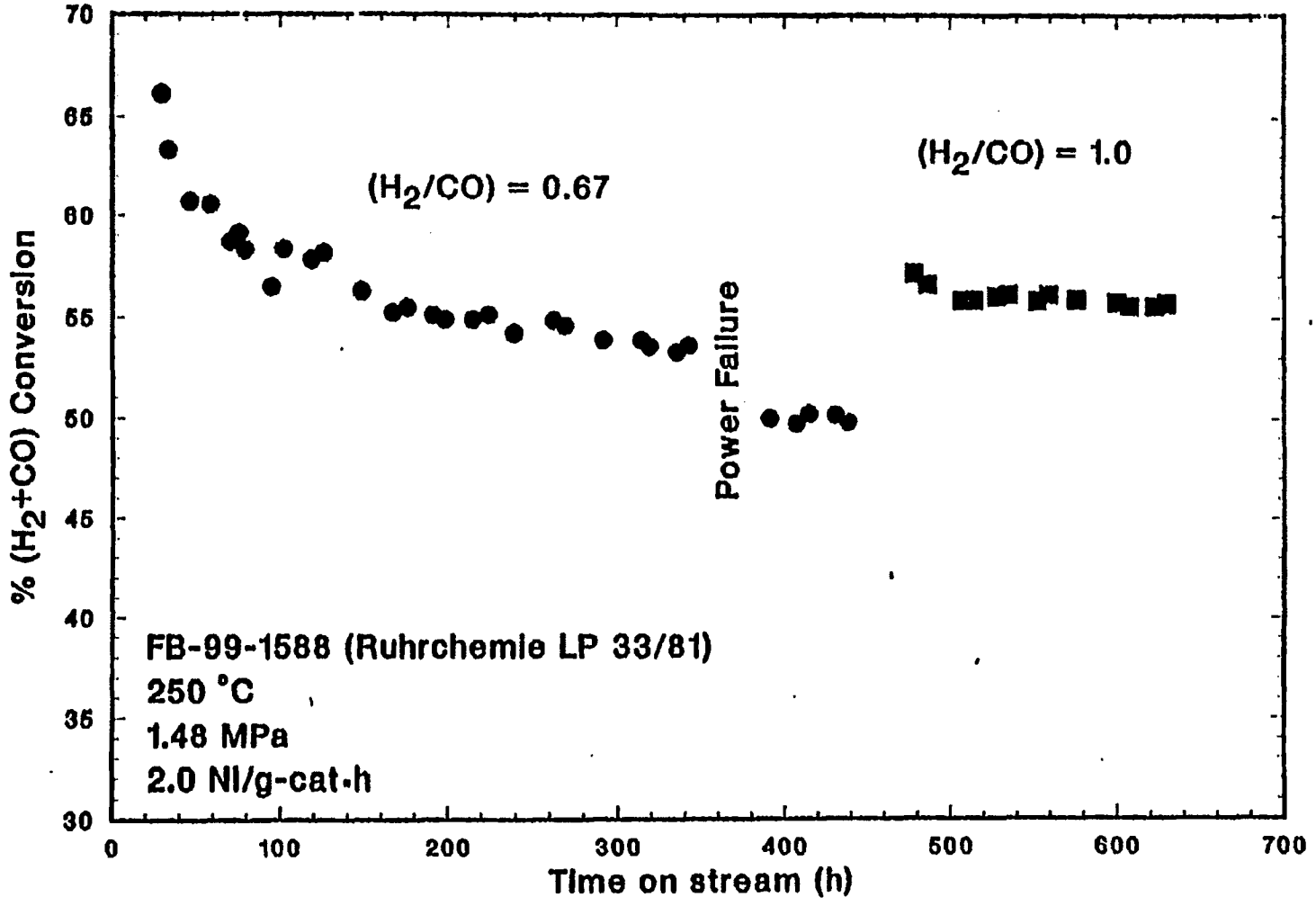

Figure 36. Stability plot, (H_2+CO) conversion versus time on stream, for run FB-99-1588.

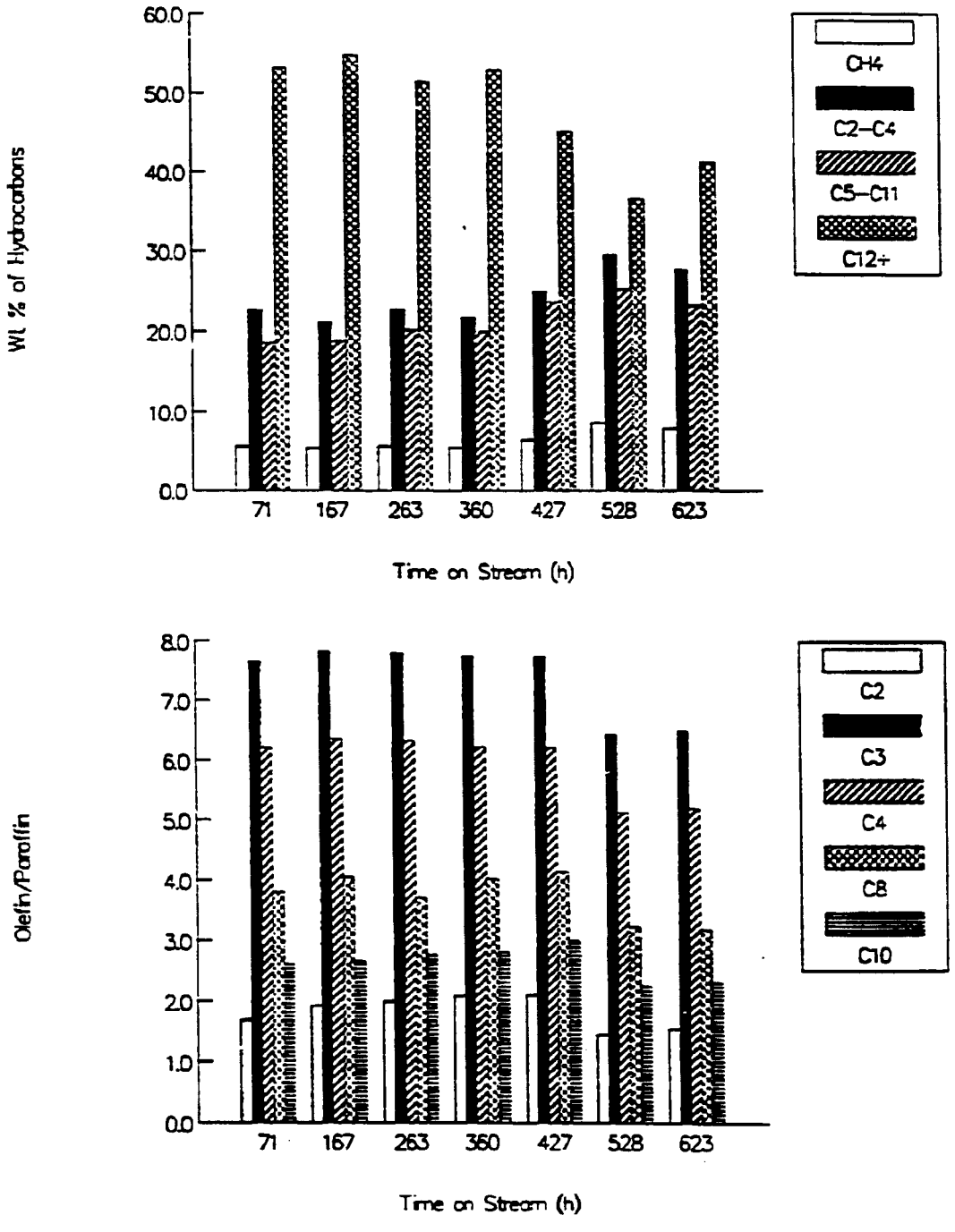

Figure 37. Effect of time on stream on Ruhrchemie LP 33/81 selectivity for run FB–99–1588: 250 °C, 1.48 MPa, 2 Nl/g–cat-h, $(H_2/CO) = 0.67$ (71–427 h) and 1.0 (528, 623 h).

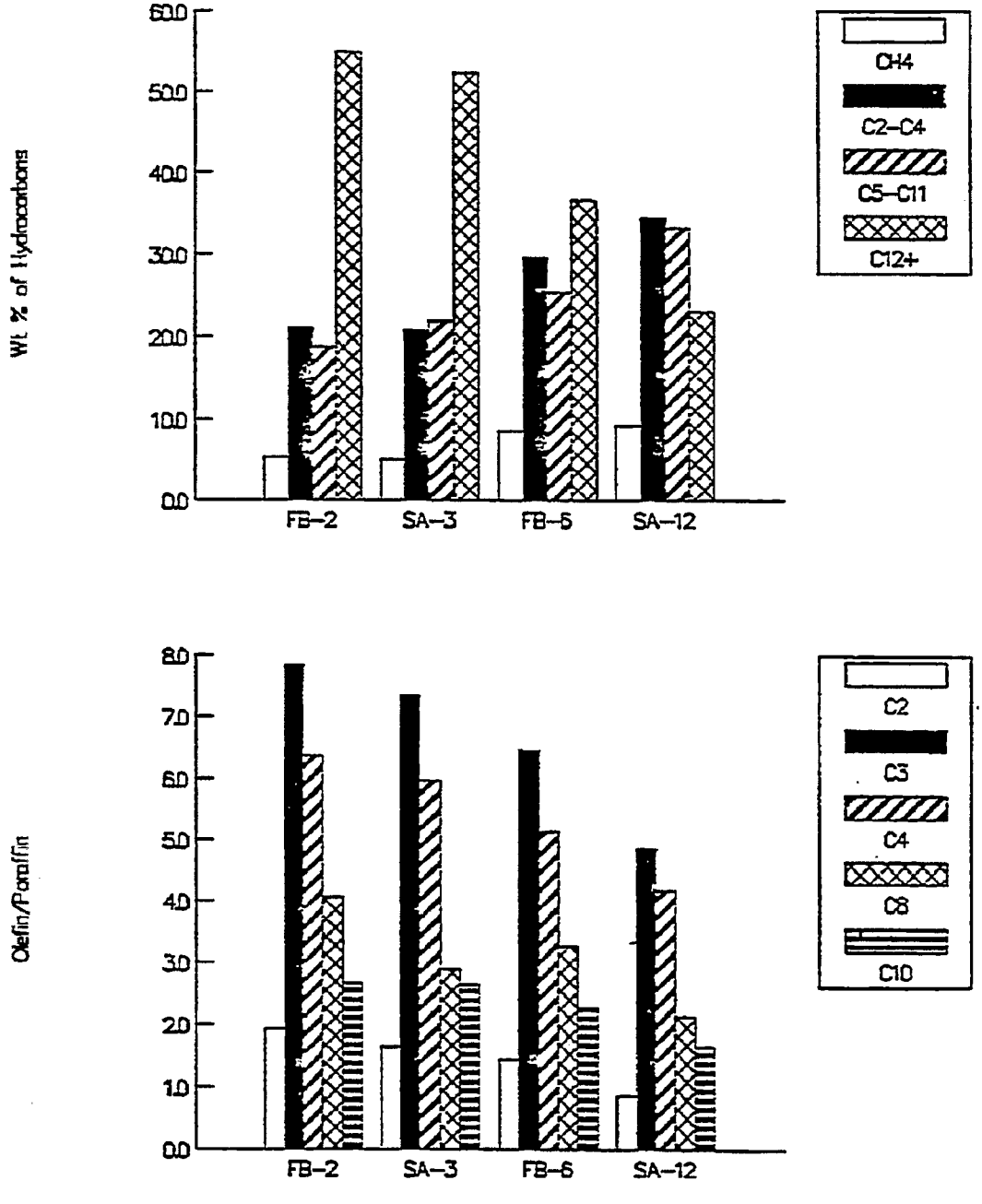

Figure 38. Comparison of fixed bed and slurry reactor selectivity with Ruhrchemie LP 33/81 catalyst (FB = FB-99-1588, SA = SA-99-0888): 250 °C, 1.48 MPa, 2.0 Nl/g-cat-h, (H_2/CO) = 0.67 (FB-2 and SA-3) and 1.0 (FB-6 and SA-12).

U.S. DEPARTMENT OF COMMERCE
Technology Administration
National Technical Information Service
Springfield, VA 22161 (703) 605-6000

DE92016986

BA

BIN: M17 11-06-03
INVOICE: 1300066
SHIPTO: 1*852037
PAYMENT: CSH*A